**University of Alberta**

Experimental Methodology Used to Investigate Transport Processes in Cap Rock

By

Anna Hoilan Ho    ©

A thesis submitted to the Faculty of Graduate Studies and Research in partial fulfillment of the requirements for the degree of Master of Science

in

Geo-Environmental Engineering

Department of Civil and Environmental Engineering

Edmonton, Alberta

Fall 2002

National Library
of Canada

Bibliothèque nationale
du Canada

Acquisitions and
Bibliographic Services

Acquisitions et
services bibliographiques

395 Wellington Street
Ottawa ON  K1A 0N4
Canada

395, rue Wellington
Ottawa ON  K1A 0N4
Canada

0-612-81409-2

Canada

University of Alberta

Library Release Form

Name of Author: Anna Hoilan Ho

Title of Thesis: Experimental Methodology Used to Investigate Transport Processes in Cap Rock

Degree: Master of Science

Year this Degree Granted: 2002

Permission is hereby granted to the University of Alberta Library to reproduce single copies of this thesis and to lend or sell such copies for private, scholarly or scientific research purposes only.

The author reserves all other publication and other rights in association with the copyright in the thesis, and except as herein before provided, neither the thesis nor any substantial portion thereof may be printed or otherwise reproduced in any material form whatever without the author's prior written permission.

#5, 7602-115 St
Edmonton, Alberta
T6G 1N5
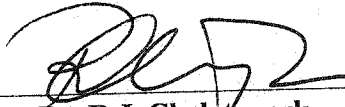
Sept. 30, 2002

Submitted to the Faculty of
Graduate Studies and Research

**University of Alberta**

Faculty of Graduate Studies and Research

The undersigned certify that they have read, and recommend to the Faculty of Graduate Studies and Research for acceptance, a thesis entitled *Experimental Methodology Used to Investigate Transport Processes in Cap Rock* submitted by *Anna Hoilan Ho* in partial fulfillment of the requirements for the degree of *Master of Science* in *Geo-Environmental Engineering*.

Dr. R.J. Chalaturnyk
(supervisor)

Dr. D.C. Sego

Dr. S.E. Guigard

Dr. B. J. Rostron

Sept. 25, 2002
**Date Approved**

# Abstract

Geological storage of $CO_2$ into deep saline aquifers has been proposed as a short-term solution. Effectiveness of geological storage is dependent on the overlying cap rock, and its ability to maintain a competent seal. Rate of $CO_2$ transport is site-specific, dependent on the geology and $CO_2$ properties.

Investigation of laboratory data is essential in understanding the fundamental processes occurring in the field. Sealing ability of low permeability cap rocks is heavily debated, and laboratory methods used to determine its behaviour are limited in capability. Development of a sophisticated testing facility required to investigate the effect of gas transport under a flexible regime of parameters and geological materials, including highly fissile stiff clays, is presented. It was designed with the intention of testing diffusion, advection, and intact adsorption on fragile materials such as clay shales. An advanced sealing mechanism design, ability to control triaxial stresses, and constant temperature control is incorporated here, with the potential for in-line electrical resistivity measurements.

Your imagination is your preview of life's coming attractions.


-- *Albert Einstein*

*For my parents, Joseph and Agnes Ho, for providing me with the opportunities.*
*And for John Ybema, for your support and encouragement.*

## Acknowledgements

# Table of Contents

## List of Illustrations

<u>List of Figures</u>

List of Tables

## 1.0  Introduction

The natural greenhouse effect is a well-understood phenomenon whereby gases such as methane, ozone, carbon dioxide, and water vapour contribute to the warming of the earth's atmosphere. Global mean annual temperature would be approximately 21°C cooler without the contribution of these gases trapping heat in the earth's atmosphere (Houghton, 1997). The addition of anthropogenic sources of methane ($CH_4$) and carbon dioxide ($CO_2$), and other human-made greenhouse gases, such as chlorofluorocarbons (CFC), has resulted in an increase in the global mean annual temperature (Houghton, 1997; United States Environmental Protection Agency (EPA) http://www.epa.gov/globalwarming.html; The David Suzuki Foundation http://www.davidsuzuki.org). Carbon dioxide is the greenhouse gas (GHG) most frequently talked about in reference to global warming, due to the large quantities of $CO_2$ emitted in the atmosphere, mostly by energy production and fossil fuel combustion. Currently, a variety of methods are being investigated in an effort to reduce these sources of GHG. An emerging technology to reduce GHG emissions into the atmosphere is by means of geological storage, whereby $CO_2$ is injected into a host formation (van der Meer, 1992; Krom et al., 1993; Tanaka et al., 1995; Bergman et al., 1997; Gunter et al., 1997).

### 1.1  Overview of Geological Storage

Injection of $CO_2$ into deep coal seams, deep oceanic beds, depleted oil and gas reservoirs, old salt caverns, and deep saline aquifers have been suggested as possible disposal receptors (Bergman et al., 1997; Holloway, 1997; Bachu, 1999). These receptors must be evaluated based on their storage potential and residence time.

Injection of $CO_2$ into coal seams results in the desorption of one molecule of methane, held in the microstructure of the coal, for every two molecules of $CO_2$ stored. Storage of $CO_2$ between mid to long residence times, depending on the geological conditions, is estimated (Bachu et al., 2000). Storage capacity of coal beds for storing $CO_2$ appears to be similar to that of deep aquifers (Gunter et al., 1997), with the added benefit of $CH_4$ production.

Deep ocean storage is proposed for depths greater than 3000m below water surface, where the density of the carbon dioxide is greater than the density of the seawater. Storing $CO_2$ in oceans can result in the formation of acidic brine, which has a lower capacity to hold oxygen compared to the surrounding seawater. Lack of $O_2$ will have an adverse affect on the conditions necessary to sustain both aquatic life and plant communities. Development of anoxic conditions, and inability for marine organisms to cope with the acidic nature of the brine suggest that $CO_2$

storage in oceans involves many hazards (Harrison et al., 1995; Freund and Ormerod, 1997). Long term effectiveness is questionable since projected residence time of $CO_2$ in oceans is likely in the order of a few hundred years (Freund and Ormerod, 1997).

Use of depleted oil and gas reservoirs, abandoned salt caverns, and saline aquifers as waste repositories are common in petrochemical and oil and gas industries (Liu and Ortoleva, 1996), and therefore the investigation into their ability as potential receptors for GHG is a natural extension of these industrial activities. Storage capacity of a single salt cavern is capable of holding 500 000m$^3$, at up to 80% of the fracturing threshold pressure (Bachu et al., 2000). The storage volume of gas reservoirs is associated with the amount of gas that is produced from the reservoir, and will determine the volume of pore space available for $CO_2$, minus a few percentage points (Holloway et al., 1996). Amount of pore space available is dependent on its abandonment time. Utilization soon after abandonment will maximize the amount of pore space available for $CO_2$ storage, as time passes pore space will become occupied with water, resulting in less available pore space for $CO_2$ (Holloway et al., 1996). Storage in depleted oil reservoirs is at a disadvantage because of its lower reservoir capacities, lower injection rates, and lower storage efficiency (Bergman et al., 1997). Storage in oil reservoirs refers to an enhanced oil recovery technique (EOR), where $CO_2$ is injected into mature reservoirs, and additional oil is recovered. Residence time associated with EOR is typically short in the order of months to several years (Bachu et al., 2000). In Alberta, the potential of storage capacity of the entire Alberta Basin alone is estimated at 20GT of $CO_2$ (Bachu et al., 1994). Estimated global storage potential of deep aquifers is in excess of 400 GT (Gunter et al., 1996). Stevens et al. (1999) present a complete summary of international storage potential in depleted oil and gas reservoirs, including case studies, and estimated volumes of sequestered waste gases.

It is postulated that deep saline aquifer storage could retain $CO_2$ in the order of $10^5$-$10^6$ years due to the large amount of pore space, mineralisation reactions and hydrodynamic trapping (Gunter et al., 1993; Law and Bachu, 1996). Hydrodynamic trapping refers to over geological times trapping of $CO_2$ gas in deep regional aquifers due to the low flow velocity. The trapping mechanism is a function of the dissolved state of $CO_2$ in the groundwater. Slow fluid flow within the aquifer will allow time for $CO_2$ and rock mineral reactions to proceed, and thus contain the $CO_2$ through mineralisation reactions (Gunter et al., 1993; Perkins and Gunter, 1996). However, the question of lateral containment in aquifers remains unanswered.

A common trait between storage mechanisms in gas reservoirs, salt caverns, and saline aquifers is the uncertainty of its ability to maintain an adequate seal, and increase the residence

time by controlling the waste fluid flow (van der Meer, 1992; Tanaka et al., 1995; Holloway et al., 1996).

## 1.2 Research Objectives

Risk assessment of long term storage of $CO_2$ requires the understanding of fundamental processes occurring in the field, including $CO_2$ movement within the injection zone, and transport processes occurring in the bounding seals or cap rock. Of the 25 largest gasfields in the world, sixteen are sealed by shales, and the remaining are sealed by evaporites (Grunau, 1987). Argillaceous rocks namely, mudstones, clays and shales, are most commonly found as top seals in natural $CO_2$ accumulations (Stevens et al., 2001), and hydrocarbon reserves (Grunau, 1987; Caillet, 1993). Due to the difficulty in obtaining representative samples, long testing times required, and sensitivity to sample preparation techniques, these class of materials have not been extensively tested. Regardless of this however, evaluation of the seal integrity for aquifers, hydrocarbon reservoirs, and salt caverns is essential in determining the likely retention time of the disposed gas. Long term stability of the seal is dependent on:

- properties of the gas

- properties of the host formation seal, i.e. its mineralogy and physical attributes (presence of discontinuities).

These properties will determine the dominant physical transport mechanisms, i.e. the permeability and diffusion occurring within the overlying seal. Retardation of gases due to physical adsorption, will also affect its transport mechanism.

Although in-situ conditions ultimately govern the probability of gas transport through the bounding seals (due to scale effects), laboratory data is essential in understanding the problem of seal integrity, and the fundamental processes which may occur under specific conditions in the field.

Currently, very few, if any experimental apparatus have been designed, which are capable of testing gas transport in water saturated geological materials under realistic conditions, and capable of applying deviatoric stresses. The main objective of this research was to design a laboratory apparatus to investigate the principles of gas transport in tight low porosity geologic materials. It was important to ensure that the principles of geotechnical engineering were incorporated into the methodology, thus increasing the complexity of the experimental design.

3

## 1.3 Scope of Work

This thesis considers potential methods of investigating gas transport in water saturated low permeability clay-rich materials, and incorporates the following:

- Detailed review of transport mechanisms (diffusion, permeability) of $CO_2$, in particular as they relate to shales;

- Development of experimental procedures suitable for the determination of gas transport under realistic in-situ stresses and temperatures;

- Design and commissioning of experimental equipment to permit execution of an experimental program; and

- Development of monitoring systems suitable for an experimental program.

Issues surrounding the permanent storage of injected CO2 involve mineral precipitation, for which reaction kinetics between CO2 and the formation minerals is a key factor. The ability to model these reactions with the experimental system was considered outside the scope of this work due to its complexity.

## 1.4 Thesis Content

A description of transport processes in geological materials and properties of $CO_2$, relevant to geological storage is presented in CHAPTER 2. Clearwater clay shale, an analog to many materials serving as seals in deep aquifer storage sites, is used to help identify the important parameters involved in designing laboratory equipment for evaluation of physical transport processes. Understanding the behaviour of gas transport processes, i.e. diffusion, permeability and adsorption, will aid in the design of the apparatus, and the issues which these processes are sensitive to.

Design criteria set forward, and intended to provide guidance in the experimental design is presented in CHAPTER 3. Realistic pressures in the Alberta Basin have been used to establish the limits of the pressure requirements. Testing conditions should be applicable under a wide range of temperatures, but exceed the critical temperature of $CO_2$ at the very least. Descriptions of the testing facility are provided.

Sealing mechanisms and membranes tested and final design incorporating an improved sealing mechanism is illustrated in CHAPTER 4. Discussion around the available options in limiting gas leakage from the specimen to the surrounding fluid is discussed.

Experimental methodology in calculating diffusion and permeability through low permeability water saturated geologic materials is presented in CHAPTER 5. Determination of adsorption capacity on intact or crushed specimens is described. Special emphasis is given to the difficulties associated with sample preparation of heavily fissile materials.

Methods used to monitor the $CO_2$ as it travels through the specimen, and downstream measurement of quantitative fluxes through the specimen are evaluated in CHAPTER 6. Details regarding potential in-line methods capable of indicating $CO_2$ concentrations are illustrated.

Concluding remarks on experimental design of the testing facility is described, and recommendations for future work are outlined in CHAPTER 7.

## 2.0 Background

Properties of a cap rock must be evaluated to determine its sealing properties. Understanding the mineralogy, pore fluid chemistry, and physical properties of the cap rock (in this case Clearwater clay shale), as well as properties of $CO_2$ were required in order to determine an appropriate range of experimental design parameters. The test parameters based on these properties are used to determine the boundaries in the experimental design. Understanding the mechanisms will also be useful in determining testing parameters.

### 2.1    Properties of $CO_2$

The disposal scenarios involving $CO_2$ are extremely broad, from shallow reservoirs to deep aquifers, and thus the behaviour of $CO_2$ will vary depending on its depth. As depth varies so does its pressure and temperature, dictating the phase in which $CO_2$ will reside. Disposal into deep aquifers, where $CO_2$ is in a supercritical state, is desired due to the increased density of $CO_2$ in that phase, and therefore a more efficient use of the pore space. Understanding the variation in the properties of $CO_2$ with temperature and pressures is necessary to evaluate its transport mechanisms.

A nonpolar molecule, $CO_2$ is currently found in the atmosphere at concentrations of 360 ppmv (parts per million by volume) (Houghton, 1997), and is a known contributor to the natural greenhouse effect. Physical properties of $CO_2$ are summarized in Table 2.1, where the triple point represents the temperature and pressure at which all three phases (solid, liquid and gas) can coexist for $CO_2$.

**Table 2.1: Carbon Dioxide Properties**

| | |
|---|---|
| Sublimation Point at 101.3 KPa | 194.4 K |
| Triple Point | 216.6 K and 517.6 kPa |
| Critical Temperature | 304.3 K |
| Critical Pressure | 7.39 MPa |
| Critical Volume | 2.147 $cm^3$/g or 94.04 $cm^3$/mol |
| Molecular Mass | 44.009 g/mol |
| Density of gas at 273.15 K and 197.7 kPa | 0.001977 g/$cm^3$ |

(Fogg and Gerrard, 1991)

6

The $CO_2$ phase diagram (Figure 2.1) illustrates its behaviour over a range of temperatures and pressures. As the gas approaches its critical point its properties, particularly density, begin to vary considerably with small changes of pressure and temperature. The supercritical phase represents the region for which the critical pressure and temperature is exceeded. Supercritical, by definition, refers to the point at which increasing pressure will not induce any changes in phase no matter how high the pressure is raised so long as the temperature is beyond its critical point (Felder and Rousseau, 1986). In other words, at supercritical pressures there is no distinct phase change that occurs, where the supercritical fluid is close to its normal liquid density, but exhibits a much lower viscosity and higher diffusivity (Kyle, 1992). It is this realm, which is of most interest in deep saline disposal scenarios.
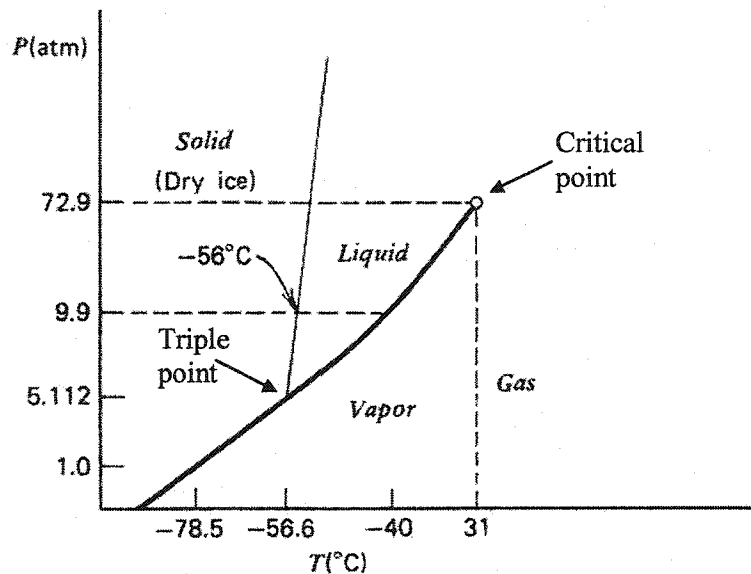


**Figure 2.1: $CO_2$ Phase Diagram**
(modified from Felder and Rosseau, 1986)

Supercritical properties of $CO_2$ significantly differ from the properties of gaseous and liquid $CO_2$. Its behaviour in geologic materials under varying pressures and temperatures is still widely unknown. In particular, its phase behaviour and reactive potential associated with $CO_2$ storage is not well understood, and continues to be investigated (White et al., 2001; Johnson et al., 2001). Theoretically, dry supercritical $CO_2$ exhibits no surface tension (Lemmon et al., 2001), and therefore would move through any microporous material. However, the existence of naturally occurring $CO_2$ deposits, which have remained under supercritical conditions, sealing gas volumes in the order of billions of tonnes by cap rocks (Stevens et al., 2000) challenges the notion of $CO_2$ movement through these class of materials, as a result of zero surface tension. Research is

currently underway to investigate naturally occurring $CO_2$ deposits, and the nature of the cap rock, as an analogue to anthropogenic $CO_2$ storage (Pearce et al., 1996; Stevens et al., 2001).

Further complexities are introduced as its thermodynamic behaviour becomes increasingly complex as $CO_2$ interactions with water and brine become a factor in geological storage (McPherson and Cole, 2000). Therefore it is important to bear in mind the varying properties of $CO_2$ with temperature and pressure, in particular under supercritical conditions. In this thesis, the notation of $CO_2$ refers to the generic properties of $CO_2$, and not specific to its phase, unless otherwise noted.

## 2.2    Ideal Aquifers

Typical in-situ conditions for $CO_2$ storage in deep saline aquifers will be used as the framework for the selection of experimental design parameters. Deep aquifers suitable for the storage of GHG have specific characteristics as identified by van der Meer (1992), Gunter et al. (1993), Bachu et al. (1994), Holloway et al. (1996):

- aquifer should be located near the source of the $CO_2$, with large enough capacities to sequester significant volumes of $CO_2$;

- top of the aquifer should be below 800m, the point at which the $CO_2$ is above its critical state (in terms of pressure and temperature, Chapter 2.4) in most aquifers;

- storage of $CO_2$ above its critical state is desired since $CO_2$ resides in its most dense phase;

- region near the injection well should be relatively permeable to allow for high injectivity of $CO_2$; and

- **$CO_2$ is less dense than the surrounding pore fluid, and will migrate to the top of the aquifer, therefore a secure aquitard/cap rock must overly the aquifer to ensure safe entrapment of $CO_2$.**

## 2.3    Effect of Scale

Although laboratory values cannot be directly related to field conditions due to a difference in scale, they provide understanding of the fundamental processes which occur. However, it is important to mention the effect of scale on the measurements of diffusive flux, permeability and adsorption. Measurements in the laboratory reflecting the properties of varying size and/or time are not the same as in the field. Particularly in cap rocks, where the average value of flow and flux is not the critical parameter, but rather the weakest point of the cap rock is critical, indicating a potential for localized flow and possible release. Aside from errors associated with averaging,

importance of the effect of scale increases with materials that exhibit greater discontinuities, and heterogeneities (Schatz et al., 1993). Scale dependence of landfill liners, for instance, illustrates the importance of diffusion and flow properties determined in the laboratory and applied to the field. More specifically, migration of contaminants in clay liners can be successfully modeled for predicting field values if the soil liner system is nonfractured, homogeneous and geometrically simple (Crooks and Quigley, 1984). In argillaceous low permeability materials, the permeability can vary considerably, and laboratory values at similar porosities may vary by a factor of three orders of magnitude due to stratification resulting in permeability anisotropy (Neuzil, 1994a). The complexities associated with fractured, low porosity, heterogeneous cap rock seals suggest that scale effects will be significant.

The limiting factor within the laboratory is the thickness of the cap rock sample, as samples which are exceedingly thin can provide data which is not applicable, however, samples which are too thick will result in exceedingly long testing times. The lower limit of sample thickness for analysis of gas transport mechanisms is 1 cm (Rebour et al., 1997).

## 2.4    Cap rock Seals

Watts (1987) classified cap rocks into two categories based on the failure mechanism of the seal. Membrane seals refer to cap rocks whose sealing capabilities are controlled by its capillary pressure, whereas hydraulic seals refer to cap rocks which exhibit sufficiently high capillary entry pressures, such that the mechanical strength of the intact rock is compromised before fluid pressures reach the capillary displacement pressure. The latter is of more interest since it describes shales and evaporites, two classes of materials that have been proposed as cap rock lithologies for geological storage. Tissot and Pelet's work (1971), translated by Hedberg (1974), was likely the first to describe hydraulic seal failure. It was suggested that a hydraulic seal could only be broken if the pressure within the fluids, formed in the porous space of the rock matrix, increased to a point where the mechanical strength of the seal was exceeded. This resulted in the formation of microfissures allowing for hydrocarbon migration through the cap rock seal. Uncertainties remain around the mechanisms which promote the formation of microfractures in argillaceous materials, evidence of its formation are largely inferred by the behaviour of fluid pressures in reservoirs as described by leak off tests (Dewhurst et al., 1999).

Theoretically, any type of lithology can act as a cap rock. However, shales are the most common, and can range from tens to hundreds of metres in thickness. Cap rock lithologies, porosity, reservoir size, geometry, thickness, and local and regional continuity are important in determining the effectiveness of the seal. Inaccurate information regarding the cap rock

properties can and have resulted in incorrect assumptions about the sealing capability of cap rocks (Grunau, 1987). Cap rocks can retard the diffusion of gases, but even perfect seals (i.e. lacking the presence of faults, fissures, etc.) are unable to prevent their migration (Nelson and Simmons, 1995; Grunau, 1987). It has been shown that multiple sequences of anhydrite and clay-rich rock formations are very effective methods of sealing against gas leakage. Miocene Anhydrite cap rock in the Zagros Fold-Belt of Iran (Grunau, 1987), and the natural accumulation of $CO_2$ in the St. Johns Dome along the Arizona/New Mexico border in the USA (Stevens et al., 2001) are examples of securely stored reservoirs of gas overlain by a complex sequence of cap rocks. Multiple sealing sequences may be inadequate in areas of high tectonic activity, and areas of increasing formation of fractures.

Cap rock thickness is an important parameter in providing confidence about the integrity of a hydraulic seal, since the probability of a continuous seal is greater with increasing cap rock thickness. Although a few inches of shale is theoretically thick enough to provide an adequate seal, it is unlikely that such a thin layer would be continuous and/or unbroken over the length of the reservoir or aquifer. In general, for hydraulic membranes, thicknesses exceeding 50m in areas of low tectonic activity are considered good (Grunau, 1987). The greater the thickness, the more likely a secure, unbreached seal would be provided by a shale formation.

Despite the high capillary pressure present in shales, diffusion across the cap rock cannot be prevented as long as a potential chemical gradient exists across the cap rock seal. Rate of diffusion through the shale can be considerable, and is dependent on its composition and physical properties. It has been suggested that there is greater diffusion through shale cap rock than through evaporite cap rock (Grunau, 1987).

Sealing characteristics of cap rock have not been proven to be predictable (van der Meer, 1992), and physio-chemical processes (formation, dissolution, and diagenesis of cap rock materials) related to its integrity remains to be addressed (Krom et al., 1993). Importance of transport mechanisms in oil and gas fields related to potential hydrocarbon losses through aquitards has received some attention (Watts, 1987; Grunau, 1987; Rostron, 1993), but the quantities of gas lost over time through cap rocks have been disputed (Leythaeuser et al., 1982; Krooss et al., 1992a; Krooss et al., 1992b; Nelson and Simmons, 1992; Krooss and Leythaeuser, 1997; Nelson and Simmons, 1997). Physical transport mechanisms through water saturated low permeability materials, such as cap rocks, are not well understood.

## 2.5    Clearwater Clay Shales

Cretaceous age clay shales used in this research program were collected from Northeastern Alberta, near Fort McMurray, in the Western Canadian Basin. These samples were collected at a depth of approximately 350m, in the Clearwater formation, which is a shallow marine deposit. Samples were obtained using a triple tube wire core. Ends of the core were sealed with polyethylene ends, and heat shrinked to the core barrel. The sealed core was placed inside a larger diameter core barrel, and sealed again.

These materials are heavily overconsolidated, consisting of uncemented clay shales, clay silts, and lenses of fine grained sands, and indurated siltstone layers. The Clearwater formation extends through a great part of Alberta, and appears at various depths throughout the Western Canadian Basin. As it changes in depth, its pore fluid chemistry and mineralogy also vary.

### 2.5.1    Alberta Basin

Two basins, Alberta and Williston, which are separated by the Sweetgrass Arch make up the Western Canadian Basin. The majority of oil and gas production in Canada comes from the Alberta Basin, which is also rich in coal resources. It covers an area of 0.8 million $km^2$, containing a volume of about 2 million $km^3$ (Mossop and Shetsen, 1994). The Alberta basin consists of a wedge, which tapers from a maximum thickness of about 6000 m east of the foothills front to a zero-edge in the northeast along the Canadian Shield, (Figure 2.2).
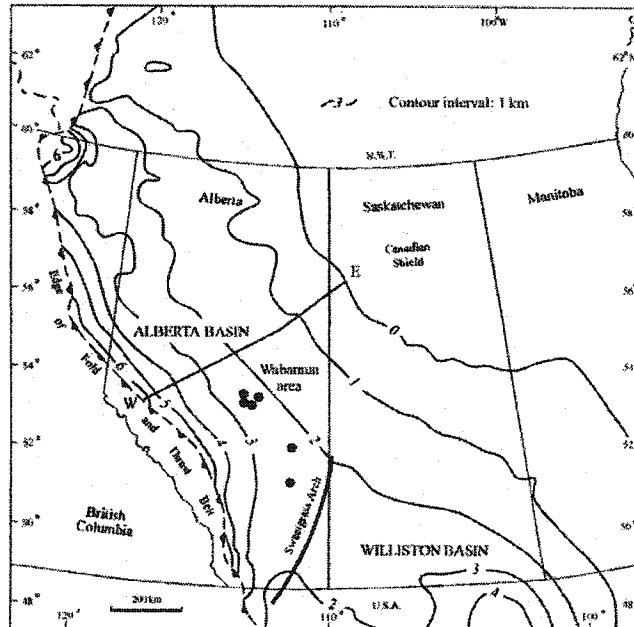
**Figure 2.2: Alberta Basin**
**(modified from Bachu et al., 1994)**

Lithology and geometry varies considerably throughout the basin. The Geological Atlas of the Sedimentary Basin (Mossop and Shetsen, 1994) describes in much greater detail the geology, history, and characteristics particular to this region. Groundwater flow in this region has velocities estimated to be in the order of 1-10 cm/year (Bachu et al., 1994).

*2.5.2    Sampling and Core Handling*

The core material was placed inside a constant temperature, moisture controlled environment following extraction, and remained in its sealed barrels until core logging commenced. Logging of the cores involved the extraction of the core from the two barrels, and the inner barrel was carefully split in half by a hand saw. Following the opening of the core, it was immediately logged (Figure 2.3, and in Appendix E), followed by the extraction of samples for various analyses, and the preservation of intact core sample for further testing. Sample preservation included wrapping the samples in plastic stretch wrap, cheesecloth, and carefully waxed. All samples were stored in a constant temperature, moisture controlled environment. Sample logging and preservation was performed as quickly as possible, as desiccation of the clay shale material was a concern.

| Depth (cm) | DS (mm) | DP (m) | Roughness | Description | Observations | | |
|---|---|---|---|---|---|---|---|
| Sec 1 0-14cm | | | | Sec1-dk clay shale fairly intact, some sand. | Sand Inclusion | | 0 4 8 12 |
| Sec 2 14-24cm | | | | Sec2-intact, but some fissures. | | | 16 20 24 |
| Sec 3 24-32cm | | | | Sec3-highly fissured clay shale in both directions. | | m.c. 2 | 28 32 36 |
| Sec 4 32-49cm | | | | Sec4-fissured clay shale. | | | 40 44 48 |
| Sec 5 49-54cm | | | | Sec5-highly fissured clay shale. Sec6-relatively intact material. | | | 52 56 60 |
| Sec 6 54-70cm | | | | Sec7-stiff intact clay shale. Sec8-highly fissured. | | | 64 68 72 |
| Sec 7 70-88cm | | | | Sec9-layered look, relatively intact. Sec10-highly fissured crumbly. | | | 76 80 84 |
| Sec 8 88-94cm | | | | Sec11-highly fissured Sec12-highly fissured clay looks layered. | | m.c.1 | 88 92 96 |
| Sec 9 94-100cm | | | | | | | 100 104 108 |
| Sec 10 100-103cm | | | | | | | 112 116 120 |
| Sec 11 103-119cm | | | | | | | 124 128 132 |
| Sec 12 119-145cm | | | | | | A.L. | 136 140 144 |

**Figure 2.3: Logging information**

### 5.2.1 Sample Mineralogy

Scanning electron microscope (SEM), transmission electron microscope (TEM), x-ray diffraction (XRD), and x-ray fluorescence (XRF) were used to determine the mineralogy of the clay shale. The SEM/TEM analysis found examples of quartz, mica, feldspars, and illite in the sample. Although quantitative determination of the minerals is not possible with this SEM analysis, it did suggest that there was an abundance of mica mineral. Carbonates (Dolomite), pyrite, various mica (muscovite, sepiolite) and feldspar (sanidine, albite) minerals were all present in the SEM analysis. Figures 2.3 and 2.4 provide two images for the SEM analysis of the uniform clay shale stratigraphy, as expected since marine deposits have not been altered by diagenesis or tectonic forces (Issac et al., 1982).

13
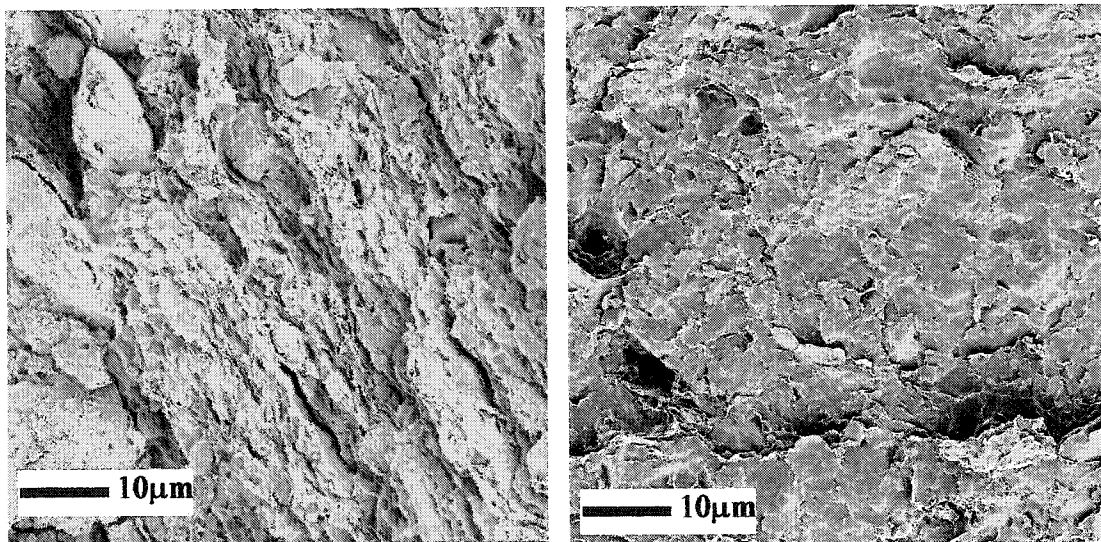
Cross Sectional View                              Plan View

**Figure 2.4: SEM Analysis 1500X Magnification**
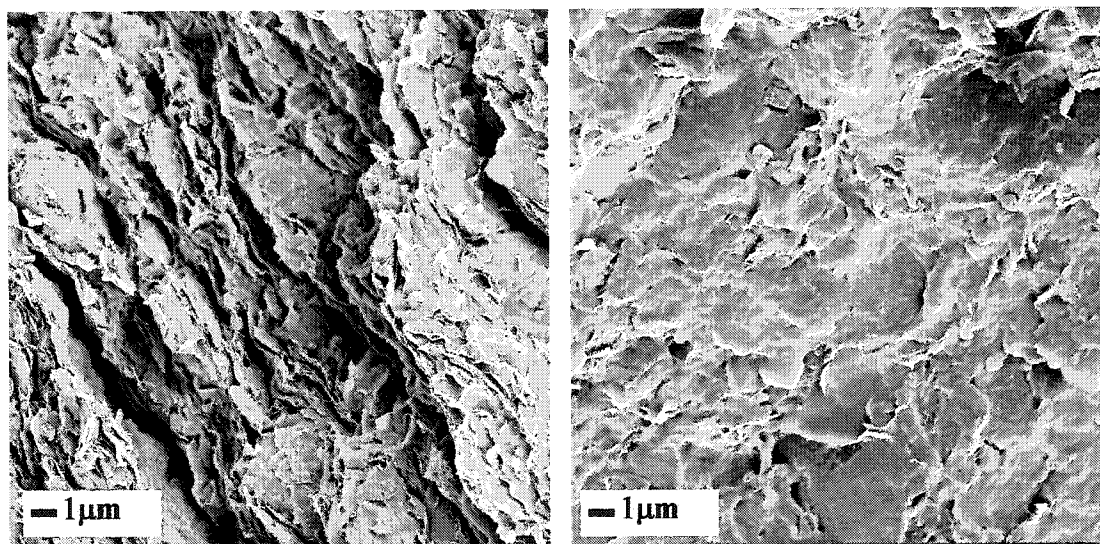


Cross Sectional View                              Plan View

**Figure 2.5: SEM Analysis 4000X Magnification**

Both XRD (University of Alberta) and XRF (University of Western Ontario) were used to determine the clay mineralogy. Quartz, muscovite, sepiloite, kaolinite, dolomite, pyrite, sanidine, and albite were identified by XRD, however quantitative amounts were unavailable. Sanidine is a potassium feldspar, and albite is a sodium feldspar. Muscovite is a mica mineral. The XRF analysis is summarized in Table 2.2, where LOI is loss on ignition.

14

**Table 2.2: X-ray Fluorescence Data**

| Oxides | $SiO_2$ | $TiO_2$ | $Al_2O_3$ | $Fe_2O_3$ | MnO | MgO | CaO | $K_2O$ | $Na_2O$ | $P_2O_5$ | L.O.I. | Total |
|--------|---------|---------|-----------|-----------|-----|-----|-----|--------|---------|----------|--------|-------|
| wt% | 62.06 | 0.74 | 16.82 | 5.24 | 0.03 | 2.28 | 0.96 | 2.42 | 1.62 | 0.14 | 7.02 | 99.34 |

Semi-quantitative XRD performed by AGAT Laboratories indicated that smectite and illite were the dominant clay minerals. Quartz ($SiO_2$) and kaolinite were also found in lesser quantities. Bulk fraction of the sample was 28.2%, and the remaining 71.8% was clay-sized fraction (<3μm as defined by the test analysis performed by AGAT Laboratories). Of the bulk fraction 50% was quartz, and the other 50% was a split of illite and smectite (21% and 29% respectively). In the clay-sized fraction smectite was the dominant clay mineral (46%), illite and kaolinite were found in quantities of 34% and 17% respectively, and the quartz accounted for the remaining 3%. It was determined that 84% of the sample was clay mineral sized. Smectitic clays present were determined to be freshwater sensitive, which was apparent upon the addition of distilled water. The addition of distilled water resulted in significant swelling of the clay shale, and swelling pressures as large as 5MPa have been previously determined for these class of materials (Golder Associates, 1981). Lack of other minerals, detected by non-quantitative XRD test suggests that feldspar, mica and dolomite minerals are in minor quantities, but it is likely to be sample dependent.

*2.5.4    Physical Attributes of Samples*

The high plasticity index, ~ 65%, obtained from the Atterberg limits (ASTM D 4318) is consistent with mineralogy, indicating a mixture of clay minerals. Indications of montmorillonite interlayered with illite can be identified by SEM (Figure 2.5). The grain size distribution was determined using a hydrometer (ASTM D 422) (Figure 2.6). The clay shale is dominated by clay fraction (<2μm) material (60%), and the remainder is silt sized (>2μm) particles. There were no particles in the sand sized range. The specific gravity of the clay shale was determined to be 2.84 (ASTM D 854). Porosity of the samples were approximately 15%. The natural moisture content of the shale ranged from 18.5% to 21% (ASTM D 2216).
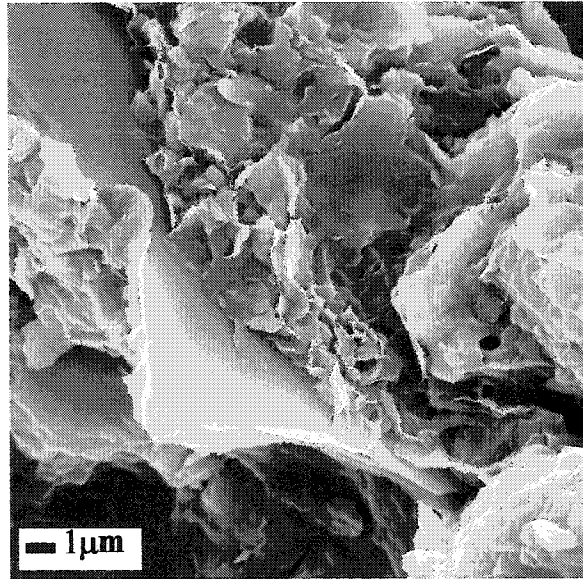
**Figure 2.6: SEM Photographs illustrating Clay Mineralogy**
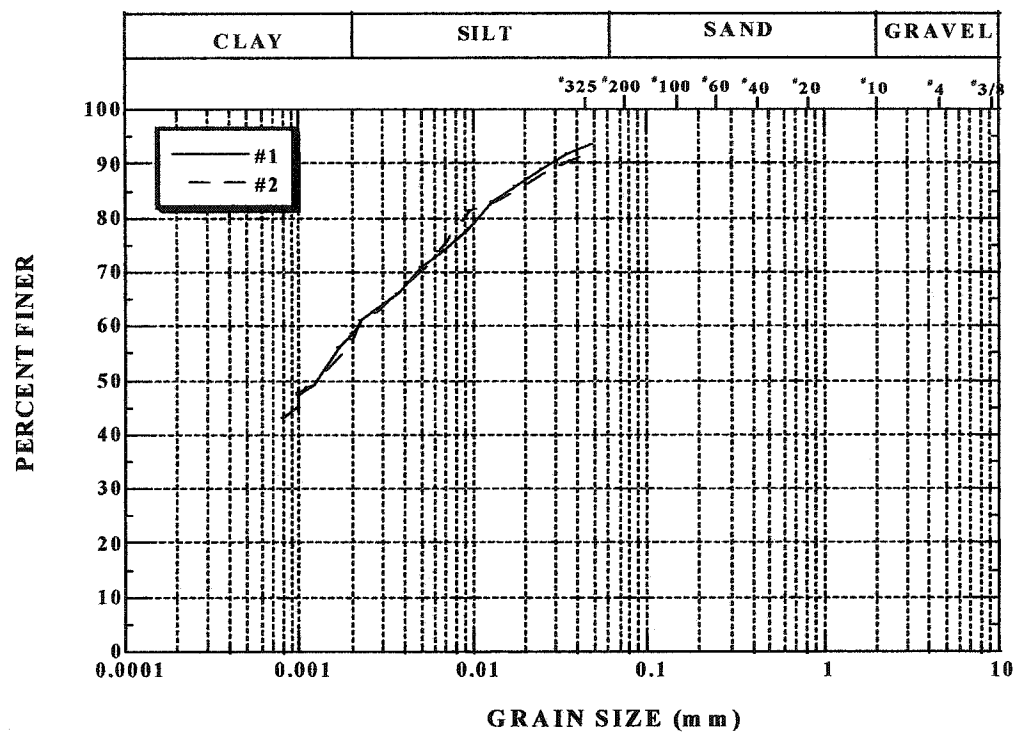


**Figure 2.7: Grain Size Distribution for Clay Shale from the Clearwater Formation**

Illite is the dominant clay mineral in stiff clays and shales (Grim, 1968, Terzaghi et al., 1996). Younger shales or shales of the Mesozoic age may have a significant component of smectitic clays (Grim, 1968). The Clearwater Formation reaches near surface in northeastern Alberta where oil sands in the McMurray Formation are heavily mined. It makes up a great proportion of the overburden during oil sands surface mining near Fort McMurray, Alberta. The Clearwater Formation is broken up into seven subsets, each with differing mineralogy, and physical properties (Issac et al., 1982) (Table 2.3).

**Table 2.3: Clearwater Formation Properties**

| Geologic Unit | Grain Sizes<br>% Sand/Silt/Clay | Clay Fraction Mineralogy<br>% chlorite/illite/kaolinite/smectite | Atterberg Limits<br>$W_L\%$ $W_p\%$ $I_p\%$ | Natural Moisture<br>$W_N\%$ |
|---|---|---|---|---|
| Kcd | 20/53/27 | 21/39/28/12 | 56/19/37 | 20.5 |
| Kcc | 2/53/45 | 15/50/15/20 | 61/22/39 | 18.0 |
| | 1/61/38 | | | |
| | 0/50/50 | 15/40/10/35 | 101/31/70 | 22.7 |
| | 0/60/40 | 15/50/20/15 | 74/23/51 | |
| Kcb | 7/47/46 | 15/55/15/15 | 58/22/36 | 16.6 |
| | 4/37/59 | 5/30/0/65 | 156/37/119 | 33.3 |
| | 8/46/46 | 10/45/10/35 | 76/22/54 | 18.4 |
| **Kca** | 2/45/53 | **5/45/10/40** | 122/30/92 | 20.9 |
| | **0/56/44** | | **92/27/65** | **18.5** |
| Kcw | 30/47/23 | 5/50/5/40 | 46/21/25 | 14.3 |
| | | 10/50/0/0 | | |
| | | 5/30/10/55 | | |
| **Samples** | **0/40/60** | **0/34/17/46** | **~ 96/33/62** | **18.5 - 21** |

(Issac et al., 1982)

Grain size distribution, moisture content, and Atterberg limits from the Kca subset are very similar to the results of the clay shale from the Clearwater formation obtained for these experiments. Mineralogy of clay shale cores as determined by AGAT Laboratories is also similar. Material obtained here is believed to be clay shale from the Kca subunit. The Kca subunit lies above the Kcw, and is directly underlain by the McMurray formation. It is characterized as a grey black, fissile, silty clay shale.

Chlorite, in small amounts, is normally associated with micas and illite (Grim, 1968). The smectite in the clay shale is likely montmorillonite, which is dominant in some clays and shales

(Grim, 1968). The presence of mixed clay mineral layers consisting of water bearing layers and contracted non-water bearing layers are not unusual, particularly in marine or lacustrine clay deposits. The most common being regularly alternating montmorillonite-illite particles (Figure 2.6) (Mitchell, 1993).

### 2.5.6    *Fissility*

The clay shales from the Clearwater formation, particularly from the Kca subunit, are characterized as gray-black, fissile, silty clay shales. Upon analysis, it was evident that the material contained many discontinuities. Improper storage, handling, sample preparation, and/or experimental setup would result in sample desiccation and disturbance, leading to erroneous data in the laboratory. To best avoid this in the laboratory, special measures are required to ensure the quality of the specimens being tested.

Although the stages of sample storage and preparation were important, it was also essential that the design of the apparatus which houses the specimen be particularly gentle on the sample to prevent the opening of fissures and discontinuities upon setup.

### 2.6    Clay-Water System

Understanding the complex nature of clay-water systems is important in assessing the transport of gases through initially water saturated clay materials. Behaviour of water in clays is quite different from its behaviour in non-clay materials, and therefore further discussion is warranted.

Due to the complex behaviour between water molecules, and clay mineral surfaces, it is not uncommon for clayey materials to be sensitive to its pore fluid chemistry, especially smectitic clays. Various theories, most notably the Guoy-Chapman and Stern models, describe the distribution of ions and water molecules along the surfaces of clay minerals (van Olphen, 1977; Mitchell, 1993; Horseman et al., 1996). Unlike non-clay materials, the term water does not simply refer to free water in the pore space. Rather, water in clays is distinguished by its position relative to the surface of the clay mineral. There are four types: interlayer, structured, diffuse layer, and free water. Interlayer refers to water present within the clay mineral structure. Structured water refers to water that is strongly adsorbed to the clay surface, and in hydrated shells of the Stern layer cations. As water molecules move away from the surface of the clay mineral, it becomes less strongly attracted to the mineral surface, this loosely held water is known as the diffuse layer. Free water resides in the porous space, and is the water which participates in fluid transport. Various mechanisms, hydrogen bonding, hydration of exchangeable cations,

attraction by osmosis, charged surface-dipole attraction, and attraction by London dispersion forces, have been used to describe the interaction between clay minerals and water, and the various types of water (Mitchell, 1993).

Classical theories of clay-water systems suggests that the layer of adsorbed water next to the clay mineral surface has a different structure, density, and viscosity than the normal pore water (Grim, 1968; Craig, 1987). It is the dipole character of the water molecule, which results in the initially adsorbed water molecules. The positive side of the water molecule is attracted to the negative charge of the clay mineral surface. Adsorbed water is able to move parallel to the clay surface, but the movement perpendicular to the mineral surface is restricted.

Cations present in the water will also be attracted to the clay mineral. Since the cations are not held strongly by the clay mineral, they can thus be replaced by other cations (cation exchange). In general, clays will preferentially hold multivalent cations over monovalent cations. A dispersed layer forms adjacent to the particle, cation concentration decreases with increasing distance from the surface until the concentration becomes equal to the normal water in the void space. The distribution of the cations on the negatively charged particle is known as its double layer, and its thickness is dependent on the valence and the concentration of the cations. Increasing the valence or an increase in the concentration will result in a decrease in the thickness of the layer. Temperature will also affect the double layer thickness, as increasing temperature will decrease the layer thickness. Diffuse double layer (or electric double layer, EDL) in a clay system is illustrated in Figure 2.7. Aside from the changes to the EDL, presence of ions disrupt the normal water structure, due to an occupation of space or by hydration of the ions by water (Mitchell, 1993).
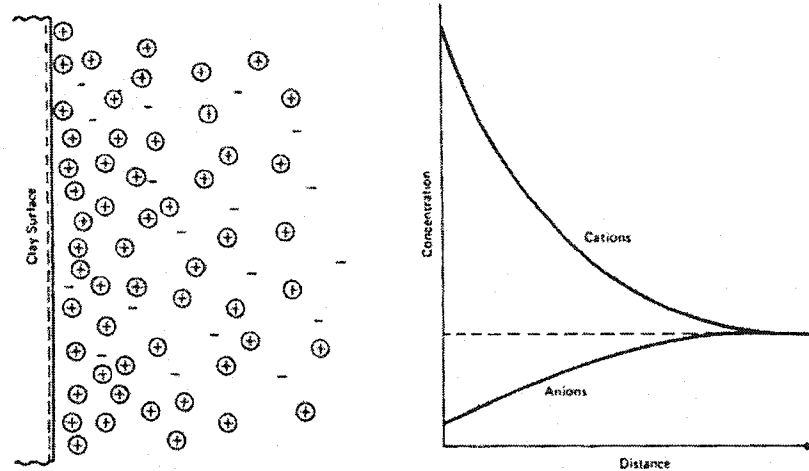
**Figure 2.8: Distributions of ions according to the theory of diffuse double layer**
(modified from Mitchell, 1993)

## 2.7    Transport Processes

### 2.7.1    Gas Diffusion

Migration of gases can occur slowly through a process known as molecular diffusion, in the absence of a pressure gradient, but in the presence of a chemical gradient (Cunningham and Williams, 1980; Cussler, 1997), which can result from temperature, pressure, fluid composition, and/or electrical field gradients (Rebour et al., 1997). In geological storage of GHG, a concentration gradient will exist on the lower boundary of the cap rock (Figure 2.8).
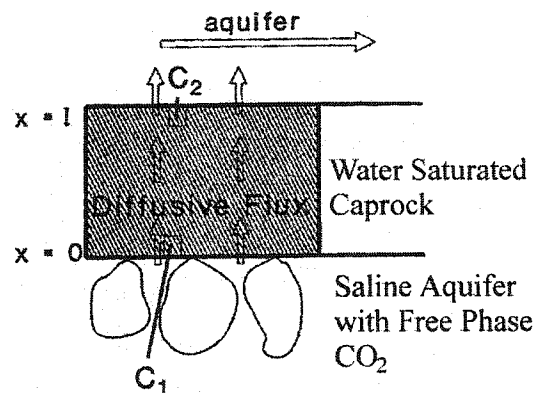


**Figure 2.9: Diffusion through Cap rock**
(modified from Krooss et al., 1998)

20

Fick's second law describes unsteady state, transient diffusion, as the rate of change of the concentration with space and time (Equation 2.1).

$$\frac{\delta C}{\delta t} = D \frac{\delta^2 C}{\delta x^2}$$

(2.1)

It refers to a general situation, where the diffusion occurs across a homogenous medium (i.e. water). However, in a heterogeneous system, such as geological material, modifications to Fick's law are required to account for the fractional volume in which diffusion occurs (i.e. volume occupied by water in the porous space, rather than the volume of the entire specimen). The solution of Equation 2.1 for the boundary condition (Figure 2.8) $0 \leq x \leq 1$, C $(x > 0, t = 0) = 0$, and C $(x = 0, t \geq 0) = C_1$ is given in Crank (1975), modified for a heterogeneous system (Equation 2.2) (Rebour et al., 1997),

$$C_2(t) = \frac{\omega S L C_1}{V_2} \left[ \frac{D_a t}{L^2} - \frac{1}{6} - \frac{2}{\pi^2} \sum_{n=1}^{\infty} \frac{(-1)^n}{n^2} \exp\left( \frac{-\pi^2 n^2 D_a t}{L^2} \right) \right]$$

(2.2)

where $\omega$ is the porosity, S is the cross sectional area, $V_2$ is the volume, L is the length, $C_1$ is the concentration, $D_a$ is the apparent diffusion coefficient, and t is the time. The apparent diffusion coefficient is the fractional reduction in the diffusion coefficient due to the tortuosity of the porous media ($\psi$), as defined by Equation 2.3),

$$D_a = \psi D_w$$

(2.3)

where $D_w$ is the diffusion coefficient for the saturating media, water. Typical values of $\psi$ for nonadsorbed ions in the laboratory are between 0.5 and 0.01 (Freeze and Cherry, 1979). Approximation from the quasi-steady state portion of the concentration-time graph, $D_a$ can be determined from its slope (Figure 2.9). The disadvantage of this approach is the extremely long testing times required to achieve quasi steady-state. Alternatively, in the limit as time goes to infinity, Equation 2.2 reduces to Equation 2.4,

$$C_2(t) = \frac{\omega S L C_1}{V_2} \left[ \frac{D_a t}{L^2} - \frac{1}{6} \right]$$

(2.4)

which allows the diffusion coefficient to be estimated from the slope of a concentration/time curve, after a time which is long compared to $\left( \frac{\pi^2 n^2 D_a}{L^2} \right)^{-1}$. For a diffusion coefficient

of $1 \times 10^{-12}$ $m^2 s^{-1}$, and a sample thickness of 10mm, testing time in the order of 1.6 years will be required for a linear concentration/time profile to develop, if the porous volume divided by the outlet volume ratio is less than 0.15 (Jenkins et al., 1970). Analysing the initial stages (transient) of diffusion requires much less time, but it is crucial that measurements of very low concentrations of gas be determined (Crank, 1975; Rebour et al., 1997). Apparent diffusion coefficients as low as $2 \times 10^{-12}$ $m^2 s^{-1}$ can be determined within a month on a 1 cm thick sample, by analyzing the initial transient portion of diffusion (Rebour et al., 1997).
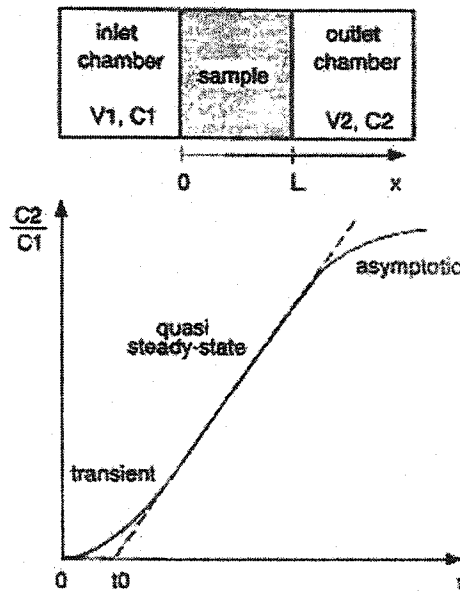
**Figure 2.10: Stages of Diffusion**
(modified from Rebour et al., 1997)

In general, two types of diffusion cells have been used to test gas diffusion in geological materials, ones which do not apply a lateral confining stress (Humé, 1993; Mackay et al., 1998), and those which are capable of providing triaxial stresses (Rebour et al., 1997; Schlomer and Krooss, 1997). The pressure rating of diffusion cells vary from atmospheric conditions (Krooss and Schaefer, 1987) to 20MPa (Rebour et al., 1997). Sealing mechanisms have been as simple as o-ring sealed devices to crimping of soft lead shim to the end cap by the confining pressure. Very thin metal shim wrapped and/or thin metal tubing has also been used to prevent the migratory effect of gas from the specimen into the confining fluid. Downstream gas analysis is typically performed with analytical units, either gas chromatographs or commercially available gas leak detectors, and often with automatically sampled systems. The lag time method of determining diffusion is the most common, which is the experimental determination of the time lag ($t_o$), from

the x-intercept of Equation 2.4. The $D_a$ can then be determined from the expression, $D_a = \dfrac{L^2}{6 \cdot t_o}$.

Of these experimental setups, the most suitable for the replication of in-situ field conditions places a sample between two end caps, held together by an adjustable strap (Rebour et al., 1997). Thin lead shim is crimped around the sample to prevent diffusion of gases radially from the specimen. The device, illustrated in Figure 2.10, is then fixed inside a confining pressure cell.
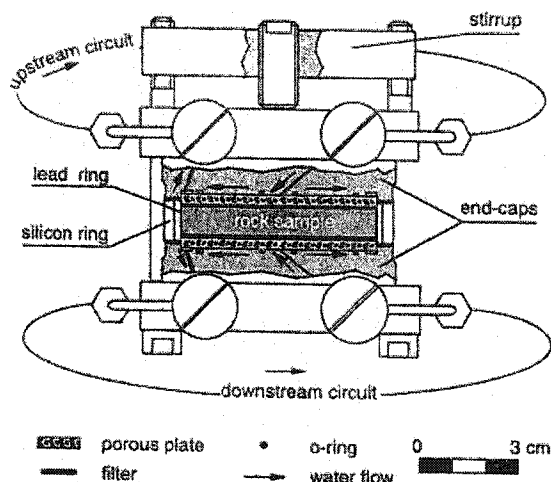


**Figure 2.11: Diffusion Cell Rebour et al., 1997**

Gas diffusion is a function of both the porous medium and gas properties. It is largely controlled by the pore space of the rock matrix (Katsube and Walsh, 1987), and the dissolution of the gas into the pore space. Increase in the porosity has been shown to increase the diffusion, (Krooss et al., 1998), however the correlation between the diffusion coefficient and rock porosity is not simple (Krooss and Leythaeuser, 1988). Decreasing porosity results in a greater restriction of the pore throat diameters, and thus has a greater influence on the flow of molecules. As the pore diameter decreases, the resistance at the molecule-wall interface increases due to greater collisions, which creates a decrease in the flux (Cunningham and Williams, 1980). As the porosity increases towards one, diffusion approaches the diffusion in water at the same temperature (Krooss and Leythaeuser, 1988). Restrictions in the pore space affect the rate of diffusion based on the size of the molecule diffusing, decreasing diffusion with decreasing molecular mass, due to the porous space acting as a sieve inhibiting the movement of larger molecules (Krooss and Leythaeuser, 1988). Diffusion is also subjected to the tortuous pathways, as well as electrostatic and size exclusion processes along the media walls, that can be affected by interactions between the water and clay minerals (Rebour et al., 1997). Thus, volume available

can be a percentage of the total porosity due to these processes, resulting in a restriction of ion diffusion into the available pore space. Generally, total porosity is not as applicable in tight clay-rich sediments as it is in coarser-grained rocks, since clays exhibit smaller interconnected pore spaces relative to fluid molecule sizes and other dissolved species (Pearson, 1999). The term diffusive or effective porosity is generally used to describe the porosity available for transport processes to occur. The influence of porous network, and tortuosity has a greater influence than the total porous volume.

A variety of factors will influence the diffusion of gases in shale materials. Temperature effects can be quite pronounced in diffusion (Thomas and Frost, 1980; Rebour et al., 1997) due to the expansion properties of gases with varying temperature. Pressure can be influential, as changes in pressure affect the solubility characteristics of $CO_2$ in water, and therefore will also affect the rate of diffusion (Krooss and Leythaeuser, 1988). It is important to measure diffusion under the appropriate in-situ stress conditions, as increases in the effective stress will result in a decrease in the effective diffusion coefficient, as illustrated with $N_2$ and $CH_4$ (Krooss and Leythaeuser, 1988). Stress-related changes in diffusive effects is thought to be a result of increased pathway tortuosity and decrease in the diffusive porosity, resulting in a reduction in gas mobility (Krooss and Leythaeuser, 1988; Pearson, 1999). Slower diffusive fluxes can occur in the presence of cementing agents, and therefore mineralogy plays a role in gas diffusion. Carbonates act as intergranular cement which prevents the diffusion into parts of the pore structure. Thus increasing carbonate content, and other cementing agents such as free silica will decrease diffusion (Thomas and Frost, 1980). Increasing pore fluid salinity results in a decrease in the rate of diffusion, as a result of increased viscosity of the pore fluid (Krooss and Leythaeuser, 1988).

Another possible mechanism of transport deals with the osmotic movement of $CO_2$, as generated by a potential chemical gradient across the cap rock. The significance of osmotic transport in geologic materials has been debated due to the poor understanding of its material properties (Neuzil, 2000). There is evidence which suggests that osmosis can occur in geologic materials under differing chemical potentials in the pore water (Neuzil, 2000). Greater details concerning the theories associated with osmotic potentials, and their impact on transport within geologic materials is described in the Petroleum Research Corporation report (1958).

### 2.7.2 Relative Permeability

Flow of fluids in porous media follows Darcy's law (Equation 2.5), where k is the permeability, $\rho$ is the density of the fluid, $\mu$ is the viscosity of the fluid, v is the apparent or Darcy

velocity, g is gravity, and dh/dl is the hydraulic gradient (Fetter, 1993). The application of Darcy's law in multiphase flow requires that each fluid obeys Darcy's law for the porous space in which it occupies. Known as the relative gas permeability theory, it suggests that partial displacement of water within the pore space occurs by the incoming gas phase. Following a modified Darcy's law (Equation 2.6), where the subscript nw represents the non-wetting fluid, $CO_2$ in this scenario, $k_i$ is the permeability of the rock matrix (Fetter, 1993).

$$v = -k \frac{\rho g}{\mu} \frac{dh}{dl} \tag{2.5}$$

$$v_{nw} = \frac{k_{rnw} k_i \rho_{nw}}{\mu_{nw}} \frac{dh_{nw}}{dl} \tag{2.6}$$

The term permeability (k) can be confused with the term hydraulic conductivity (K). Hydraulic conductivity is dependent on the properties of both the porous medium and the fluid properties, and has by the dimensions of length per time. Permeability is an intrinsic property of the porous medium, and has the dimensions of length squared. The two terms are related by equation 2.7, with $\rho$ and $\mu$ as a function of temperature.

$$K = k \frac{\rho g}{\mu} \tag{2.7}$$

Displacement of water is dependent on the size of the pore throats, intrinsic permeability, and the interfacial tension between the fluids, the influencing factors on displacement pressure. Displacement pressure, or capillary threshold pressure, is the difference between the gas pressure and the pore water pressure, and describes the force required for gas to enter the porous space. Once capillary displacement pressure is exceeded, flow of the non-wetting phase will occur by two phase Darcy flow (Ingram et al., 1997; Schlömer and Krooss, 1997; Hildenbrand et al., 2002). According to Darcy's law modified for multiphase flow, the effective gas permeability (or relative gas permeability) will be lower than the permeability of a single phase. This is a result of greater competition for the available porous space. Influx of the gas phase occurs as a result of expulsion of the water phase, according to Darcy's law.

However, applicability of Darcy's law for multiphase flow in tight, low permeability clay rich materials is heavily disputed, due to the extraordinarily high capillary threshold pressures which exist in these hydraulic seals, as discussed in section 2.3.

In low porosity clay sediments, the majority of water molecules are strongly adsorbed to the clay mineral, and little water is available in the free phase (section 2.6). Water molecules closer to the clay surface are more strongly occluded to the mineral, due to their hydrophilic nature. As dewatering takes place closer to the adsorbed layer, greater gas pressure is required to displace this water, and often requiring pressures which are significantly greater than the overburden stress (Figure 2.11). Thus, the displacement of water due to the influx of gas is difficult.
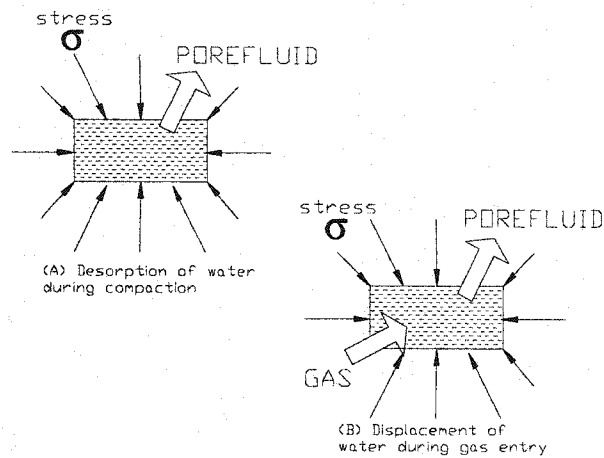


**Figure 2.12: Desorption of Water from Compact Clays**
(modified from Rodwell et al., 1999)

Due to the complex behaviour of surface bound water in clays, and the distribution of ions and water molecules along the surfaces of clay minerals, growing consensus suggests that it is improbable that gas migration will occur with desaturation of the water phase (Rodwell et al., 1999; Harrington and Horseman, 1999; Gallé, 2000). Any measurement of relative gas permeability in low permeability clay shales is likely to occur only in highly fractured media. High gas pressures may lead to the development or reopening of existing discontinuities, resulting in gas flow by an increase in the overall volume. Presence of discontinuities is currently believed to play an important role in the migration characteristics of this class of materials, as it seems unlikely that gas will migrate by relative permeability. However, this is debated, as gas permeability measurements in water saturated, low porosity, clay-rich materials have been achieved (Hildenbrand et al., 2002).

Typical methods of determining permeability in soils and rocks are based on Darcy's law, where the coefficient of permeability can be measured based on the hydraulic gradient and quantity of flow, knowing the cross-sectional area. These methods generally refer to the constant head permeability test (for permeable materials), and the falling head permeability test (for low

permeability soils) (Head, 1982). These methods are not suitable for the determination of extremely low permeabilities (as expected in clay shales), or relative gas permeabilities. Constant flow techniques have been capable of measuring permeabilities as low as $10^{-22}m^2$ (Krooss et al., 1998), but are suitable only under low confining stresses. Measurement of water permeability in low permeability materials can be done for tight shales exhibiting permeabilities as low as $7x10^{-22}$ $m^2$ (Katsube et al., 1991). Permeability of tight rocks, such as shales, is strongly dependent on the effective stress of the sample, as illustrated in Figure 2.12, where permeability decreases with increasing effective stresses (Katsube et al., 1991; Schlömer and Krooss, 1997; Krooss et al., 1998). The effective stress-permeability relationship is lithology dependent (Schlömer and Krooss, 1997).
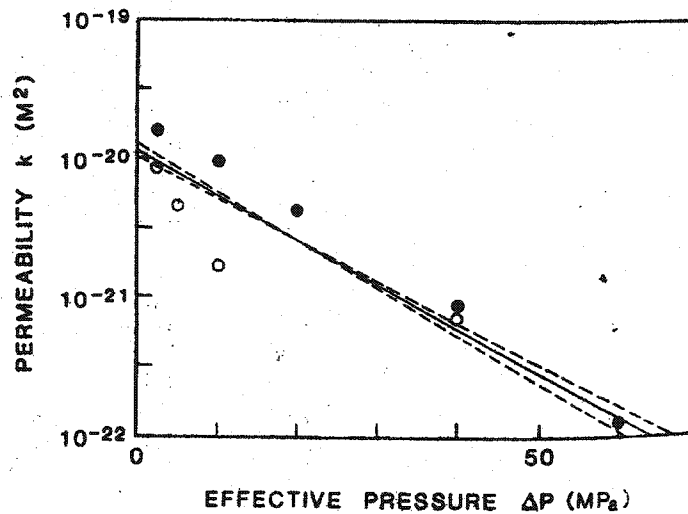


**Figure 2.13: Vertical Permeability as a Function of Effective Stress**
(modified from Katsube et al., 1991)

Extremely low permeabilities (around $10^{-24}$ $m^2$ under a hydrostatic confining pressure of 10 MPa) have been measured by utilizing a pressure pulse technique (Brace et al., 1968; Hsieh et al., 1981; Neuzil et al., 1981). A less desirable method, because it is unable to account for fracture permeabilities, is the degassing technique (Schettler and Parmely, 1991). Degassing rock samples are placed under equilibrium conditions at a known pressure, the pressure is dropped in a step-wise manner, and the rate of gas produced is calculated as a function of time.

Experimental systems put in place to investigate relative gas permeability has some similarities to diffusion cells. Odeometer type setups have been used (Gallé, 2000), as well as

27

isotropic environments (Harrington and Horseman, 1999), and triaxial-type, where a controlled application of the axial stress is unavailable, and thus may not result in an isotropic environment (Schlömer and Krooss, 1997). However, more recent advances to the experimental setup by Schlömer and Krooss (1997) have resulted in a controlled application of axial stresses (Hildenbrand et al., 2002). Determination of gas transport properties utilizing isotropic confining stresses during gas injection is currently the bested suited experimental design at determining relative gas permeability measurements (Harrington and Horseman, 1999). Samples are sealed by means of a copper or Teflon heat shrink membrane. Tapered end caps and hose clamps are used to secure the membrane, as illustrated in Figure 2.13.
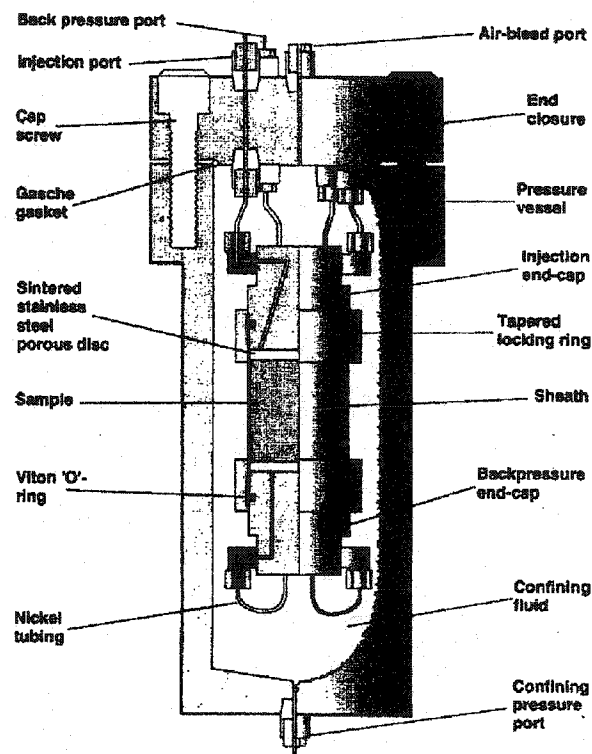


**Figure 2.14: Triaxial Setup by Harrington and Horseman (1999)**

Parameters and processes which influence gas migration through clay-rich rocks include porosity, pore size distribution, surface adsorption, capillary entry pressure, matric suction, stress history and total and effective stress (Rodwell et al. 1999). Pore throat size is related to its stress history, and maximum burial depth. Equivalent pore size radii were shown to significantly vary with interfacial surface tension and wetting angle of the two fluids, in this case $CO_2$/water and $N_2$/water (Hildenbrand et al., 2002). Low permeability mudstones, shales, and other clay rich, heavily overconsolidated materials will exhibit extraordinarily high displacement pressures due to its tight porous structure. Harrington and Horseman (1999) conducted gas flow experiments in

water saturated Boom clay under uniform and isotropic stress conditions, and high gas pressures. Exceedingly high gas pressures required for gas injection resulted in high pore pressures, which caused the sum of the effective stresses and pore pressure to exceed boundary stresses. An unbalanced internal tension was imposed on the clay fabric resulting in preferential gas pathways, as a result of hydrofracturing. Gas pathways tended to propagate along the bedding planes in naturally sedimented material, and gas breakthrough pressures were generally lower in samples that were parallel to the bedding rather than normal to the bedding. In reconstituted materials, where there is no oriented fabric, gas pathways tended to propagate normal to the minor principal stress, and a trend indicating gas pathways formed in the direction of the maximum stress gradient was also observed.

Although gas transport in low porosity clay-rich materials has been studied previously (Horseman et al., 1996; Gallé, 2000), a consensus on its behaviour has not been reached (Hildenbrand et al., 2002), and thus investigations into understanding gas migration behaviour is on-going (Rodwell et al., 1999).

*2.7.3  Gas Adsorption*

Determination of gas adsorption on solids has been categorized into dynamic (thermal-desorption) and static (volumetric, gravimetric) methods. Dynamic methods are generally employed at low pressures, and typically use a non-adsorbing carrier gas, which is flowed continuously throughout the experiment. Static methods involve successive doses of gas brought in contact with the absorbent. Gravimetric methods determine the amount of gas adsorbed through the determination of the change in weight before and after adsorption. This method requires an accurate and sensitive balance to achieve a level of accuracy in adsorption measurements. Advantages of gravimetric methods are shorter experimental time, and direct measurement of gas adsorbed. However, shales will adsorb much less than traditional absorbents, and therefore small errors associated with the sensitivity of the balance can result in significant errors.

The most common method of determining the adsorption capacity of materials with low adsorption capacity is by the volumetric test method. The adsorptive capacity of clay shales has not been investigated extensively. Some experimental work in the area of Devonian shales has been done utilising a volumetric test method (Lu et al., 1995), which determines the volume of gas adsorbed, and relates it to the total moles of adsorbate by an equation of state (EOS). The apparatus consisted of a reference cell and sample cell, and the sample cell was constructed of stainless steel to endure high pressures, and to minimize the extraneous adsorption effects. A

constant temperature environment is crucial for adsorption testing, particularly in materials which are not particularly adsorptive. There is not a lot of data on the adsorption behaviour of shales, and the data which does exist is primarily performed on crushed cores.

Although adsorption in clays is small in comparison to zeolites, and other commercial adsorbents, the adsorption of $CO_2$ onto clay minerals can be significant. Total adsorption is affected by the burial depth, carbonate content, organic content, lithology, depositional environment, overpressured fluid zones, history, and tectonic stress (Thomas and Frost, 1980). X-ray diffraction and infrared absorption illustrated that carbon dioxide was able to penetrate the clay structure on thin homoionic smectitic clays tested at $-70^{\circ}C$ (Fripiat et al., 1974). Although it was initially believed that carbon dioxide had only dissolved into the pore space, it was shown by Thomas and Bohor (1968), and later confirmed by Fripiat et al. (1974) that penetration into the interlamellar space was possible.

Equilibrium gas adsorption measurements made on four different clay minerals illustrated that the increased specific area of minerals such as montmorillonite resulted in an increased equilibrium gas adsorption in comparison to other clay minerals (0.210 mmol of $CO_2$/g of clay) (Volzone et al., 1999). However, these tests were not conducted under supercritical conditions, but in the gaseous realm, under elevated temperatures between $80-110^{\circ}C$. Other studies which have investigated methane gas adsorption in shales suggest that as much as $5cm^3$/g (approximately 15.3 mmol/g at room temperature and 7.5 MPa) is adsorbed (Lu et al., 1995). Total organic carbon (TOC) present in the shale can be directly related to its adsorption capacity of methane if the amount of TOC is greater than 1%. However, in shales with less than 1% TOC, adsorption capacities were a function of the clay minerals present. Adsorption capacity in shales with low TOC is due to the adsorption into the ultramicropore ($<5\text{Å}$) structure of clay minerals, which can be determined by the Brunauer, Emmett, and Teller (BET) method (Schettler and Parmely, 1991). Size and charge of the exchangeable cation will affect the ability for the carbon dioxide to penetrate the clay; more specifically less adsorption was found for divalent than monovalent cation substituted clays (Thomas and Bohor, 1968). Effect of residual water on carbon dioxide adsorption was not considered, however, Thomas and Bohor (1969) hypothesized that hydration of the shales could prevent the adsorption of carbon dioxide between the layers. In highly compacted materials, shales and coals, adsorption becomes severely retarded by the low gas diffusion through small pore volumes, despite the large internal surface area for adsorption (Thomas and Frost, 1980).

Adsorption isotherms tested around the critical point of a gas have not been well documented. Carbon dioxide adsorption by clays has not been studied extensively, due to its low adsorptive capacity, and its lack of application. Comparison between adsorption under in-situ stress conditions, the kinetics of the adsorptive behaviour in relation to transport processes and adsorption in crushed and intact samples has not been studied.

This experimental system developed in this research has the ability to test both crushed and intact adsorption of geologic materials, and can provide an excellent comparison between intact and crushed adsorption on similar materials. Providing adsorption data under realistic in-situ conditions.

### 2.7.4 Equations of State

Measuring adsorption using a volumetric method typically requires the application of an equation of state (EOS) to determine the amount of gas adsorbed. The ideal gas law (Equation 2.8) is the most basic EOS, and is a reasonable assumption for the behaviour of gases as its pressure decreases and temperature increases. A modification of the ideal gas EOS, is the van der Waals EOS, incorporating two additional terms (Equation 2.9). The $a/v^2$ term accounts for attractive forces between molecules, and b is a correction for the volume that is occupied by the molecules (Kyle, 1992). The modifications to van der Waals EOS have enabled a more accurate determination of fluid behaviour in the two phase region. The most common modifications include the Redlich-Kwong (Equation 2.10), Soave (Equation 2.11) and the Peng-Robinson (Equation 2.12) equations. Application of the various EOS are described in various thermodynamic texts (Lewis and Randall, 1961; Çengel and Boles, 1989; Kyle, 1992),

$$PV = nRT \tag{2.8}$$

$$P = \frac{RT}{v-b} - \frac{a}{v^2} \tag{2.9}$$

$$P = \frac{RT}{v-b} - \frac{a}{T^{1/2}v(v+b)} \tag{2.10}$$

$$P = \frac{RT}{v-b} - \frac{a(T)}{v(v+b)} \tag{2.11}$$

$$P = \frac{RT}{v-b} - \frac{a(T)}{v^2 + 2bv - b^2} \tag{2.12}$$

where P is the pressure, R is the gas constant, T is the temperature (in Kelvin), $v$ is the specific volume, and a and b are the attractive and repulsive terms respectively. The attractive term in the modifications of van der waals are temperature dependent.

The extended Redlich-Kwong EOS has been used in combination with finite difference codes to model and describe the thermodynamic and transport properties of $CO_2$ under potential storage scenarios (McPherson and Cole, 2000).

## 2.8 Summary

Storage of $CO_2$ under supercritical conditions requires that the gas pressure and temperature exceed 7.31 MPa and $31.1^0C$.

Based on the geological material chosen as an analogue for cap rocks in geological storage, it was determined that pore fluid chemistry can be and, in this case, is an important influencing factor for the mineralogy present. Assessment of the clay shales from the Clearwater formation suggested that it is from the Kca subunit, characterized by a gray-black, highly fissile material. Therefore, the handling of the samples during sample preparation, and during experimental setup, must be closely considered to minimize desiccation and disturbance of the specimen prior to experimentation.

Current understanding of gas transport in tight clay-rich materials suggests that gas is impermeable under water saturated conditions, without the presence of discontinuities. Creation of pathways under a dilation of existing network of discontinuities, or the creation of new ones due to the increase in gas pressure could potentially result in significant losses. Gas flow in low permeability clays is non-Darcian (Harrington and Horseman, 1999), and does not result in a significant reduction in water saturation, due to the complex physio-chemical interactions between clay mineral surfaces and water (Rodwell et al., 1999). Therefore, an overall increase in the specimen volume is expected during gas flow. However, migration of gas can occur by diffusion, with or without the presence of discontinuities as long as a potential gradient exists. The rate of gas diffusion under in-situ conditions will be a determining factor of the risk assessment associated with geological storage. Migratory effect of $CO_2$ can be retarded by its adsorption as it travels through the cap rock. Role of adsorption in intact specimens will indicate its effectiveness in reducing the probability of gas migration. Comparison between crushed samples, and intact water saturated samples is of interest when identifying the retardation of $CO_2$ in the field.

In general, diffusion, permeability and adsorption are influenced by the porosity, pore size distribution, tortuosity, percent saturation, and mineralogy. Diffusion and permeability are also a function of the pore fluid salinity, and effective stress. Adsorption and diffusion are influenced by the diffusing gas molecule size. Adsorption is also related to the exchangeable cation of the clay mineral and specific surface area. Permeability can be affected by the surface adsorption, capillary entry pressure, and stress history.

Although many of the parameters which influence gas permeability are also the ones which determine gas diffusion in water saturated media, no correlation between the two transport mechanisms has been found (Krooss and Leythaeuser, 1988). Correlation between adsorption and transport parameters in low permeability materials has not been evaluated.

While dominant transport mechanisms are highly contentious issues, a growing consensus suggests that gas flow in water saturated tight clay materials is not possible in the absence of discontinuities. However, diffusion will always be present. The testing apparatus designed here will be able to investigate a variety of different scenarios which will occur in geological storage conditions. This apparatus can provide the basis for the development of a framework for which dominant modes of gas transport can be established.

## 3.0 Experimental Design Considerations

It is extremely difficult for experimentally derived material properties to be directly related to field conditions, due to sampling issues and scale dependency. They can provide enormous value, however, in understanding the fundamental mechanisms occurring at the field scale. To maximize the value of experimental programs, the analysis of transport mechanisms in the laboratory must be representative of in-situ field conditions. Based on this design premise, this chapter describes the design criteria associated with the apparatus which houses the specimen, and to other peripheral equipment required to accurately and precisely measure the response of clay shale when exposed to a significant concentration of $CO_2$.

Investigation of gas transport mechanisms in low permeability (less than $10^{-22}$ m$^2$) fissile water saturated clay shales refers to diffusion and relative gas permeability. Retardation processes such as adsorption will also influence the transport properties of $CO_2$. The experimental apparatus, described in the subsequent chapter, was designed with the intention of testing all three mechanisms utilizing one setup. It was anticipated that utilising one apparatus would ensure uniformity in the results, and ensure comparable studies be undertaken.

### 3.1  Guiding principles

A triaxial cell is the best suited apparatus to incorporate the testing of gas transport in low permeability (less than $10^{-22}$ m$^2$) water saturated geologic materials, and incorporate principles of geotechnical testing. In geotechnical testing, the ideal triaxial cell allows for the independent control of the three principal stresses, $\sigma_1$, $\sigma_2$ and $\sigma_3$ illustrated in Figure 3.1. Most often the cylindrical compression test, studying changes in volume, and the determination of pore pressure responses and dissipation rates under isotropic conditions are most typical of triaxial applications in geotechnical engineering (Bishop and Henkel, 1964). However, the significant testing times required by adsorption and diffusion of gases must be considered in the design. Numerous considerations to reduce potential sources of error are incorporated in the concept of the testing facility.
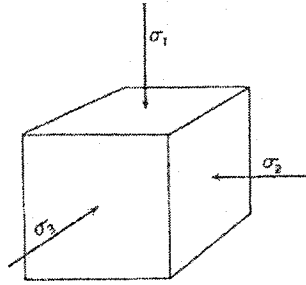
**Figure 3.1: Stresses**

Thus, using a triaxial cell concept, modified for isotropic stress conditions, the following design criteria were determined to be important in this type of testing.

- Capable of testing under a wide range of temperatures and pressures, indicative of geological storage situations

- Re-saturation of specimens with compatible pore fluids

- Incorporation of a true triaxial environment, to best replicate in-situ conditions

- Designed with the intention of testing permeability, intact adsorption, and diffusion of gases under pressures indicative of deep saline aquifer conditions.

- Design should be adaptable to include the determination of gas permeability under conditions of deformation.

- Design should be flexible, and easily modified to accommodate a variety of core types and sizes.

- Ease of sample loading, reducing the set-up time required, and the minimization of sample preparations are desirable to avoid potential desiccation and sample disturbance prior to testing.

- Either the implementation of a relatively gas impermeable membrane should be used, or alternatively the gases must be insoluble in the cell fluid. (Chapter 4)

- Membrane should remain flexible enough so that the lateral confining pressure is not carried by the membrane. (Chapter 4)

- An adequate sealing mechanism on the upper and lower end caps must be in place to ensure no leakage from the specimen into the cell fluid or vice versa. (Chapter 4)

## 3.2 Temperature Limits and Control

Experimental apparatus must be capable of operating under a variety of temperatures, from room temperature to at least critical temperature (31.1°C), and ideally to 60°C for greater flexibility. The geothermal gradient in the Alberta Basin ranges from 30°C to 70°C, with an approximate geothermal gradient of 45°C/km near the site in which these clay shales were obtained (Bachu and Burwash, 1994). Resulting in $CO_2$ disposal at approximately 40°C (assuming a surface temperature of 9°C), depending on the specific aquifer conditions. Deep saline disposal at a depth of 800m is proposed, where $CO_2$ resides in its supercritical state. These ranges of temperatures will enable $CO_2$ storage testing to occur under a variety of conditions. Based on these considerations a temperature range of 20°C to 60°C was chosen as a design basis for the experimental system. This range is illustrated in Figure 3.2, relative to the phase behaviour of $CO_2$.
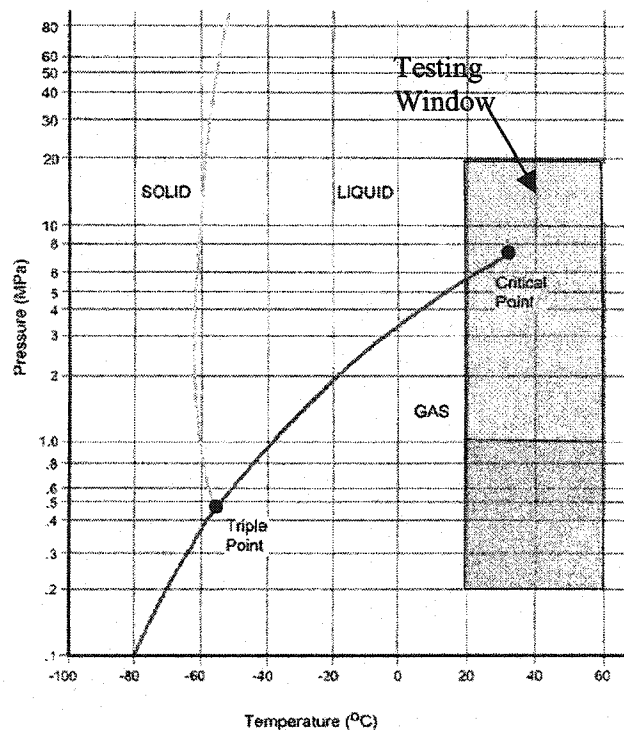


**Figure 3.2: Applicability of Testing Framework in Field Conditions**

Fluctuations in temperature will affect gas properties such as density, viscosity as well as the gas solubility, rate of diffusion, and adsorption. Rate of diffusion cannot tolerate changes greater than 1°C, however, the tolerance for adsorption measurements is far more stringent. Fluctuations

of $\pm$ 1°C will result in a difference in almost 10% of the density, and changes within $\pm$ 0.1°C can result in density fluctuations as great as 1% around the critical point of $CO_2$ (Span and Wagner, 1996). Therefore, strict temperature control is required if accurate and precise measurements of gas volumes are to be made. In measuring adsorption by volumetric means, the amount of gas adsorbed is calculated based on the temperature and pressure of the gas, and therefore poor temperature control will result in large uncertainties in determining gas volumes.

To achieve the required temperature accuracy and stability, the triaxial cell, gas and water lines were all submerged within a constant temperature water bath, which was monitored by Precision Platinum RTD Temperature Probes (Azonix 1011). A Proportional-Integral (PI) control system was set up to obtain tight control on the water bath. Two mixers were placed inside the bath to ensure excellent circulation of water throughout the bath. A 750 watt heating element was placed inside the water bath to supply the necessary heat to maintain a constant temperature. Power delivery to the heating element was provided by the PCI data acquisition board which transmitted the voltage to a 4 to 20 mA converter, and solid state relay (SSR) driver. The Labview control system received information from the SSR driver, and the corresponding energy input was provided to maintain a constant temperature. An overall accuracy in measurement was ±0.02°C, and the accuracy of the control was determined to be ±0.05°C. Temperature control data is illustrated in Appendix B. A bellows diaphragm equipped with an LVDT (Linear Variable Displacement Transducer) placed inside the constant temperature bath determined change in gas volume.

3.3    Pressure Limits and Control

Within the Alberta Basin the freshwater pressure gradients are approximately 10kPa/m, while more saline formations will have a pressure gradient of 12 kPa/m (Bell et al., 1996). For conditions of deep saline disposal at a depth of 800m, these gradients would result in $CO_2$ storage at a pore pressure of approximately 10 MPa, depending on the specific aquifer conditions. Confining pressure based on a saturated unit weight of 20kN/m$^2$ at 800m will be 16MPa. Apparatus design must allow for the application of at least 16 MPa confining stress and a gas pressure of 10 MPa. The testing facility is capable of testing from 200 to 20 000 kPa (Figure 3.2). The physical stainless steel apparatus limits the upper limit of the operating pressure, which could be easily modified to accommodate significantly higher pressures.

Determining PVT (pressure-volume-temperature) data requires accurate application of pressures. Adsorption of $CO_2$ will likely be very small (in the order of 0.2 mmol/g, Volzone et al., 1999), and therefore small changes in the pressure will have an effect on the calculation of the

volume adsorbed. Although, control on pressure fluctuations is not as stringent as the regulations on temperature.

ISCO 500D series syringe pumps, with Nitronic 50 construction of all wetted parts, and a heavy duty graphite-impregnated Teflon seal, were used to deliver gas pressures to the cell. It is capable of operating to a maximum pressure of 25.9MPa (3750 psi) to an accuracy of 0.5% of the full scale. These pumps operate best under liquefied gas conditions. It also limits the potential for gas losses through the seals, and changes in pressure have less effect on gas density under liquefied conditions. Operation under liquefied gas conditions (temperatures and pressures around 298K (~25°C) and 7.5MPa respectively) will result in changes in 0.5% changes in density, within this 0.5% accuracy window. This change in density can be reduced to 0.3% if the temperature of the pump is lowered to 293K. Changes in the pressure can effect the rate of diffusion, although its sensitivity to pressure is exceeded by the stringent control of the syringe pumps.

The pump syringe is heated to 25°C, and is wrapped in insulation and tape to minimise heat loss to the atmosphere. All of the flow lines leaving the pumps pass through a heat exchanger, which is controlled by an Isotemp refrigerated circulating water bath, bringing up the temperature of the flow lines to the testing temperature prior to entering the main temperature bath.

3.4    Pore Fluid Determination

In the laboratory, back saturation with fluids which match the in-situ pore fluid chemistry, is always preferred when conducting transport type experiments, especially in deep clays. In the analysis of the Clearwater Formation it was evident that the significant presence of smectitic clays, and the results of the quantitative XRD, would require saturation of the pore space with pore fluids of similar chemistry. Changes to the pore fluid could result in significant changes to the structure of the clay shale fabric. There are several methods in which pore fluids have been extracted from stiff clay shales to determine their properties.

Pore fluid extraction is often required to determine the chemical composition of pore fluids, and has been relatively well documented. Balasubramonian (1972) presents and compares various methods of obtaining the pore-water chemistry, and concludes that:

i)    the immiscible liquid displacement or gas extraction methods are suitable for sandy and silty materials, but these methods are unadvisable for other materials

38

ii)     centrifuging is also capable of providing good results for sands and silts, but is unsatisfactory for smaller particle sizes because of the difficulty in separating the fluid from the clay particles

iii)    low pressure mechanical squeezers are limited to soft sediments

iv)     **dilution, leaching, and high pressure squeezing methods can often be applied to fine grained materials**

Dilution and leaching methods are similar, both requiring addition of distilled water, and subsequent removal of water by filtration or application of a small suction. The natural water content is back calculated from the amount of water extracted and the dilution factor. Cave et al. (1994) compared the leaching approach to the high pressure squeezing method (mechanical extraction) of obtaining pore fluid, and determined that the leaching method held some potential in determining the true pore fluid composition. However, the computations required in the leaching method are cumbersome due to the possible dissolution of the mineral phases, which falsely increases the ionic concentration. Adsorption and/or ion exchange processes between aqueous and solid phases create non-linear water-rock interactions, and thus can potentially cause more variabilities between the dilution and mechanical extraction techniques. Despite some advances in using this technique it is still considered to be far less reliable than the mechanical extraction technique.

Utilizing high pressures to extract pore fluids is analogous to the natural process of consolidation except under accelerated conditions. A seven year study of pore fluid extraction from a variety of geological materials by mechanical extraction, concluded that very few samples could not be treated successfully using this method (Reeder and Entwisle, 1994). The mechanical extraction method appears to be the most widely used, and most successful method of obtaining pore-water from cores. However, there are some limitations to the mechanical extraction method. Concentration of the pore fluid exhibits a dependency on the applied pressure, particularly with monovalent ions. Morgenstern and Balasubramonian (1980) found that an increase in the stress applied, resulted in a decrease in sodium or potassium ions, and an increase in calcium and magnesium concentrations. They observed an overall decrease in total salinity at higher stresses, believed to be a result of the dilution of pore water with water from the double layer, and a membrane effect preventing the flow of salts in highly consolidated clayey sediments. Balasubramonian (1972) determined that the maximum squeezing pressure where no adsorbed water was removed is below 4.8MPa (700psi).

Entwisle and Reeder (1993) suggest that the main constraint on the amount of water collected is the stiffness of the sample to be squeezed. A maximum constrained modulus between 100 and 250 MN/m$^2$ is an acceptable range for this test method (Reeder and Entwisle, 1994). Moduli exceeding this range are typically too stiff to be able to obtain pore fluids utilising the high pressure squeezing technique. The minimum moisture content of a sample of 8% is suitable for this technique.

Improper storage of samples can affect the quality and accuracy of the fluid extracted. Presence of pyrite, and its exposure to oxygen can result in a scatter of $SO_4^{2-}$ data (Neuzil, 1994b).

Although it appears that the dilution technique holds much promise for low porosity, and low moisture content materials (Cave et al., 1994), it has yet to be proven as a suitable substitution for the mechanical extraction technique (Reeder and Entwisle, 1994). This technique was supported by the work of Morgenstern and Balasubramonian (1980) in the Bearspaw shale and Morden shale, as well as a subsequent seven year study described by Entwisle and Reeder (1993), who maintained that the mechanical extraction technique is ideal for clays and mudrocks, where other methods fail.

### 3.4.1 Relationship between Electrical Conductivity and Total Dissolved Solids

Often the extraction of pore fluid from stiff shales utilising the mechanical squeezing technique yields small amounts of pore fluid. Unfortunately, a full analysis of the pore fluid can generally not be accomplished given such small sample volumes. Therefore, the relationship between electrical conductivity and the total dissolved solids is an excellent way to correlate the salinity of the pore fluid for reconstruction, without requiring a large volume of pore fluid.

The relationship between electrical conductivity (EC in dS/m) and total dissolved solids (TDS in mg/L) or ionic strength (I in mol/L) is well established (Griffin and Jurinak, 1973; Reddy and Raju, 1990), and typically follows the general relationship in Equations 3.1 and 3.2, and illustrated in Figure 3.3.

$$I = 0.0127 \times EC \qquad (3.1)$$

$$TDS \approx 640 \times EC \qquad (3.2)$$
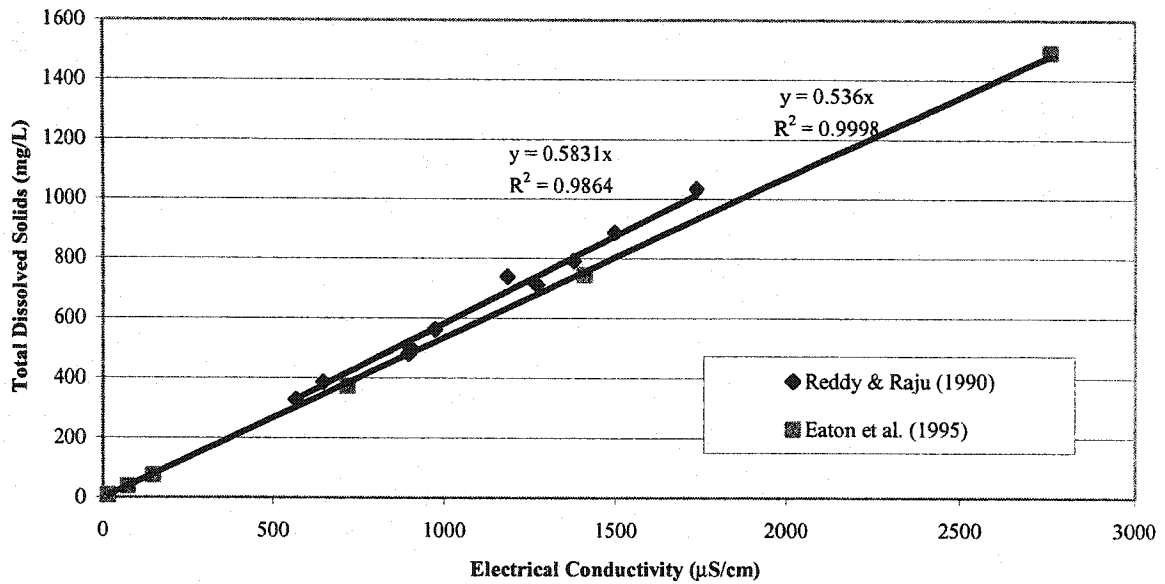
**Figure 3.3: Relationship between total dissolved solids and electrical conductivity**

## 3.5 Volume Change

Changes of gas volume are sensitive to fluctuations in temperature. Determining the gas volume at the upstream boundary conditions requires that gas temperature be relatively stable. Changes in ±0.1°C can result in a 1% change in density.

## 3.6 Summary

The ability to operate under a variety of pressures and temperatures increases the flexibility of the testing apparatus. It was determined that the tolerable limits of temperature changes in the laboratory would be less than 0.1°C. Tolerance of changes in pressure were determined to be less stringent, and within the accuracy of the syringe pumps chosen for the experimental set-up. Re-saturation with synthetic pore fluid was determined to be essential in the case of these clay shales obtained from the Clearwater formation, and may be influential in other materials, and thus very case-specific. Pore fluid salinity, in particular, can have an effect on the diffusion coefficient, and thus should be re-created to as close to field conditions as possible. Thus, incorporated in the design of the geotechnical testing apparatus, capable of applying triaxial stresses under these limitations, is a methodology to examine transport processes in cap rocks. It was determined that the best method of achieving this would be to utilize a modified triaxial cell with appropriate membrane technology prevent gas migration from the specimen to the cell fluid.

41

## 4.0 Sealing Mechanisms & Membranes

For the type of experimental program envisioned for the infrastructure developed in this research, the determination of a method which limits the gas mobility from a specimen into the confining fluid is one of the most important criteria in the laboratory design. Its importance increases with increasing testing times, as gas leakage from the specimen during a diffusion test will result in significant errors. The tolerable limits of gas migration from the specimen are dictated by the expected diffusive fluxes across the sample, and adsorption capacity of the sample.

The diffusion coefficient for $CO_2$ in water at $25°C$ is $1.92 \times 10^{-9}$ $m^2/s$ (Cussler, 1997). Diffusion coefficients for $CO_2$ in brine solutions are lower than in pure water, but in the same order of magnitude (Renner, 1986; Wang et al., 1996). A decrease in the diffusion coefficient from pure water will be observed in porous medium as a result of increased wall effects, due to tortuous pathways, electrostatic and size exclusions along the walls, and complex interactions between water molecules and clay minerals. Diffusion will only occur in the porous space, and volume available for diffusion to occur is likely a fraction of the total porosity. In general, total porosity is not as applicable in tight clay-rich sediments as it is in coarser-grained materials, since clays exhibit smaller interconnected pore spaces relative to fluid molecule sizes and other dissolved species (Pearson, 1999). The apparent diffusion coefficient of hydrogen through an argillaceous rock with a porosity of 23% was $2 \times 10^{-12}$ $m^2/s$ (Rebour et al., 1997), and diffusion coefficients of light hydrocarbons in geological materials with porosities between 0.4 to 16.5%, ranged from $10^{-10}$ to $10^{-13}$ $m^2/s$ (Krooss and Leythaeuser, 1988). Molecular weight of the diffusing species plays a significant role in its diffusive characteristics, with increasing molecular weight, resulting in a decrease in diffusion coefficient (Krooss and Leythaeuser, 1988).

Considering that the amount of $CO_2$ which will be adsorbed to the clay surface may be in the order of 0.2 mmol/g (measured on montmorillonite samples, Volzone et al., 1999), the losses through the membrane and seals become extremely important. As losses through the membrane and sealing mechanisms may be inaccurately read as adsorption or transport through the specimen. For the $CO_2$ to access the available surface area in the clay, it must diffuse into the small porous spaces prior to adsorption, thus the process is diffusion-limited. Thus, the time required for the determination of adsorption at steady state is likely in the order of months.

In a conventional triaxial cell set-up, the sample is segregated from the solution that applies the cell pressure by a latex membrane, where water is the permeant and the confining fluid.

Under higher differential pressures, i.e. in oil sands testing, thicker neoprene or silicone membranes are used (Sterne, 1981), although some experimental set-ups at larger differential pressures have utilised latex membranes (Al-Hawaree, 1999). In general, errors associated with flow measurements are a result of leaks within the apparatus, unsaturated membranes, and preferential flow (Tavenas et al., 1983). Leaks in the apparatus leading to leakage past the membrane seal and/or leakage through the membrane itself can result in significant error. Preferential flow between the sample and the membrane will result in higher flow measurements than what is actually occurring within the sample. Preferential flow can be reduced or even avoided by increasing the effective lateral stress. Ensuring saturation of the membranes will also reduce potential errors. Utilisation of gas rather than water as the permeant will result in larger errors if latex membranes are used, due to the migration of gas from the sample to the confining fluid, unless a $CO_2$ insoluble fluid is used.

## 4.1   Cell Fluid

Utilising a low solubility cell fluid limits the mass transfer of $CO_2$ from the specimen when the cell fluid approaches its $CO_2$ saturation point. Therefore, change in concentration of $CO_2$ with respect to time can be determined for a given volume of cell fluid, which approaches zero at infinite time. This rate of change can be calculated and accounted for in the laboratory analysis. However, solubilities which are too great will decrease the overall sensitivity of the analysis.

Grozic (1999) tested gassy sands under triaxial configurations at relatively low pressures using viton coated latex membranes. Since testing was performed in 3-4 hours, it was concluded that minimal diffusive losses through the membrane would have resulted in that time, which allows for the use of water as the confining fluid. However, adsorption and diffusion tests in tight clays can result in significantly longer tests. It is not uncommon for diffusion through a 1 cm long tight clay specimen to require a testing time of one month (Rebour et al., 1997).

Sobkowicz (1982) outlined a variety of options in altering the cell fluid to minimise the diffusion of $CO_2$ from the sample to the confining fluid, among them were low gas solubility fluids such as mercury, silicone oil and glycerol. Although silicone oil ($F_3C_3H_7CH_3SiO$) can be used to reduce the diffusive escape of most permeants, due to its viscous nature (Tavenas et al., 1983), its $CO_2$ solubility increases substantially with pressure, rendering it ineffective for $CO_2$ isolation systems (Wedlake and Robinson, 1979). A better cell fluid was determined to be glycerol ($C_3H_8O_3$) in preventing gas diffusion from the specimen (Sobkowicz, 1982). Solubility of $CO_2$ in glycerol is in the order of $10^{-5}$ mol/cm$^3$, only slightly lower than the $CO_2$ solubility in water at the same temperature (Vazquez et al., 1994), results in a solubility of 14 mmol in 1.4L of

cell fluid versus 0.2 mmol/g adsorbed in montmorillonite clay (Volzone et al., 1999). Despite having exhibited solubility characteristics which are too great for $CO_2$ segregation systems, using glycerol and silicone oil as cell fluids results in an increase in the equipment set-up time in comparison to water. An additional error associated with the use of low solubility confining fluids is that the calculation of solubility with time can be altered by the presence of gas bubbles entrained in the cell fluid during set-up. Testing conducted by Sobkowicz (1983) demonstrated that upon disassembly of the apparatus, trapped $CO_2$ between membranes and in the cell fluid (glycerol) was observed.

Expected experimental time will have a significant influence over the applicability of utilising a low solubility fluid as the confining fluid to prevent migration of gases from the specimen. Small diffusive fluxes ($10^{-11}$ to $10^{-14}$ m$^2$/s of $H_2$ and light hydrocarbons in low porosity argillaceous rocks, Krooss and Leythaeuser, 1988, Rebour et al., 1997) and low adsorptive capacity of shales (0.5 to 5 cm$^3$ of $CH_4$/g of Devonian shale, Lu et al., 1995) suggests that the amount of gas loss due to solubility in cell fluids can result in a decrease in the sensitivity of the analysis. Solubility of $CO_2$ into the cell fluid should be much less than the $CO_2$ diffusion/adsorption in these sample materials. A comparison of $CO_2$ solubility in different fluids versus the likely rate of adsorption is shown in Table 4.1.

**Table 4.1: Expected Adsorption Values compared to Expected Losses in Solubility**

| Cell Fluid | Solubility | | Expected Adsorption | Reference |
|---|---|---|---|---|
| | mol/cm$^3$ | in 1.4L | mmol/g | |
| glycerol | $10^{-5}$ | 14 mmol | - | Vazquez et al., 1994 |
| silicone oil (at P ~ 5.7 MPa) | > 0.9lb/lb Si | > 36 mol | - | Wedlake and Robinson, 1979 |
| $CO_2$ on montmorillonite | - | - | 0.210 | Volzone et al., 1999 |
| $CH_4$ on Devonian Shale | - | - | < 15 | Lu et al., 1995 |

Mercury is an excellent fluid at preventing migration of $CO_2$ from the specimen to the surrounding fluid, due to the insolubility of $CO_2$ in mercury, and is illustrated in Appendix A.

Initial cell design attempts to incorporate a double-barrelled triaxial cell. In the double barrel design, the outer barrel houses the confining fluid (typically water), and the inner barrel contains mercury which prevented the diffusion of gases from the sample into the confining fluid, separated from the specimen by a latex membrane (Figure 4.1) (Fredlund, 1973; Al-Hawaree, 1999). The double barrel technique is capable of preventing gas migration from the specimen to the cell fluid, however, it is a difficult test method to work with in terms of experimental set-up. Mercury was found to be difficult to work with, hard to clean up, and a hazardous substance which requires significant laboratory equipment and safety precautions to handle properly. Any leaks in the membrane and/or membrane seals results in mercury entrainment into the sample, porous stones, and displacement into the flow lines. Leakage results in awkward, complicated, and cumbersome cleanups, and in extreme cases may result in pump damage if proper mercury traps are not in place.
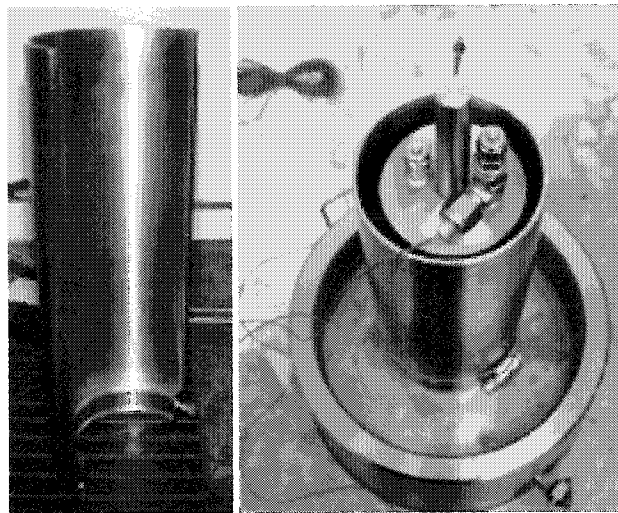


**Figure 4.1: Mercury Containment Device**

It was determined that the use of mercury in the laboratory was not the most ideal method of preventing gas migration from the specimen into the cell fluid. Therefore, after significant investigation into the potential of double barrelled triaxial cells, previously used in unsaturated soil mechanics, it was determined that a new testing technique must be developed and applied in the testing of low permeability cap rock materials. Research into various cell fluids illustrated that the potential to reduce gas migration from the specimen below anticipated adsorption and diffusive fluxes (Table 4.1) was unlikely. Therefore, the investigation into new materials for membranes was initiated.

## 4.2   Membranes

Changes in membrane material can reduce the loss of gases from the specimen. Materials such as polyethylene film, Teflon film, copper and other metals all have lower diffusivity to gases than latex. If a relatively impermeable membrane is not available, a combination of low diffusivity membrane with a low solubility cell fluid may be suitable, depending on the specific test conditions.

Typical polyethylene heat shrink is made with linear low density polyethylene (LLDPE), however, not all LLDPE are equal. Varying properties in the LLDPE will result in varying gas diffusivity properties. Shrink film is usually made with LLDPE or VLDPE (very low density). Essentially, the lower the density of the polyethylene the greater gas migration rates. Other factors are thickness, film orientation and cross linking. Crosslinked shrink film appears to have the lowest gas migration of around 3.12 $cm^3/cm^2$ per day of $CO_2$ (ASTM D3985) (http://www.syfan.co.il/sytec_701.html). Similarly, a variety of Teflon (PFTE) heat shrink films exist. Diffusion through Teflon heat shrink is approximately 1.4 $cm^3/cm^2$ of $CO_2$ would migrate through it over a 24 hour period (ASTM D-1434) (http://www.dupont.com/teflon/films/index.html). It is important to note the diffusing gas in these experimental values, as $O_2$ transmission is often lower by one order of magnitude than $CO_2$ transmission due to a difference in molecule size (e.g. for the same polyethylene film with a $CO_2$ diffusivity of 3.12 $cm^3/cm^2$, its $O_2$ diffusivity is 0.76 $cm^3/cm^2$ over a 24 hour period (http://www.syfan.co.il/sytec_701.html).

Using thin foil, and sealing with PTFE or PE heat shrink may reduce the diffusion through polymeric membranes. Possibility of a diffusive flow path between the layers of wrapped lead shim or aluminum foil may be a concern. Addition of silicone grease between the layers of lead shim may decrease the potential for gases to move between layers (Sobkowicz, 1982), however, sealing to the end caps may become a challenge. Teflon heat shrink used in combination with thin walled aluminum tubing has been used in permeability testing (Schlömer and Krooss, 1997).

Seamless thin walled copper and aluminum membranes have been used successfully in the testing of competent shale materials (Harrington and Horseman, 1999; Krooss et al., 1998), and in some cases in combination with layers of thin lead shim (Krooss et al., 1998). However, thin walled larger diameter copper membranes can be difficult to procure. Plans to silver solder copper shim to form a membrane both in the lab, and in the machine shop resulted in failed attempts at constructing a proper seal. Laboratory testing illustrated that as little as 5 psi internal pressure placed on the membrane resulted in a leak through the soldered joint. It was concluded

that the soldering was ineffective due to the added stiffness of the joint, resulting in failure occurring at a weak point along the seam.

Plans to machine down commercially available water drainage pipe as a means of creating a thin-walled membrane were unsuccessful. Reduction of the pipe to the desired membrane thickness was not possible, and the formation of pinholes in the membrane was always present. Uneven diameter and thickness of the membrane was an additional problem. This is especially difficult with low grade commercial products, as quality of the copper and the dimensions can vary considerably.

The electroforming process, whereby molecules of copper are deposited onto a mandrel to the desired thickness and removed, is capable of producing very thin walled seamless copper membranes of a variety of sizes. An inherent risk associated with electroformed copper is that poorly electroformed copper can potentially enhance gas diffusivity if inclusions and open porosity are left. However, well done electroformed copper should be 100% dense, and will behave similarly to wrought copper with the same grain size, which is practically impermeable to gas diffusive effects (Shelby, 1996). Using reputable manufacturing facilities can avoid the need for metallography tests, used to identify potential inclusions in the electroformed copper.

A summary of the types of membranes and their potential in $CO_2$ isolation systems is illustrated in Table 4.2. The data for copper is the diffusion coefficient of $O_2$ at temperatures between 800 to $1600^{\circ}C$, and diffusion is expected to decrease significantly at temperatures present under the current test conditions (Barrer, 1951).

Table 4.2: Gas Permeability through Membranes versus specimen

| Membrane Type | Gas Permeability (@STP) | | Apparent Diffusion Coefficient, $m^2/s$ | Expected gas concentration through specimen at test conditions $mol/m^3$ | Reference |
|---|---|---|---|---|---|
| | $cm^3/cm^2$ in 24hrs | in 30 days in set-up $cm^3$ | | | |
| Polyethylene | 3.12 | 7488 (0.307 mol) | - | - | http://www.syfan.co.il/sytec_701.html |
| Teflon film | 1.4 | 3360 (0.136mol) | - | - | http://www.dupont.com/teflon/films/index.html, |
| Copper, $O_2$ (800-1600°C) | - | - | $\sim 10^{-9}$ | - | Pastorek and Rapp, 1969 |
| $H_2$, 23% porosity | - | - | $4.6 \times 10^{-11}$ | $7.47 \times 10^{-6}$ | Rebour et al., 1997 |

4.3   Sealing Mechanisms

Regardless of the membrane selection, it is imperative to effectively seal the membrane against both the upper and lower end caps to ensure isolation of the cell fluid and pore fluid. Preventing communication between the pore fluid and the cell fluid was difficult to achieve with an o-ring. The addition of hose clamps were unable to provide a uniform seal on the o-rings, and therefore provided zones whereby leakage could occur. It was determined that a sufficient seal could not be assured utilising these methods.

In order to eliminate the sealing uncertainty associated with hose clamps, smooth seamless confining rings, with bevelled edges were designed. These confining rings were meant to secure the o-rings in the o-ring grooves, and therefore provide adequate sealing by providing a physical force (Figure 4.3). However, during testing, it was determined that the confining rings were cumbersome and difficult to work with. They were only able to provide a seal part of the time, and their potential failure or success was not always easy to determine. In some cases, the seal was broken upon disassembly of the test cell. Assembly of thin metal membranes utilising the confining ring was also prone to tearing of the metal. It was, therefore, concluded that the confining rings were easier to work with in theory rather than in practise. Due to the fissility of potential shale samples, significant care would be required during experimental set-up. However,

utilising the confining rings resulted in significant effort and time required to set-up the apparatus, likely subjecting the specimen to significant disturbance and desiccation. In some cases, the sample showed signs of crushing and disturbance upon disassembly. Consequently, confining rings were not incorporated in the final design of the experimental system.
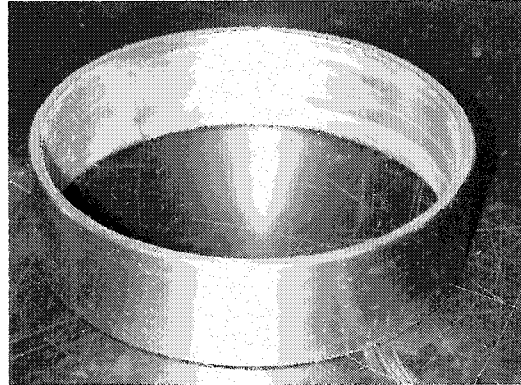


**Figure 4.2: Bevelled Confining Ring**

Introduction of metal membranes resulted in increased difficulty in sealing to the end caps due to their rigidity. It was determined that o-ring seals utilising some type of confining ring or split ring would not provide a reliable seal. Due to the substantial increase in cost of copper membranes in comparison to latex or polyethylene membranes results in a need for an increased reliability of the sealing mechanism, as membrane failure leads to higher experimental costs.

Previous experimental setups utilising metal membranes sealed the specimen using thick pieces of Teflon rope, which provided a physical seal between the cell wall and the end cap (Krooss and Schaefer, 1998). This set-up segregates the lateral and axial stresses, similar in concept to a Hoek cell design (Hoek and Franklin, 1968). However, it is unable to provide controlled axial loads (maximum axial load is 100kN). Tapered end caps sealed by hose clamps have also been utilised to provide seals against copper membranes (Horseman and Harrington, 1999). However, tapering end caps can cause potential tears in the membrane, if the taper slope is too great. Stiffness of the metal membranes may create difficulties associated with uniform sealing along the end cap and sample. It was noted that Horseman and Harrington (1999) did eventually shift from metal membranes to Teflon heat shrink. It is likely that the rigidity of the metal membranes caused some difficulty in the experimental set-up with the tapered end cap design. The increased flexibility and decreased stiffness of the Teflon membrane makes it easier to handle and potentially a better seal under these conditions.

49

For the current research, it was desirable to create a sealing mechanism which would ensure a dependable and repeatable seal during each setup. A sealing mechanism, modeled after a Swagelok fitting, was designed to allow a rigid membrane to slide freely inside the seal until the fittings were tightened. This more sophisticated approach to sealing relies on a series of o-rings separated by brass washers, to provide an active compression against the copper membranes (Figure 4.2). The active seal is achieved by mechanical exertion of a force on a series of o-rings, creating an active seal between the copper tubing to the end caps. If required, a concentric silicon ring can be cast around the copper tubing as a back-up seal around the copper during early stages of pressurization.
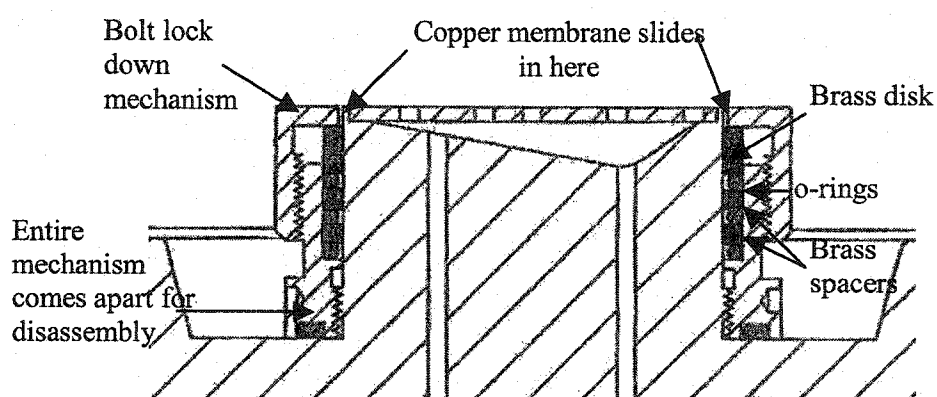


**Figure 4.3: Seal Compression Ring**

Copper membranes employed were specifically designed for the flow cell by electroforming. An inside diameter of 63.6mm ±0.03mm; length of 70 mm ±0.5mm, and a thickness of 0.15mm ± 0.03 mm were the copper membrane specifications. A maximum thickness of 0.5mm is the maximum acceptable wall thickness in the current sealing design.

## 4.4    Summary

Membranes and the mechanisms used to seal them are likely one of the most important factors in the experimental design for determination of slow transport processes. Expected values of diffusion and adsorption are in the order of $10^{-12}$ to $10^{-14}$ m$^2$/s and 0.2 mmol/g respectively. Therefore, changes to a low solubility cell fluid alone will not provide adequate enough measures against $CO_2$ migration into the cell fluid. Although, a variety of membranes can be and have been used in this type of testing, the most suitable are gas impermeable metal membranes. Adaptations of the sealing mechanism are required if stiffer seals, such as metals are to be used.

Therefore, due to the low diffusion rates, the likelihood that adsorption will be diffusion limited, and the total amount of $CO_2$ adsorbed will be small, the membrane and sealing mechanisms must ensure that gas migration is lower than the observed fluxes.

Traditional o-ring seals alone, typically used in triaxial cells were not capable of providing a sufficient seal. Previously designed confining rings increased the opportunity for tearing of the copper membrane. Although, many of these sealing mechanisms are able to provide a seal some of the time. The probability of an adequate seal should be greater, given the time required for a setup, and the cost of the membranes. Therefore, confining rings, hose clamps, split rings were all abandoned for a more secure and sophisticated means of sealing, modeled after the Swagelok fitting.

## 5.0   Final Design & Methodology

### 5.1   Final Design of Flow Cell

A modified triaxial cell capable of continuous operation up to a maximum of 20MPa cell pressure, and 120°C maximum operating temperature, with a safety factor of 1.5 was designed to test transport mechanisms in low permeability clay shales. Photos and Autocad schematics are illustrated in Appendix A. It was designed with flow ports exiting the cell from the bottom, and a stacking recess, with the intention of allowing several cells to be assembled on top of one another inside a constant temperature bath. It is built with isotropic stress conditions in mind, however, it can be easily adapted to test deviatoric stresses by changing the top cap design. Axial and confining stresses were applied by the same source. A pressure relief valve was placed in the top cap for safety purposes.

A variety of confining fluids can be used in this set-up, however water was the intended confining fluid, decreasing the time required, for assembly and disassembly. Approximately 1.4L of cell fluid can be placed inside the triaxial cell. Cell configuration allows for the testing of diffusion, permeability and adsorption, and allows for water saturation of the sample prior to the introduction of a gas phase. The design incorporates ease in specimen assembly to minimise the potential for desiccation, crushing, and sample disturbance. The sample is placed between two porous stainless steel stones, and a radial drainage plate on the upstream side ensures even distribution of the gas along the diffusing and advective front of the sample.

Sample size was dependent on the size of the cores, and the ease to trim these cores. In this case, the fissility of the clay shale cores suggested that the size of the specimens were best left as close to the size of the original cores as possible, to reduce the difficulty associated with preparing the sample. End cap diameter of 63.5mm (2.5") was chosen based on the ease of sample preparation, as samples available were slightly larger than 63.5mm in diameter. A schematic of the high pressure fluid cell design is illustrated in Figure 5.1, and detailed plans are contained in Appendix A.
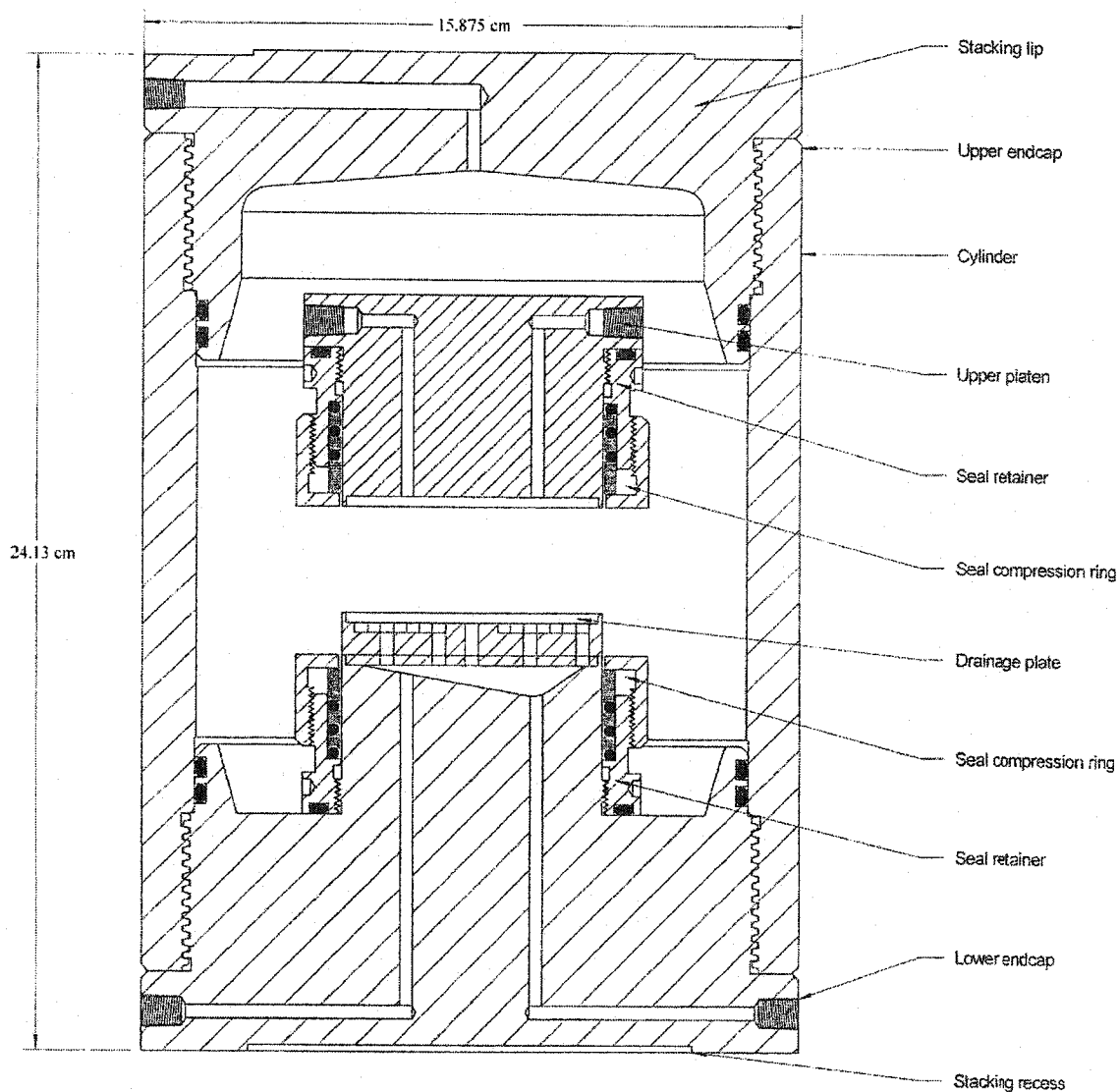
**Figure 5.1: Modified Triaxial Cell**

The triaxial flow cell encompasses several features intended to aid in sample preparation, and experimental setup. The drainage plate, shown in Figure 5.2, was designed with the intention to facilitate water drainage following saturation of the sample. The sloping drainage face, below the drainage plate, which radially displaces the fluid phase, is initially water filled, and upon the commencement of the experiment, water is displaced by a supercritical $CO_2$ phase.
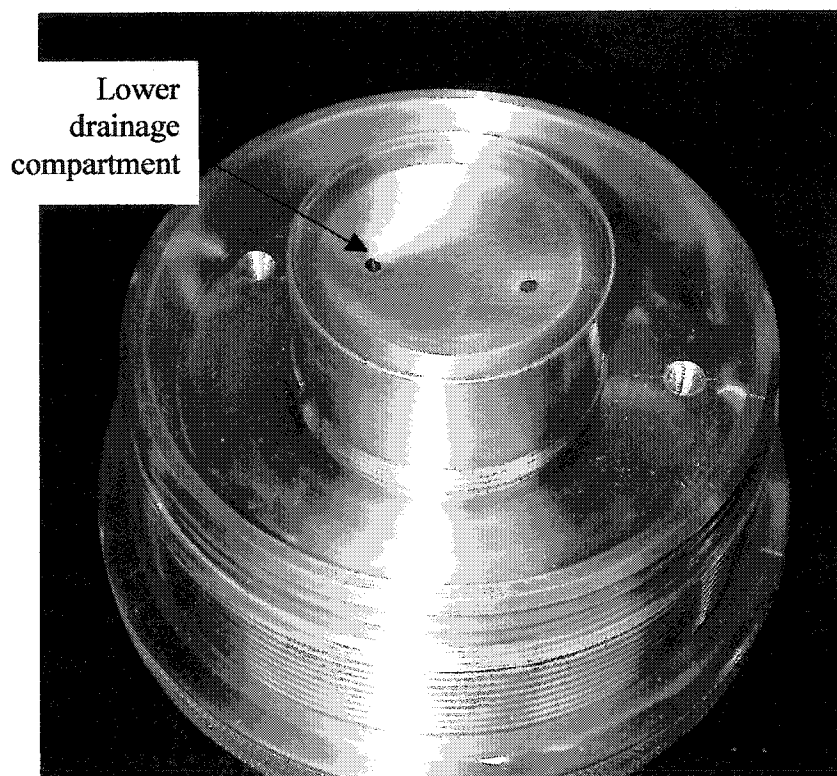
**Figure 5.2: Drainage Face**

A comparison of the current techniques used to measure relative gas permeability and gas diffusion in low permeability materials is illustrated in Table 5.1.

**Table 5.1: Comparison of Design**

| | Ho | Gallé | Rebour | Mackay | Krooss | Horseman |
|---|---|---|---|---|---|---|
| **Sample Handling** | Gently seats the sample, no sample movement | no sample movement (odeometer ring) | no sample movement | no sample movement (odeometer ring) | some potential for sample movement, no fixed end cap | some potential for sample movement, no fixed end cap |
| **Triaxial Stress Application** | isotropic: single source application of confining stress deviatoric: capability of applying an axial load | odeometer type set-up, $1^D$ | no application of deviatoric stresses | odeometer type set-up, $1^D$ | similar to Hoek cell design, segregation of major and minor principal stresses. Prior to more recent testing, there was axial stress limitations | only isotropic stress, not capable of applying deviatoric stresses |
| **Sealing Mechanism** | seals by a tightening mechanism which physically activates o-rings on both the top and bottom end caps | no lateral stress | wrapped lead shim, followed by concentric silicon cast ring | no lateral stress | requires significant force and time; sealed by Teflon rope between the cell wall and end caps | hose clamp seal to tapered end caps |
| **Membranes** | capable of utilising any membrane type | no membrane required | lead shim and cast silicone ring | no membrane required | capable of utilising any membrane type | polymeric heat shrinkable membranes, limitation of membrane use associated with taper slope |
| **References** | Current design of this thesis | Gallé, 2000 | Rebour et al., 1997 | Mackay et al., 1998 | Schlömer and Krooss, 1997; Krooss et al., 1998 | Harrington and Horseman, 1999 |

## 5.2 Saturating Fluid

Clay rich materials are unique because the interparticle spaces are of submicroscopic dimensions, they possess very large specific mineral surface areas, exhibit strong physio-chemical interactions between the water molecules and the mineral surfaces, have extremely low permeabilities and a very pronounced coupling between the hydraulic and mechanical responses (Mitchell, 1993; Horseman et al., 1996), resulting in a very complex class of materials.

The percentage of free phase water available will effect the transport properties within the clay material, as transport is a function of the available porosity (Pearson, 1999). The addition of electrolytic solutions will affect the clay structure. Changes in the pore fluid chemistry can result in a change in the thickness of the electric double layer. In particular, smectitic clays are sensitive to pore fluid chemistry. Increased salinity results in a decrease in the electric double layer (EDL). A previously saline saturated clay material, subjected to distilled water will result in a flocculated structure due to an expansion of its EDL.

Prior to the commencement of the gas flow experimentation, a specimen is back saturated with a synthetic pore fluid, similar to its pore fluid in-situ. Although this is not always necessary it can be crucial depending on the mineralogy of the specimen. Pore fluid also affects the diffusion characteristics, as increasing the salinity of a solution will decreases its diffusion, and therefore it is best to replicate in-situ conditions when possible. Modifications to the experimental apparatus designed by Balasubramonian (1972), to improve the sealing mechanism and water collection, was used to extract pore fluid from these clay shale materials. Approximately 15% moisture content is obtained from the sample following the pressure squeezing. About 5-7% of the water is removed at 700psi.

It is likely that only small amounts of pore fluid will be available for determination of the ionic concentration. Therefore, electrical conductivity measurements of the pore fluid are useful in determining the ionic strength (Section 3.4.1). Electrical conductivity of the extracted pore fluid was determined to be approximately 4dS/m, by measurement using the Horiba Cardy Twin B-173 conductivity probe. This probe has measurement range from 1 µS/cm to 19.9 dS/m, an accuracy of 2% of full scale, and requires at least 1mL of fluid. Conductivity values for the Clearwater aquifer and the Upper McMurray formations are 2.28 and 5.59 dS/m respectively (Thimm, 1999), conductivity of the clay shales from the Clearwater formation determined by pore fluid extraction is appropriate considering it lies between these two formations.

## 5.2.1 Pore fluid on Diffusion Properties

General conclusions from previous experimental work determined that solubility of nonpolar substances in aqueous electrolytic solutions will always be lower than its solubility in pure water, under the same conditions, and is known as the salting out effect (Markham and Kobe, 1941; Wiebe and Gaddy, 1941; Ellis and Golding, 1963; Takenouchi and Kennedy, 1965; Malinin and Savelyeva, 1972). Therefore, increasing the concentration of the salt solution will decrease the solubility of gaseous $CO_2$. In addition, electrolyte type is a factor, whereby solubility of gaseous $CO_2$ in electrolyte solutions exhibiting lower activity coefficients will result in higher solubility. Differences in solubility of different molecules are a function of its size, with decreasing solubility for increasing molecule size. For instance, the solubility of gaseous $CO_2$ in chloride solutions increases from $CaCl_2 < NaCl < KCl$ (Figure 5.3) (Malinin and Savelyeva, 1972; Freeze and Cherry, 1979).

Perkins and Gunter (1996) observed a temperature effect on the solubility of carbon dioxide, indicating a decrease in the salting out parameter with increasing temperature. The effect of temperature on the salting out effect was determined to decrease with increasing temperature to a minimum of 150°C, at which point the salting out effect increases with increasing temperature (Ellis and Golding, 1963). This point re-iterates the importance of a stable temperature testing environment.
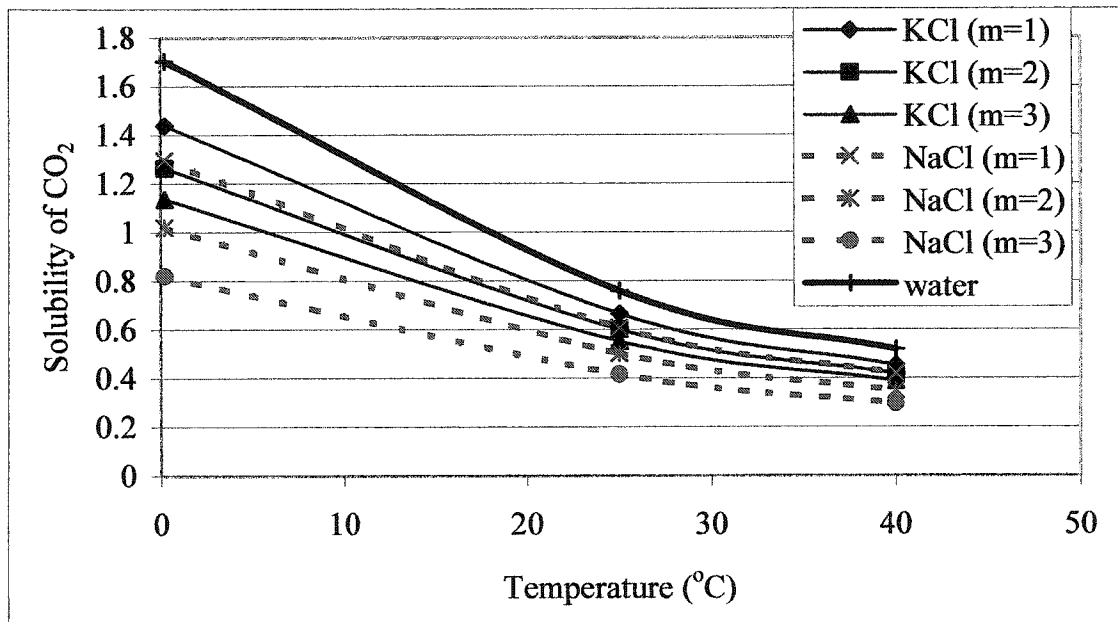


**Figure 5.3: Effect of Temperature on Solubility**
(Based on data from Markham and Kobe, 1941)

Solubility of water in supercritical $CO_2$ has not been tested extensively, and the data is conflicting. Some have reported that supercritical $CO_2$ is immiscible in water (Holloway and Savage, 1993; Cussler, 1997). However, there are indications that supercritical $CO_2$ behaves in a similar manner to gaseous $CO_2$ solubility, that is, increasing in solubility with decreasing temperature, increasing pressure and decreasing salinity, with solubility in pure water of approximately 5% (Enick and Klara, 1990).

In the field, increasing hydrodynamic trapping of $CO_2$ is best suited by an aquifer which possesses a lower ionic strength (Gunter et al., 1993; Perkins and Gunter, 1996). In the cap rock, solubility affects transport processes in that the rate of gas diffusion through saturated media is a function of its solubility, and therefore is dependent on its pore fluid characteristics. Increases in pore fluid salinity will result in a decrease in the solubility, and thus a decrease in the gas diffusion rate (Krooss and Leythaeuser, 1988). The decrease in diffusion was thought to be a result of increased viscosity of the brine solution in comparison to the water.

## 5.3 Volume Change

A high pressure volume change device was utilized in the determination of the volumetric flow throughout the testing. It was calibrated using a $CO_2$ pump upstream, and the change in volume measured by the changes in the volume of water in the downstream pump, all contained at the desired temperature (40°C in this case). Water was used to measure the downstream volume because the changes in its properties with temperature fluctuations are much smaller than those with gaseous $CO_2$.
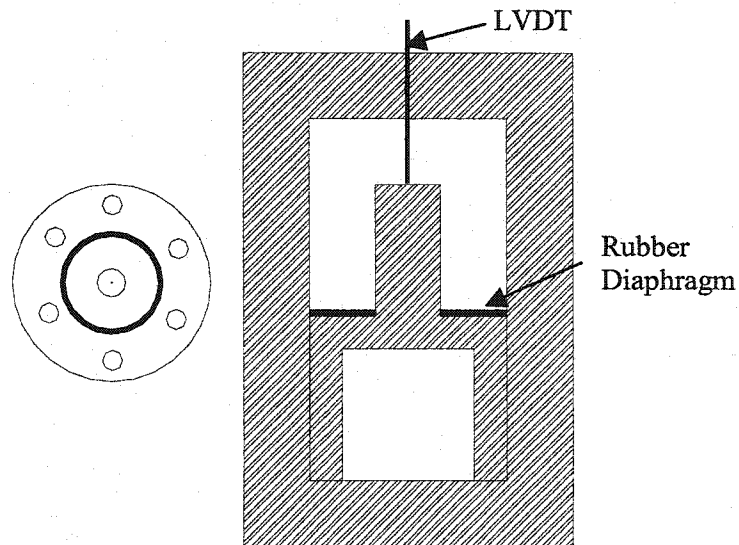


Figure 5.4: Schematic of Volume Change Device

A four way valve changes the direction of the piston, and therefore dictates which compartment is providing the gas flow. Each direction is calibrated against the change in the LVDT (Appendix D). The rubber diaphragm seals the two compartments.

## 5.4    Sample Preparation & Setup

Fissile, stiff samples have been a challenge to prepare in the laboratory. Cores obtained from the field were initially placed in double lined core barrel, and brought back to the University to be logged and analysed. Following logging and analysis of their physical properties (illustrated in Appendix E), select materials were taken and preserved in wax. The best method for obtaining 10mm thick samples was to extract the shale directly from the wax cores, which were used to preserve the samples. The entire sample preparation procedure should be carried out inside a temperature and moisture controlled environment to prevent unnecessary desiccation during sample preparation. Samples were extracted from waxed cores by using a modified odeometer ring. This ring, which had an extremely sharp edge and was the same diameter as the end cap, was gently pushed into the core, while still in the wax, and using a sharp blade any excess material and wax was removed. The cross sectional area of the sample faces can be carefully trimmed to a smooth surface using a surgical blade. The sample preparation ring provided some confining stress to the sample throughout the entire preparation stage to prevent the opening of discontinuities. The minimum thickness required is 10mm, however sample sizes as large as 40 mm can be accommodated in this apparatus.
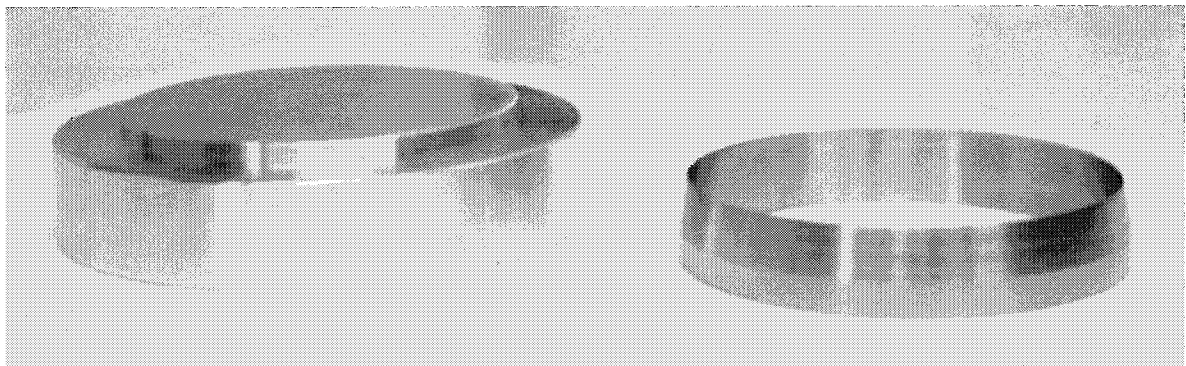


**Figure 5.5: Sample Preparation Tool**

Following extraction, the sample is placed on top of a pre-saturated porous stone, which is resting on a pre-saturated bottom end-cap. Above, porous stone and top end cap are carefully placed on top of the sample, and the thin (0.15mm) copper tubing is placed over top of the entire assembly (Figure 5.6). Copper membrane is carefully sealed on both the top and bottom end cap

59

by a series of o-rings held in place by a sealing assembly. As the assembly is tightened the extrusion of the o-rings creates an active seal on the copper membrane.
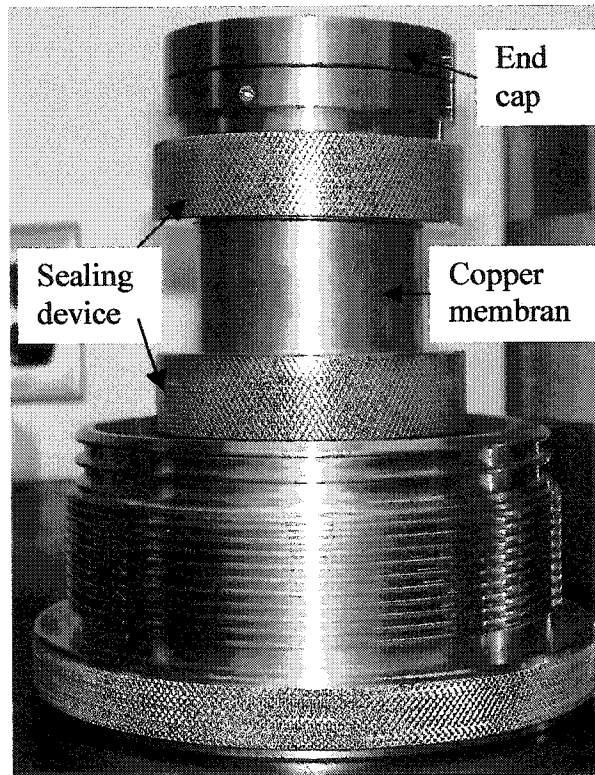


**Figure 5.6: Copper membrane Assembly**

Upon assembly of the sample a staged approach of applying confining stress and pore pressure can be employed to bring the specimen to the desired test conditions. Saturation should be performed with synthetic pore fluid, and crude water permeability measurements should be taken to ensure sample saturation. Once permeability measurements are stable, it can be assumed that saturation is achieved. The literature suggests that the saturation of low permeability materials can take up to one week to achieve (Katsube et al., 1991).

An overall schematic of the laboratory setup is illustrated in Figure 5.7. Three syringe pumps (ISCO 500D series) are used for the application of confining pressure, upstream $CO_2$ gas pressure, and downstream $N_2$ pressure. The $CO_2$ pump should be operated at lower temperatures, such that the fluid is in a liquid state, and then sent through a heat exchanger to approximately the desired temperature before entering the water bath, where temperature is maintained at a constant value.
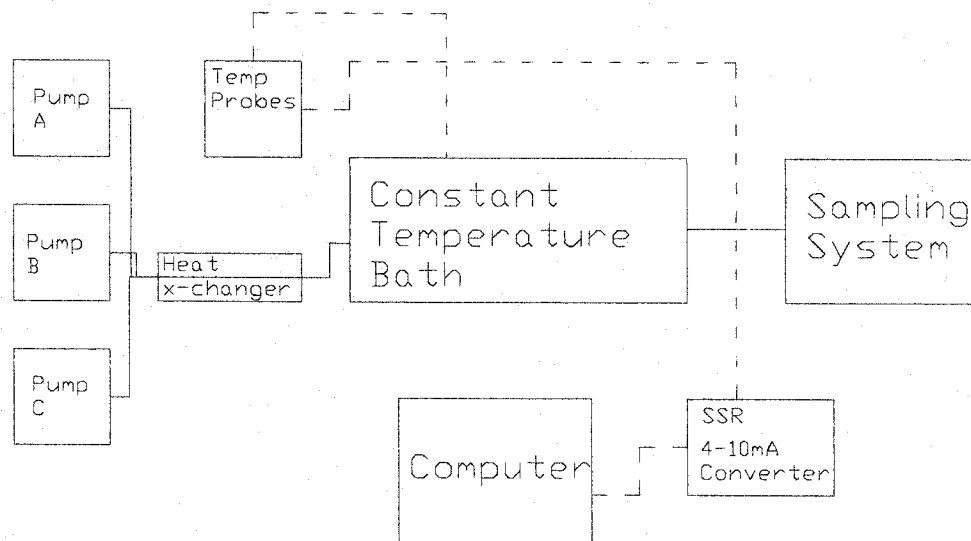
**Figure 5.7: Schematic of Laboratory Setup**

Inside the constant temperature bath is a preheating coil (where a volume of $CO_2$ can reach the desired temperature in the bath prior to test commencement) a high pressure volume change device, a heating element, and the triaxial cell (Figure 5.8).
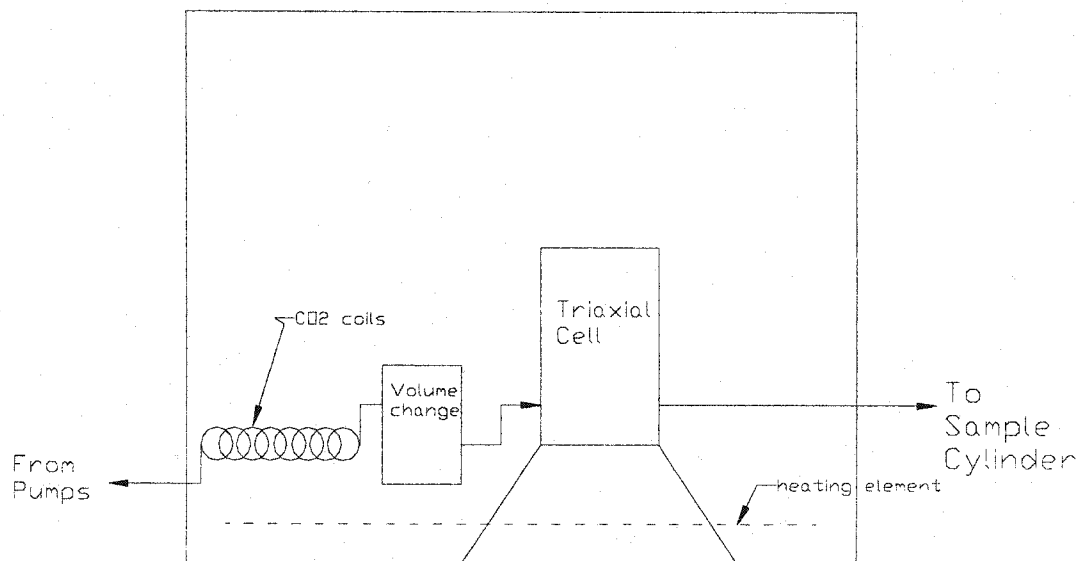


**Figure 5.8: Schematic of Setup Inside Temperature Bath**

The schematic diagram of the triaxial cell provided in Figure 5.9, illustrates the experimental set-up of the equipment. Flow lines 1 and 4 represent the downstream gas lines, whereas 2 and 3 are the upstream lines.
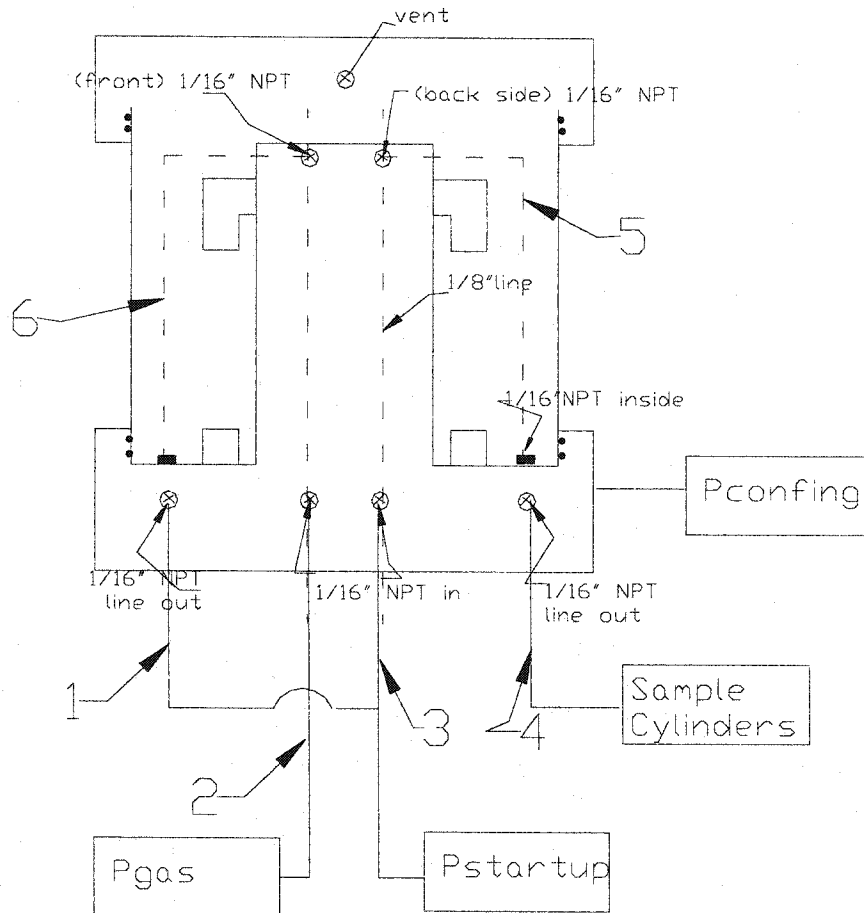


**Figure 5.9: Schematic of Cell Setup**

During saturation the synthetic pore fluid is brought in contact with the specimen by lines 3 and 4. Saturation of the sample is determined by permeability measurements, and upon stable permeability coefficients, saturation of the sample will be assumed. Synthetic pore fluid is removed from the flow lines by a slight differential pressure between the $CO_2/N_2$ and water lines. A slope designed into the base of the bottom end cap prevents fluid pooling during this pore fluid displacement phase of the test. It is essential prior to the start of the experimentation that all syringe pumps and flow lines are sufficiently shielded from ambient temperature disturbances.

## 5.5   Set-Up Procedure/Saturation Phase

The initial stages of sample setup are important, and may require significant time, particularly in clay shale materials. Saturation time is likely to exceed one week (Katsube et al., 1991), as permeability through these materials is low ($10^{-22}$ m$^2$). Initial saturation can be performed on one sample face, or to decrease the saturation time, by both faces. Thus, introduction of the synthetic pore fluid both in the upstream (1 and 4) and downstream (2 and 3) lines can achieve saturation. While sample saturation is occurring, initiation of the temperature control system can be started, and will take approximately 2 or 3 days to reach its optimum control of $\pm0.05$ °C. During this time, the volume of $CO_2$ in the pre-heated coils submersed in the water bath, can be slowly brought to temperature with the increase in the bath temperature.

1.  Connect synthetic pore fluid syringe pumps to top and bottom flow lines of the triaxial cell

2.  Place the triaxial cell inside the constant temperature water bath.

3.  Start the PI control system of the temperature bath.

4.  Fill $CO_2$ into the pre-charging vessels and coils, at the testing pressures. Ensure appropriate volume for the desired test.

5.  Allow sufficient time to ensure that temperature bath is stable, and that the $CO_2$ has been brought to desired testing temperature.

6.  Saturation is monitored by the change in pressure applied, similar to the pulse-decay measurement of permeability (Brace et al., 1968), however not to the same degree of accuracy. Thus, permeability measurements will be approximate, however, the goal is to ensure water saturation prior to the commencement of the test.

## 5.6   Diffusion

Following the setup procedure, temperature control adjustment, and sample saturation, the following procedure can be used to determine the diffusion across a shale cap rock within the modified flow cell.

1.  Evacuation of brine from the top flow lines (1 and 4 in Figure 5.9) by a water saturated $N_2$ gas. This provides an inert gas boundary condition downstream at the start of a test. Water saturation of the gas ensures that desiccation of the sample by the gas boundary condition does not occur.

2. Evacuation of brine from the bottom end cap (2 and 3 in Figure 5.9) and introduction of $CO_2$ concentration. Once this upstream boundary condition is imposed, the diffusion test begins. Similar to the $N_2$ gas, the $CO_2$ gas upstream is also water saturated. Water saturation can be achieved by running the gas stream through a partially filled water vessel.

3. Constant $CO_2$ pressures and temperatures are to be maintained at greater than critical values of 7.39 MPa and 31.1°C respectively, throughout each test. This ensures that the $CO_2$ remains supercritical throughout the test.

4. Constant temperature environment in the water bath ensures that the fluctuations in temperature do not result in significant changes to the gas density.

5. Utilising the automatic gas sampler (described in Chapter 6), $CO_2$ samples are taken at regular intervals, during the test. This gas sampler system is flexible and can accommodate a variety of gas sample sizes, therefore the anticipated volume of gas should be correlated with the sample cylinder volume.

6. Diffusion coefficient can be determined according to Fick's second law, modified for heterogeneous systems (Equation 2.2). Analysis of the transient portion of the concentration with time curve will result in significantly lower testing times (Section 2.7.1). Frequent sampling of the downstream gas phase is required, and the plot of downstream/upstream gas concentration ratio with time takes place throughout the test, until an adequate fit is obtained.

## 5.7 Gas Permeability

Following the setup procedure, temperature control adjustment, and sample saturation, the following procedure is used to determine the diffusion across 10 mm of shale cap rock within the modified flow cell. Similar initial set-up is required for the gas permeability measurement as in the diffusion test.

1. Evacuation of brine from the top flow lines (1 and 2 in Figure 5.9) by water saturated $N_2$ gas, for the downstream boundary condition.

2. Evacuation of brine from the bottom end cap (3 and 4 in Figure 5.9) and introduction of $CO_2$ concentration.

3. Downstream gas pressure is adjusted for the desired change in pressure across the specimen. This will impose the condition of gas flow versus gas diffusion, described in Section 5.6.

4. Monitor the gas volume into and out of the sample. Non-linear flow with respect to pressure difference is expected.

5. Measuring the concentration downstream of the sample, will also indicate if only diffusion is occurring, by matching the data with the diffusion test.

## 5.8    Adsorption

The experimental apparatus has the ability to test both crushed and intact adsorption of geologic materials. It provides a means of performing comparative testing to determine the adsorptive capacity, as well as investigate the ability of $CO_2$ to be retained by adsorption in cap rocks.

1. Generally, crushed samples are tested dry, and therefore does not require pre-saturation of the specimen prior to testing. Intact adsorption will likely desire as close to in-situ conditions, and therefore similar techniques employed to saturate the sample in diffusion and permeability testing should be performed.

2. Once saturation is finished, and temperatures are fixed inside the temperature bath, introduce a known volume of gas into the triaxial cell.

3. It is desired to limit the loss of $CO_2$ due to its solubility into the free pore fluid in the flow lines. Thus it is desired to turn off the downstream pump, and close off the vessel as close to the specimen as possible. Placing a valve immediately exiting the triaxial cell, and utilising 1/16" flow lines can significantly reduce the amount of free volume synthetic pore fluid.

4. Once the volume of $CO_2$ has been placed inside the triaxial cell, monitor both the changes in pressure (measured by the syringe pump), and the change in volume (measured by the high pressure volume change device)

5. Relate the pressure to volume adsorbed by the appropriate EOS.

It is essential in adsorption testing that all lines and pumps are properly isolated from the external temperature variations.

## 5.9 Calibration

Pressure transducers in the syringe pumps were calibrated against a dead weight table hydraulic pressure calibrator. The LVDT (Linear Variable Displacement Transducer) for the high pressure volume change device was calibrated against the volume reading from the syringe pumps. The ISCO 500D syringe pumps have an accuracy of 0.5% of its full scale, with a range of 0.001 to 204 mL/min. The temperature probes were factor calibrated, and prior to their implementation within the laboratory, they were tested between the temperatures of 0°C to 60°C. Operation of the temperature control bath was investigated over weeks to determine its effectiveness at maintaining temperature values within the required range. Calibrations are illustrated in Appendix D.

## 5.10 Summary

Approximately 5-7% of the available water is removed from the clay from the sample following the pressure squeezing at 700psi. Re-saturation with a synthetic or reconstituted pore fluid can be formulated based on the pore fluid electrical conductivity, and the presence of ions in the XRD analysis.

The flow cell designed in this research has the ability to test intact and crushed adsorption, diffusion of gases through water saturated media, and relative permeability of gases through low permeability water saturated material. Fluctuations in gas temperature during experimentation is strictly controlled by the constant temperature water bath within 0.05°C of its setpoint. Evacuation of pore fluid from the bottom flow lines, and the introduction of $CO_2$ are facilitated with the design of the drainage face on the bottom end cap. Downstream flow lines can also be evacuated of any existing pore fluid for $N_2$, reducing the effect of gas diffusion through synthetic pore fluid. Volume of the flow lines was limited to minimize the lag time. Damaging effects due to the fissility of the shale is minimised by careful sample preparation techniques, and ease of loading incorporated into the triaxial cell design. Diffusivity of $CO_2$ into the cell fluid was reduced through the use of an electroformed copper membrane sealed with an active compression seal. This mechanism provides a dynamic seal against leakage from the ends of the membrane and the end cap.

Synthetic pore fluid remaining in the lines should then be drained from the triaxial cell, and displaced to carbon dioxide at a pressure of 7.5 MPa (or gas pressure greater than its critical point of 7.39 MPa).

Diffusion experiments consist of a zero pressure gradient across the sample, whereas relative permeability measurements are determined by inducing a differential pressure across the sample. Adsorption of $CO_2$ onto the clay surfaces, and interpore spaces can be achieved by monitoring the change in pressure with respect to time. Sample preparation of stiff fissile materials requires the most time, and poses the greatest challenges throughout the course of the experimental design and setup.

## 6.0 Monitoring Methods

Quantitative determination of the dominant transport processes occurring within a specimen (diffusion or relative gas permeability) requires analysis of the concentration of $CO_2$ downstream of the sample. This can be achieved in a variety of methods. However, the important factor among the methods is the time lag between $CO_2$ exiting the sample, and the point of capture. It is important to ensure that the distance to the measurement device is not limiting.

### 6.1   Point of Measurement

Measurement of real-time data is always preferred over methods, which are a function of gas solubility or kinetics. If gas solubility or kinetic measurements cannot be avoided, the method must ensure that the data collection is not limited by these mechanisms. That is, if $CO_2$ diffusion through the water or brine saturated flow lines limits the movement of $CO_2$ to its end destination, and is slower than gas migration through the sample, it will provide erroneous data.

The time required for $CO_2$ to travel from the sample to the point where it is measured must be much less than the time required for it to move across the sample. Gas transport through low permeability ($<10^{-22}$ $m^2$) geological materials is extremely slow, potentially exceeding 1 month for a diffusion test. Consequently, it is best to reduce the lag time to be as close to a real time measurement as possible. For the downstream fluid in the experimental setup, it is desirable to choose a fluid which provides the least restriction in the movement of $CO_2$ from the sample to the point of data collection. Comparison of $CO_2$ diffusion through $N_2$ versus water indicates that water or brine will be more restrictive. Nitrogen is also an inert gas, which will limit the potential for any interactions between $CO_2$ and the ions in the free solution.

At 1 atm and 25°C, the diffusion coefficient of $CO_2$ through nitrogen and water is 0.165 $cm^2/s$ and $1.92 \times 10^{-5}$cm/s respectively (Cussler, 1997). Since, the diffusion through electrolytic solutions will be lower, nitrogen is the best choice. Nitrogen is also a good choice because it is inert. Good design also dictates that reducing the volume through which $CO_2$ must travel after exiting the sample and arriving at the sampling point will also decrease the lag time.

### 6.2   Sampling Techniques

Quantitative determination of specific gas content is usually performed outside of the experimental setup. Sampling methods are often cheaper as they require less laboratory hardware. In-line methods under these operating pressures can be quite costly. Sampling techniques can occur by manual sampling techniques using sampling cylinders and by-pass

valves, or by a more sophisticated set-up utilising an automatic sampling system, automatic systems are preferred due to the length of testing times. A variety of analytical techniques can be employed to determine the concentration of $CO_2$.

The current sampling system to be used in this testing, as illustrated in Figure 6.1, steps down the pressure prior to the gas stream entering the pneumatic selector valve. The selector valve automatically determines the sample cylinder in which it will sample into, and as determined by the time interval set for sampling. A variety of cylinder sizes can be accommodated in this setup, as determined by the test requirements.
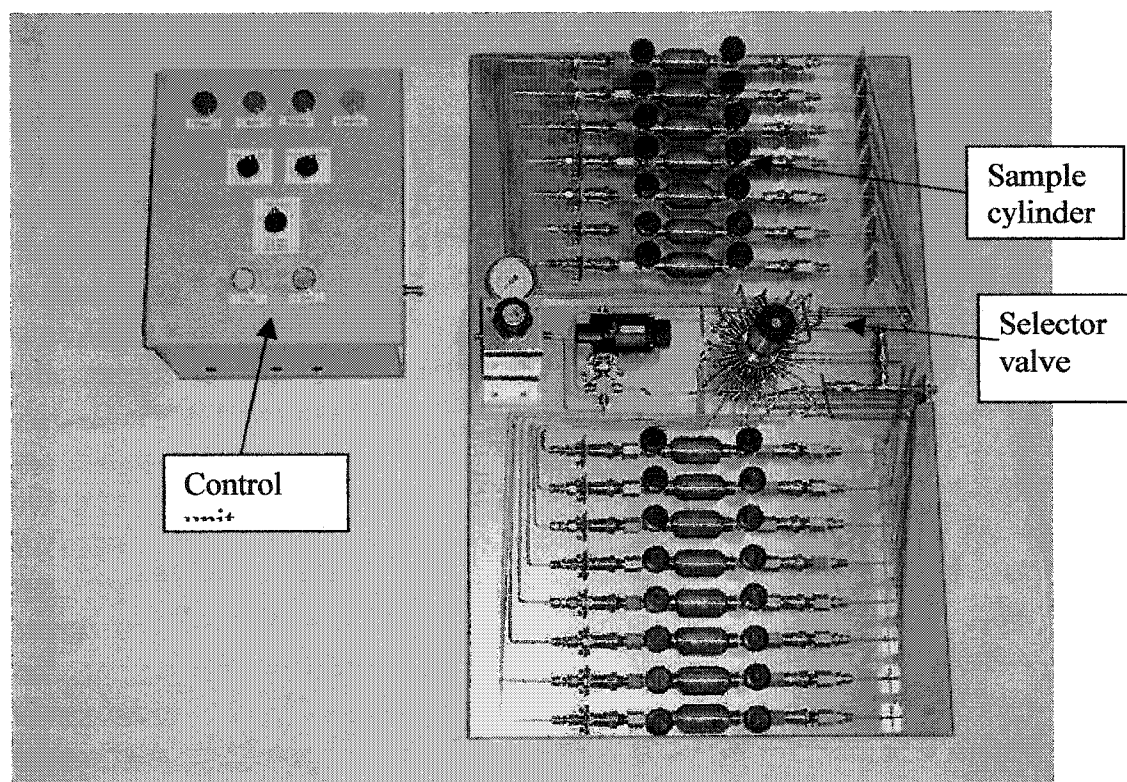


Figure 6.1: Automatic Gas Sampling System

The automatic sampling system is a simple, but sophisticated and flexible method of sampling gases from the triaxial cell, which can be subsequently sent to a laboratory for analysis of $CO_2$ concentration or other constituents.

5.4    Analytical Methods

Currently there are various methods which can be used to determine the concentration of $CO_2$ in a given gas sample. Some of these methods can be used in-line with the experimental apparatus, while others require gas sampling, depending on the experimental set-up.

### 6.3.1 Gas Chromatograph

Gas chromatographs (GC) are commonly used (Krooss and Schaefer, 1987; Schlömer and Krooss, 1997; Rebour et al., 1997) to determine concentrations of $CO_2$ in an unknown gas stream. It is one of the most powerful and popular methods of determining gas concentrations.

Its accuracy is most dependent on the quality of the sample, and possible sources of contamination from the source to the GC. However, operating parameters of the GC (i.e. retention times, band widths, peaks, column temperature and mobile phase flow rates) can also contribute to possible errors (Bruno and Svoronos, 1989).

### 6.3.2 FTIR

Fourier Transform Infrared Spectroscopy (FTIR) is a quantitative method of determining the concentration of a substance. It relates the changes in the spectral response to the change in concentration. A relationship between the changes is typically, although not always, a linear relationship (Günzler and Williams, 2001).

### 6.3.3 Titration

Solubility of $CO_2$ into distilled water and titrated against either sodium carbonate or sodium hydroxide to form sodium bicarbonate can be used to determine the concentration of $CO_2$. Colorimetric determination from clear to pink identifies concentration of $CO_2$ in the solution, using phenolphthalein as an indicator (Eaton et al., 1995). Potentiometric precipitation titrations using silver, mercury or platinum indicator electrodes are also possible, rather than using a colour indicator.

Sources of error can be significant utilising this method, as 300ppmv of $CO_2$ resides in the atmosphere (Houghton, 1997). It is important to prevent possible contamination of the sample by ambient sources during titration, which is difficult to avoid during titration as well as in sample preparation. Aside from the significant time and effort required for this analysis, it is extremely difficult to prevent free $CO_2$ losses into the atmosphere at larger concentrations, and $CO_2$ contamination by the ambient sources at small concentrations. In order to minimize laboratory error, analysis should be conducted as soon as possible after sampling.

### 6.4 Electrical Resistivity (Conductivity)

Measurement of electrical resistivity, or its inverse conductivity, has been used extensively in the delineation of contaminated geological materials (Weemees, 1990; Chan et al., 2000). It has been used in the laboratory to monitor the movement of contaminants across geologic materials (Chan et al., 2000). It is a very sensitive measurement, and varies with changes in mineralogy,

pore fluid characteristics, pressure and temperature. Electrical resistivity exhibits the greatest variation in comparison to other physical properties of rocks and minerals (Telford et al., 1990).

## 6.4.1 Mapping the movement of $CO_2$

Most rocks and minerals in their dry state are poor conductors, and thus exhibit large resistivities. In clay-free rocks the resistivity is determined mainly by the amount of water present (percent of saturation), its salinity and its distribution through the rock porous space (Parkhomenko, 1967). Degree of water saturation has a significant effect on the resistivity (Brace and Orange, 1968), however in the case of fully saturated porous media the resistivity becomes a function of the salinity, pore structure, and tortuosity (Telford et al., 1990). Confining pressure also influences resistivity, however at high pressures resistivity is largely a function of porosity (Brace and Orange, 1968). Other important factors include the mobility, concentration and degree of dissociation of the ions, as well as the volume and arrangement of the pores (Telford et al., 1990).

The presence of clays complicates the electrical resistivity response. Typically, clayey materials will exhibit less resistivity than clay free materials because of the higher cation exchange capacity (CEC) of clays. The higher the CEC the lower the resistivity (Weemees, 1990). Consolidated shales, dolomite, and clays typically exhibit electrical resistivites of 2-20x$10^3$ $\Omega$m, 3.5x$10^2$-5x$10^3$ $\Omega$m, 1-100 $\Omega$m respectively (Telford et al., 1990). The relationship between resistivity and salinity is further emphasized in clay rich media by the effect that salinity bears on the structure of the clay itself. Salinity of the pore fluid will alter the thickness of the clay electric double layer (EDL). Compressed EDL is associated with higher salinities, while an expanded EDL represents lower salinity pore fluids. Salinity dependence is related to the relative mobility of the ions in the pore space from the free water to the double layer near the solid surface, resulting in a complex change in the resistivity due to the difference in free water ions and double layer ions, which follow an alternating electrical field (Parkhomenko, 1967). Since ions in the double layer are more restricted, it results in an increase in the conductivity. In general, the increase in conductivity plays a more significant role in dilute pore fluids than saline pore fluids. All else equal, increasing the salinity increases the conductance. Heavily fractured media is found to have a lower electrical resistivity, particularly if the surfaces are rough a (Stesky, 1986). This is likely due to the increase in fracture porosity.

In general, pore fluid chemistry, physicochemical properties of the pore walls, concentration of ions in the pore space, effective stress, confining pressure, extent of fracturing, interconnectedness of the pore space, the degree of saturation, the clay content, and the salinity of

the pore water all effect the resistivitiy of clays (Brace et al., 1965, Stesky, 1986; Demir, 1988; Sen et al. 1988).

Significant complexities are involved with the quantitative measurement of electrical resistivity in clays. However, assessment of relative changes of electrical resistivity may yield interesting data on the movement of $CO_2$ in the specimen without requiring significant research into the complexities surrounding the electrical response of saturated clays. Although, quantitative measurements are not required, for this relative drainage approach, a stable reading over long testing times (in excess of one month) are required. Fluctuations in the reading of a single solution will yield inaccurate and unreliable data.

Qualitative data on $CO_2$ movement through the specimen can provide information regarding the path and/or distribution of $CO_2$ as it migrated. A definitive point of breakthrough should be identifiable by this means. Given the potential for this monitoring method, an extensive program was initiated to examine its potential for the use in the experimental program. The following section descries the outcome of this investigation.

Circular platinum mesh wires were used as electrodes. Platinum is typically the metal of choice, since it would have no reaction with the saline pore fluid during the experiment. Two meshes were placed, one on either side of the sample, while the third was placed downstream, with a porous stone on the other side, Figure 6.2.
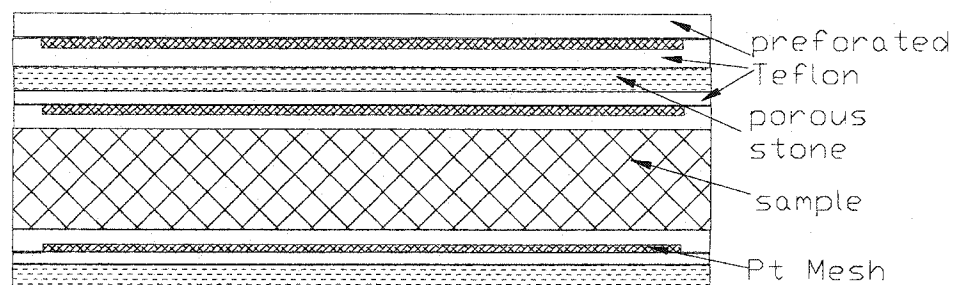


**Figure 6.2: Electrical Resistivity Set-up in Triaxial Cell**

The middle electrode was a common electrode between the two measurements. Measurements were taken across the sample, and then across the porous stone, in a pulsed DC manner, shorting out the circuit following each reading. Electrodes were segregated from the metal porous stones by means of a thin (2mm) Teflon perforated plate. It was anticipated that a baseline for the electrical resistivity could be achieved during sample saturation. Following saturation, sufficient time would be allowed for the sample to achieve a baseline reading of

electrical resistivity. It was anticipated that once $CO_2$ entered the triaxial setup, the changes in resistivity would allow for a qualitative mapping of gas migration in the specimen, and potentially identify pathways in which $CO_2$ was moving. Breakthrough would be identified once changes in the downstream pair of electrodes were observed. If changes in the downstream are slow, then it could be hypothesized that the entrance of $CO_2$ was slow, and therefore slow even migration through the porous space could be expected. However, if a large amount of $CO_2$ was found (i.e. a spike), it was thought that a preferential flow path was found through the specimen.

Relative changes in resistivity or resistance was of more interest than the actual values of electrical resistivity through the specimen. Baseline resistivity readings for the clay specimen could be achieved by obtaining readings during saturation. As the change in resistance would indicate information about the movement of $CO_2$. Calibration of this technique involved the measurement of water, and increasing concentrations of brine solution. Additions of small, known concentrations of $CO_2$ would also allow for the determination of the sensitivity of the setup to $CO_2$ addition.

Despite the potential for resistivity measurements to provide significant data concerning the behaviour of $CO_2$ in the specimen, it was not successful in the laboratory. Details regarding the problems in the laboratory are described in Section 6.4.4. Further analysis of electrical measurements is also described in the following section.

### 6.4.2    Hydroxide Absorber

Utilising electrical conductivity in the laboratory has the potential to monitor quantitative changes in $CO_2$ concentration over time. It has been used in biological and environmental systems in the monitoring of atmospheric $CO_2$ absorption, and has been successful in providing a stable and continuous measurement of changes in $CO_2$ concentration as indicated by the continual monitoring of electrical conductivity of a hydroxide solution, in the order of months (Ko and Juang, 1983; Govind et al., 1997).

Theoretically, absorption and reaction of $CO_2$ will occur with any hydroxide solution, which changes the electrical conductivity of the solution. Utilising a simple solution such as potassium hydroxide (KOH) is thought to be better than NaOH and LiOH based on their solubility and specific conductance characteristics (Ko and Juang, 1983). For a concentration of $1 mol/dm^3$, the specific conductance of LiOH, NaOH and KOH at 25°C is 0.139, 0.158 and $0.184 \times 10^{-3}$ $ohm^{-1}cm^{-1}$ respectively (Ko and Juang, 1983). It has been suggested that the use of $Ba(OH)_2$ is a suitable, and potentially better choice than KOH due to its lower solubility product ($5.1 \times 10^{-9}$), thus almost complete conversion of $CO_2$ to $BaCO_3$ is achieved (Govind et al., 1997). Utilisation of either

Ba(OH)$_2$ or KOH solutions are acceptable in this application, and have been used in the monitoring the amount of CO$_2$ in a particular system (Ko and Juang, 1983; Tanaka and Fritz, 1987; Govind et al., 1997; Ahmed et al., 2000).

Exposure of 37% KOH to atmosphere for 10 months illustrated that 14.5% of CO$_2$ could be absorbed and converted to 45.5% K$_2$CO$_3$, resulting in a decrease in the specific conductance from 0.64 to 0.25 ohm$^{-1}$cm$^{-1}$ (Ko and Juang, 1983).

In the laboratory, a solution of KOH was placed inside a 150mL Teflon lined, stainless steel sample cylinder downstream from the triaxial cell. As gas enters the cylinder the CO$_2$ reacts with the KOH, and forms K$_2$CO$_3$ (Equation 6.1)

$$2KOH_{(aq)} + CO_{2(g)} \Leftrightarrow H_2O_{(l)} + K_2CO_{3(aq)} \qquad (6.1)$$
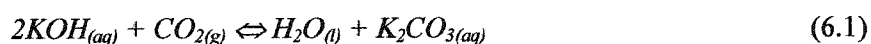
As the reaction proceeds the electrical conductivity of solution in the sample cylinder decreases. Due to the corresponding changes in conductivity as a result of the less conductive K$_2$CO$_3$ formed at the expense of the more conductive KOH (Ko and Juang, 1983). Two platinum electrodes fed into the sample cylinder, sealed by a Conax connector (Figure 6.3), measured the changes in conductivity.
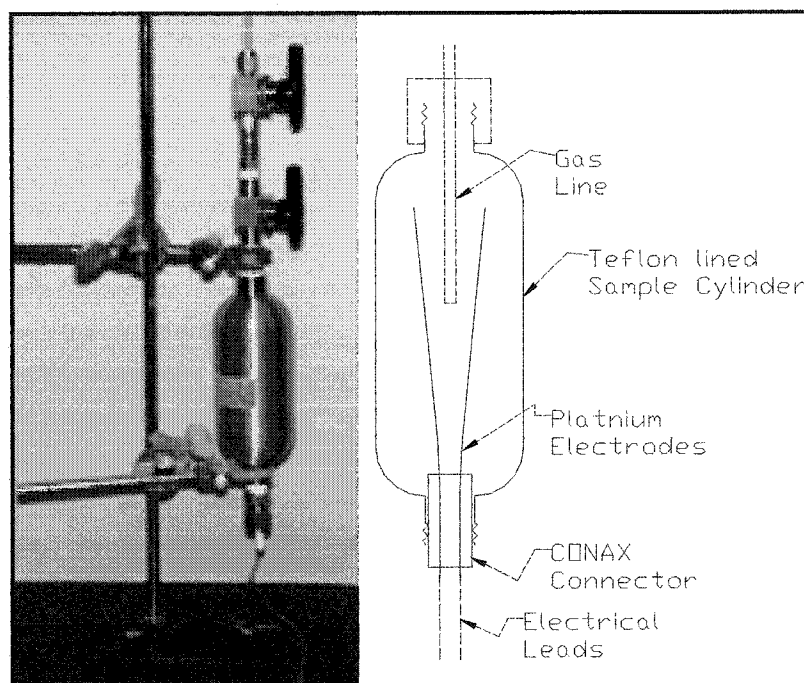


**Figure 6.3: KOH Absorber Setup**

### 6.4.3 Measuring Electrical Resistivity in the Laboratory

Resistivity is related to the resistance through a medium, and is a function of the distance between the electrodes and their cross-sectional area (Equation 6.1), where R is the resistance in $\Omega$, L is the distance between the electrodes in m, A is the cross sectional area in $m^2$, and $\rho$ is the resistivity in $\Omega m$. The experimental geometry determines the correlation between the resistivity and the resistance, known as the geometry correction factor.

$$R = \rho \frac{L}{A}$$ (6.1)

The geometry correction factor is a constant value under the assumption of a homogeneous isotropic medium, that the electrodes work as perfect conductors, and that the current supply source is perfect (Weemees, 1990). Calibration of the setup can be made by a series of measurements of electrical resistivity and resistance using a variety of solutions, to determine the geometry correction factor. Slope of the resistivity-resistance curve will provide the geometry correction factor for the circuit. Applying a known voltage (V, in volts) through the medium of interest at a constant, known current (I, in amperes) will provide the resistance (R) of the medium according to Ohm's law (equation 6.2).

$$V = IR$$ (6.2)

Electrical conductivity ($\sigma$) is the reciprocal of the electrical resistivity ($\rho$), and can be expressed as an $(\Omega m)^{-1}$ or more commonly as dS/m, where 1 ampere/volt is equal to 1 S (siemens). In older literature the term mmhos/cm is commonly used, and is equivalent to 1 dS/m. The properties of the medium will dictate which notation is more convenient, i.e. conductivity or resistivity.

The measurement of electrical resistivity can be achieved using a fairly simple electrical circuit. A resistor in series with the medium of unknown resistance of interest, operating at a constant, known voltage, can be used to determine the resistivity of the unknown medium. Increased stability of the measurements, and decreasing the potential charging effects from occurring between the electrodes can be achieved by the addition of FETS (Field Effect Transistor) in the circuitry. These FETs act as voltage gates, allowing current to flow through the circuit, or eliminating the potential for current to flow, and effectively creating a ground effect where by the entire circuit is short, and has no current (Figure 6.4). This helps to eliminate any

75

potential charging or capacitance effects occurring between the electrodes. Introduction of FETs results in a pulsed DC voltage being sent through the circuit, in this case for a 35 msec time interval, while data is acquired, resulting in dynamic measurements. Stability of the electrical circuitry, of the voltage source, and the accuracy of the data logging system was determined by placing a constant electrical resistance pot in the circuit, in the place of the testing medium. The disadvantage of dynamic measurements is that back averaging data to reduce scatter and noise in the system is not applicable. Greater fluctuations and noise issues may potentially arise due to dynamic measurements.
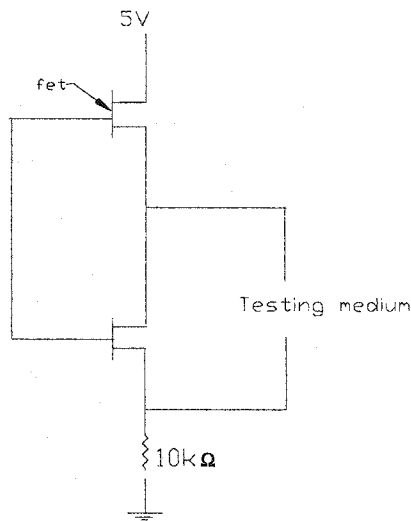


**Figure 6.4: Electrical Circuitry**

The 10kΩ resistor in series with the medium was used to determine the current. Base line testing of the ability for the electrode configurations to measure a steady drop in voltage (referring to a constant resistivity measurement) was initially investigated. The drop in voltage across the specimen was measured and data was logged by Labview.

*6.4.4    Sources of Error*

There are several possible sources of error that the two test methods involving conductivity/resistivity measurements may have in common, and some initial tests are illustrated in Appendix C. Although, some noise is inherently a part of laboratory readings, often backaveraging techniques are utilized to reduce significant scatter in electrical readings. However, due to dynamic measurements obtained in the laboratory to avoid charging effects from occurring between the electrodes, back averaging is not effective nor representative. At the time of initial testing, it was not possible to isolate the source of the noise in the laboratory. Poor

connections and resistance in the lead could have affected the sensitivity of the readings, and could have been the source of the noise. Noise fluctuations in comparison to the constant resistor are illustrated in Figure 6.5, in a solution of KOH contained within the Teflon lined sample cylinder.
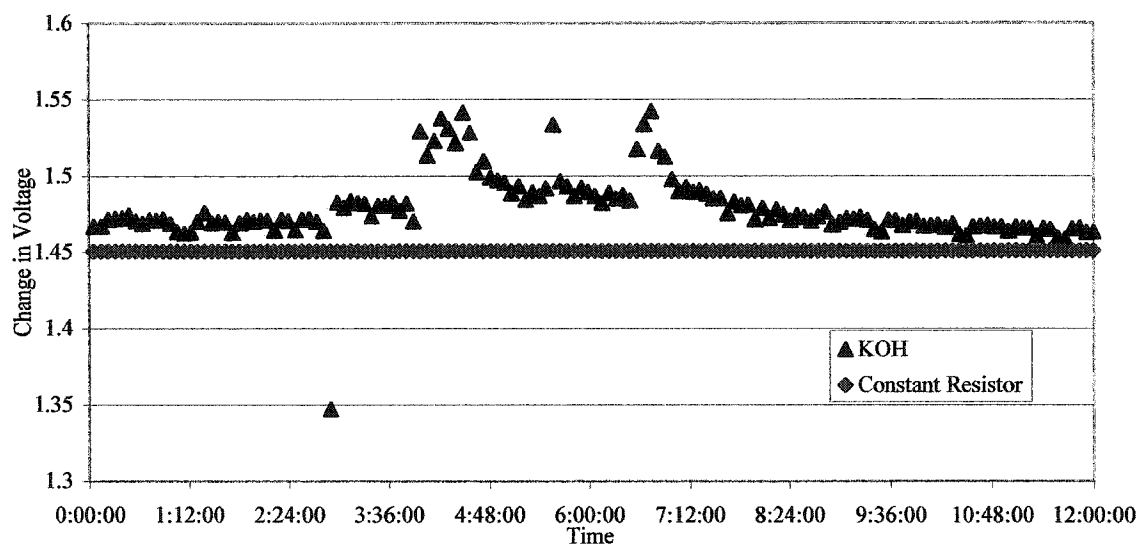


**Figure 6.5: Electrical Resistivity Measurement with Time (KOH in sample cylinder)**

Obtaining good electrical contact, especially with the current electrodes can be difficult. Often electrodes are dipped in soft solder, or are constructed of tinfoil or mercury (Parkhomenko, 1967). However, corrosion at the point of contact can cause difficulties during long term testing. Connections between the leads and the electrodes could have posed potential errors. It was difficult to avoid rusting of the soldered joints in both water and brine. Ensuring secure contacts can be difficult, especially when the majority of the contacts are submersed in water. Careful consideration of the contact areas, and the potential for a short must be identified. The contact between the electrical lead and the wire mesh is extremely important, and it was found that some corrosion at that point may have lead to unstable results.

Other possible sources of noise were determined to be the ambient temperature fluctuations, improper experimental electrode setup and the effect of the solution itself. Although techniques to prevent external laboratory noise were not implemented, i.e. the addition of shielded wiring etc., it was not done because constant resistance measurement devices put along side the laboratory measurements did not yield much fluctuation within the same time. It was determined

that it was potentially a sensitivity to temperature in the solution, or the electrode setup. However, the amount of noise that was seen by the wires was not expected.

It was felt that changes in ambient air temperatures could have possibly lead to the fluctuations in resistivity. Therefore, the temperature of the room was mapped, and ultimately the KOH absorber was placed inside the constant temperature water bath. It was determined that the temperature was not the ultimate cause in the noise found in the laboratory. However, no correlation between the temperature and voltage readings were found. Upon isolation of the resistivity measurements from fluctuating ambient temperatures, spurious readings were still present.

Greater difficulties were observed in the measurements of resistivity across the clay specimen. It was initially felt that the variations were due to the inability to properly isolate the system from external sources of conducting materials. Potential for surrounding conductive materials to short the circuit, and provide noise to the electrical measurements can cause significant noise problems if not properly isolated. Due to the application of high pressures in the modified triaxial cell, it was determined that nonconducting porous stones such as ceramic and corundum could not be used. Utilising fused glass beads as porous stones was difficult because the uniformity of the porous space could not be confirmed. It was difficult to ensure that the beads were fused to the desired pore space opening. Further crushing of the glass beads within the triaxial cell at high confining pressures may occur, particularly under deviatoric stresses. Nickel porous stones were employed due to the ease and availability of their usage. The segregation of the nickel porous stones from the electrodes was achieved by placing perforated Teflon disks between the porous stones and the electrode. Metallic membranes or mercury barrier used to prevent gas diffusion was another source of possible noise. Segregation of the electrodes from the metallic membranes was difficult, and additional latex or thin polyethylene shrink film was thought to provide additional shielding. To ensure additional protection, it was determined that the diameter of the wire mesh would be cut smaller than diameter of the end caps, and set inside the perforated Teflon disks for added protection from the surrounding metal.

Unfortunately, reduction in the noise of the system, and the occasional spiking was not successful. It was determined that noise was an inherent part of the system, and that stable resistivity measurements within the triaxial cell could not be achieved. Electrical resistivity across the clay specimen was aborted due to the instability, and significant noise experienced in the readings. It was assumed that the instability was due to the length of the line, the contact with or short due to the surrounding metal, which could not be removed, and/or poor contacts. The

investigation into the qualitative use of $CO_2$ was placed on hold, to decide the next steps. Due to the nature of the test, electrical noise would have a significant effect on the measurement of $CO_2$ changes in resistivity.

Resistance in the leads can affect the accuracy of the measurement of resistance. Generally, this can be reduced by having a three or four lead system, whereby two leads send a known current through the wire, and the other leads are used to measure the voltage drop across the wire. From this information, the resistance of the wire can be calculated with a minimum effect from the leads and connectors. This is the case for high precision RTD temperature probes, which were used in measuring and controlling the temperature of the water bath. In addition, these temperature probes were constructed of platinum wire and coil, reducing the source of error. The lack of noise from the constant resistance pot suggested that the two electrode system was not causing a problem, however, it was not anticipated that the extra length in the wiring to the triaxial cell was creating an antenna effect for the noise.

Although, at the time it was felt that the wiring was not shielded properly, and was therefore receiving outside noise, it was later determined that the cause of the problem was due to inadequate laboratory grounding. Laboratory measurements were halted, to seek out the problem associated with the large noise and spiking. In July of 2002, it was determined the laboratory contained no true ground, and therefore noise would have a significant influence on measurements. The additional wire length between that of the resistor and the laboratory setup was substantial. And in effect was acting as antennas in noise pickup. Therefore, no further experiments were conducted with respect to electrical resistivity, both quantitative and qualitative.

The possibility of isolating the noise issue, and finding a proper solution to the electrical resistivity technique requires that a proper ground be in place, in order to determine that the noise issues are in fact related to the experimental configuration of the electrodes, poor contacts, and other potential sources of error.

### 6.4.5   *Possible Solutions to the Noise Problem*

During the course of the testing it was determined that the noise of the system was inherently a result of its setup, and therefore the 2 electrode system was not able to accurately measure the electrical resistivity in the medium. It was possible that the leads, which were taking the resistivity measurements from the setup, were causing a certain amount of noise, which was affecting the overall result of the setup. The following could be tried to reduce laboratory noise:

- change the setup to a four electrode system

- twist the leads, this reduces AC noise, and helps to prevent electrical pickup from other sources of equipment

- if twisting is not an option, shielded coaxial wire is can be used to remove any environmental noise from affecting the reading

Next steps would likely have involved additional shielding of the wires, to reduce the effect of the resistance in the line, and a reduction in atmospheric noise; and the improvement of contact connections. However, in the laboratory setup, it was not possible to twist the leads going to the laboratory setup. In conclusion, it is likely that the source of noise is from the pickup of ambient noise within the laboratory, and peripheral equipment in neighboring laboratories which has resulted in spiking and increased noise levels. Decreasing the noise can be achieved by shielding the wires going to the sample setup. However, in order for shielding to be effective, the shield itself must be properly grounded. If it is not properly grounded, then the shield itself can add to the noise, and increase the reading of the noise. Given the large sources of noise present in the laboratory, it was difficult to isolate the problems in the lab from laboratory technique, to noise in the laboratory electrical power system.

6.5    Data Acquisition

Both the Azonix 1011 temperature probes, and the ISCO syringe pumps have an RS-232 serial communication port, such that temperature, pressure, volume, and flow rate data can be collected and recorded by the LABview data acquisition system. Based on the information collected by the acquisition software, the LABview PI control loop controlled the voltage output to the water bath based on the information from the temperature probes, providing a constant temperature environment for which the cell operated under. Electrical resistivity measurements and the constant resistance control data was also monitored and collected by the same system. The lab in its current configuration is capable of sampling automatically throughout the course of the testing. Samples are then sent to a laboratory for analysis of $CO_2$ content.

6.6    Summary

It is important to determine the acceptable lag time between the point at which $CO_2$ exits the specimen, and the point at which its concentration is measured. However, the upper limit of travel time of $CO_2$ through the sample, will likely be determined by the flow of $CO_2$ by means of relative gas permeability. However, it is estimated that this will require a time period in the order of two weeks. The limiting factor is therefore the time it takes the $CO_2$ to move through the

sample which should be far greater than the time it takes the $CO_2$ to migrate from the downstream side of the specimen to its final sampling destination point.

There are a variety of methods which can be utilized to determine the changes of $CO_2$ concentration, from the very labour intensive titration techniques, to the automatic gas chromatography (GC) techniques. Gas chromatographs are used the most frequently, due to their ability to test very low to very high concentration levels.

Continuous measurements of $CO_2$ using electrical conductivity measurements, over extended periods of time, have been utilized. Although efforts to determine the qualitative and quantitative measurements of $CO_2$ in the laboratory using electrical measurements were not entirely successful, an interim method of obtaining quantitative $CO_2$ values can be used. Sample collection, and subsequent testing in a laboratory will be able to provide adequate information on the transport behaviour of gases in clay shales. Modifications to the laboratory setup, and the introduction of a proper ground may result in more positive results concerning the determination of electrical resistivity/conductivity in the laboratory.

# 7.0 Conclusions

Cap rock integrity is one of the most important factors in determining the risk and reliability of deep saline aquifer disposal. Despite the fundamental importance of cap rock, it has received little attention in past research efforts associated with aquifer disposal. Increasingly, more focus is being paid to the state of the cap rock in selected greenhouse gas disposal sites. The ability to accurately test gas transport mechanism in the laboratory to answer fundamental questions associated with its migration properties will be invaluable.

Due to a difference in scale effects between the laboratory and the field, it is imperative that the laboratory be set-up to best suit realistic field conditions, in order to obtain reasonable data. Currently, $CO_2$ storage in deep aquifers is proposed in aquifers whose top depth is greater than 800m, which in general is the point at which supercritical $CO_2$ exists.

In this research, experimental apparatus to investigate the movement of $CO_2$ through clay shales, an analogue to potential cap rock materials, was designed. Gas permeability, diffusion and the role of adsorption on gas transport in the laboratory can be achieved in this testing facility. It is capable of maintaining temperatures to $0.05°C$, and utilises high pressure syringe pumps with the an accuracy of 0.5% of its full scale range.

Specialised sealing devices have been incorporated into the design of the modified triaxial flow cell, such that thin (0.15mm) metal membranes can be utilized, and effectively sealed to the end caps. Gas impermeable membranes used in the experimental set-up, and stringent temperature control allows for the determination of intact adsorption of geologic materials.

An in-line method of determining the movement of $CO_2$ across the specimen was evaluated. An unsuccessful attempt at utilising electrical conductivity measurements to evaluate the movement of $CO_2$ through the specimen was investigated. In the current laboratory set-up the samples will be automatically sampled, extracted and its concentration will be determined in the laboratory.

This research potentially provides a means of fundamentally testing the risk associated with gas transport in saline aquifers. It is easily modified to suit a variety of material types, core sizes, and test conditions.

## 7.1  Recommendations for further research

Utilising electrical resistivity measurements in the laboratory is possible, if the noise issues can be determined and isolated.  As a first measure, it would be ideal to isolate the general noise issues associated with improper grounds.  It would be very difficult to isolate the issues related to the electrical response of clays or solutions under such variability.  Options to shield the wire, or incorporate a four electrode design would not be as valuable until the problem of grounding is resolved.

The next steps include the assessment of gas permeability in tight clay shales to determine the applicability of Darcy's law for these class of materials.  Evaluation of the dominant transport mechanism present in tight clay shales under the situation of geological storage.  Determine the potential for clay shales to adsorb $CO_2$ in water saturated intact specimens.  It is of interest to determine the differences between adsorption in crushed and in water saturated intact specimens.  Assessment of discontinuities and its effect on the flow characteristics is also of interest.  Clay shales are only one class of materials thought to be potential cap rock materials in GHG storage.

The current testing facility can be used to determine the transport mechanisms in a variety of applications, as it is not solely applicable to clay shales.

# References

ASTM D-422. Standard test method for particle-size analysis of soils (D-422-63). Annual book of ASTM standards (2002) V.04.08 p.10-17.

ASTM D-854. Standard test for specific gravity of soils (D-854-92). Annual book of ASTM standards (2002) V.04.08 p.93-99.

ASTM D-1434. Standard test method for determining gas permeability characteristics of plastic film and sheeting. Annual book of ASTM standards (2002) V.15.09 p.194-205.

ASTM D-2216. Standard test method for laboratory determination of water (moisture) content of soil and rock (D-2216-92). Annual book of ASTM standards (2002) V.04.08 p.218-222.

ASTM D-3985. Standard test method for oxygen gas transmission rate through plastic film and sheeting using a coulometric sensor (D3985-81). Annual book of ASTM standards (2002) V.15.09 p.472-477.

ASTM D-4318. Standard test method for liquid limit, plastic limit, and plasticity index of soils (D-4318-84). Annual book of ASTM standards (2002) V 04.08 p.567-580.

Ahmed, M.K., R. Geetha, N.K. Pandey, S. Murugesan, S.B. Koganti, B.Saha, P.Sahoo, M.K. Sundararajan. 2000. Conductometric determination of carbon in uranium carbide and its solution in nitric acid. Talanta V.52 p.885-892.

Al-hawaree, M. 1999. Geomechanics of $CO_2$ sequestration in coalbed methane reservoirs. MSc. Thesis, University of Alberta. 196pp.

Bachu, S., M. Brulotte, M. Grobe, S. Stewart. 2000. Earth sciences report 2000-11: Suitability of the Alberta subsurface for carbon dioxide sequestration in geological media. Alberta Energy and Utilities Board, Alberta Geological Survey. 86pp.

Bachu, S. 1999. Sequestration of $CO_2$ in geological media: criteria and approach for site selection in response to climate change. Energy Conservation and Management V.41 p.953-970.

Bachu, S. and R.A. Burwash. 1994. Geothermal regime in the Western Canada Sedimentary Basin, chapter 30. In Geological Atlas of the Western Canada Sedimentary Basin. Mossop, G.D. and I. Shetsen (eds.) p.437-454. Alberta Research Council and Canadian Society of Petroleum Geologists.

Bachu, S., W.D. Gunter, E.H. and Perkins. 1994. Aquifer disposal of $CO_2$: hydrodynamic and mineral trapping. Energy Conservation and Management V.35 no.4 p.269-279.

Balasubramonian, B. 1972. Swelling of compaction shale. PhD Thesis, University of Alberta. 236pp.

Barrer, R.M. 1951. Diffusion in and through solids. Cambridge University Press. 464pp.

Bell, J.S., P.R. Price, and P.J. McLellan. 1994. In-situ stress in the Western Canada Sedimentary Basin, chapter 29. *In* Geological Atlas of the Western Canada Sedimentary Basin. Mossop, G.D. and I. Shetsen (eds.) p.439-446. Alberta Research Council and Canadian Society of Petroleum Geologists.

Bergman, P.D., E.M. Winter, Z-Y. Chen. 1997. Disposal of power plant $CO_2$ in depleted oil and gas reservoirs in Texas. Energy Conservation and Management V.38 suppl. p.S211-S216.

Bishop, A.W. and D.J. Henkel. 1964. The measurement of soil properties in the triaxial test. Edward Arnold Ltd. 228pp.

Brace, W.F., A.S. Orange, and T.R. Madden. 1965. The effect of pressure on the electrical resisitivity of water-saturated crystalline rocks. Journal of Geophysical Research, V.70 no.22 p.5669-5678.

Brace, W.F., and A.S. Orange. 1968. Further studies of the effects of pressure on electrical resisitivity of rocks. Journal of Geophysical Research, V.73 no.16 p.5407-5419.

Brace, W.F., J.B. Walsh, and W.T. Frangos. 1968. Permeability of granite under high pressure. Journal of Geophysical Research V.73 p.2225-2236.

Bruno T.J., and P.D.N. Svoronos (eds). 1989. CRC handbook of basic tables for chemical analysis. CRC Press Inc., Florida, USA. 517pp.

Caillet, G., 1993. The cap rock of the Snorre Field, Norway: a possible leakage by hydraulic fracturing. Marine and Petroleum Geology, V.10 p.42-50.

Cave, M., S. Reeder, and J. Artaz. 1994. Preliminary evaluation of physical and statistical methods to determine the chemical composition of clay pore waters. Hydraulic and hydrochemical characterization of argillaceous rocks proceedings of an international workshop, June 7-9 p.235-246. Nottingham, UK.

Çengel, Y.A. and M.A. Boles. 1989. Thermodynamics: an engineering approach. Mc-Graw Hill Inc., USA. 867pp.

Chan, C.Y., H.M. Buettner, R. Newmark, and G. Mavko. 2000. Conductivity measurements of sand-clay mixtures: A modified experimental method. Journal of Environmental and Engineering Physics, Vol 5, Issue 3 p.15-26.

Craig, R.F. 1987. Soil Mechanics, 4th Ed. Chapman & Hall. 410pp.

Crank, J. 1975. The mathematics of diffusion, 2nd Ed. Oxford University Press. 414pp.

Crooks, V.E. and R.M. Quigley. 1984. Saline leachate migration through clay: a comparative laboratory and field investigations. Canadian Geotechnical Journal V.21 p.349-362.

Cunningham, R.E. and R.J.J. Williams. 1980. Diffusion in gases and porous media. Plenum Press, New York, USA. 275pp.

Cussler, E.L. 1997. Diffusion: mass transfer in fluid systems, 2$^{nd}$ Ed. Cambridge University Press, USA. 580pp.

Demir, I. 1988. The interrelation of hydraulic and electrical conductivities, streaming potential, and salt filtration during the flow of chloride brines through a smectite layer at elevated pressures. Journal of Hydrology V.98 p31-52.

Dewhurst, D.N., Y. Yang, and A.C. Aplin. 1999. Permeability and fluid flow in natural mudstones, *In:* Aplin, A.C., A.J. Fleet, and J.H.S. Macquaker (eds). Muds and mudstones: physical and fluid-flow properties, Geological Society, London, Special Publications No. 158, p.23-44

Eaton, A.D., L.S. Clesceri, and A.E. Greenberg (eds). 1995. Standard methods for the examination of water and wastewater, 19$^{th}$ Ed.

Enick, R.M. and S.M. Klara. 1990. $CO_2$ solubility in water and brine under reservoir conditions. Chemical Engineering Communications V.90 p.23-33.

Entwisle, D.C. and S. Reeder. 1993. New apparatus for pore fluid extraction from mudrocks for geochemical analysis, chapter 15 *In:* Manning, D.A.C., P.L. Hall, and C.R. Hughes (eds) Geochemistry of clay-pore fluid interactions, p.365-388. Chapman and Hall, London.

Ellis, A.J. and R.M. Golding, 1963. The solubility of carbon dioxide above 100°C in water and in sodium chloride solutions. American Journal of Science V.261 p.47-60.

Felder R.M., and R.W. Rousseau. 1986. Elementary principles of chemical processes, 2$^{nd}$ Edition. John Wiley & Sons. 668pp.

Fetter, C.W. 1993. Contaminant hydrogeology. Macmillan Publishing Company, USA. 458pp.

Fogg, P.G.T., and W. Gerrard. 1991. Solubility of gases in liquids: a critical evaluation of gas/liquid systems in theory and practice. John Wiley & Sons, USA. 332pp.

Fredlund, D.G. 1973. Volume change behaviour of unsaturated soils. PhD Thesis. University of Alberta. 490pp.

Freeze, R.A., and J.A. Cherry. 1979. Groundwater. Prentice-Hall, Englewood Cliffs, New Jersey, USA. 604pp.

Freund, P. and W.G. Ormerod. 1997. Progress toward storage of carbon dioxide. Energy Conservation and Management V.38 Suppl. pS199-S204.

Fripiat, J.J., M.I. Cruz, B.F. Bohor, and J.Jr. Thomas. 1974. Interlamellar Adsorption of Carbon Dioxide by Smectites. Clays and Clay Minerals V. 22 p.23-30.

Gallé, C. 2000. Gas breakthrough pressure in compacted Fo-Ca clay and interfacial gas overpressure in waste disposal context. Applied Clay Science V. 17 p.85-97.

Grim, R.E. 1968. Clay Mineralogy 2$^{nd}$ Ed. McGraw-Hill Inc., New York. 596pp.

Govind, R., C. Gao, L. Lai and H.H. Tabak. 1997. Continuous, automated and simultaneous measurement of oxygen uptake and carbon dioxide evolution in biological systems. Water Environment Research V 63 p.73-80.

Golder Associates. 1981. Geotechnical assessment Gulf-Aostra Surmont project Proceeding no. 960952, appendix F – laboratory testing. Calgary, Alberta, Canada.

Griffin, R.A. and J.J. Jurinak. 1973. Estimation of activity coefficients from the electrical conductivity of natural aquatic systems and soil extracts. Soil Science V. 116 no.1 p.26-30.

Grozic, J.L.H. 1999. The behaviour of loose gassy sand and its susceptibility to liquefaction. PhD Thesis. University of Alberta.

Grunau, H.R. 1987. A worldwide look at the cap rock problem. Journal of Petroleum Geology V. 10 no.3 p.245-266.

Gunter, W.D., T. Gentzis, B.A. Rottenfusser, and R.J.H. Richardson. 1997. Deep coalbed methane in alberta, canada: a fuel resource with the potential of zero greenhouse gas emissions. Energy Conservation and Management V.38. Suppl. p.S217-S222.

Gunter, W.D., S. Bachu, D.H-S. Law, V. Marwaha, D.L. Drysdale, D.E. MacDonald, T.J. McCann. 1996. Technical and economic feasibility of $co_2$ disposal in aquifers within the Alberta Sedimentary Basin, Canada. Energy Conservation and Management V.37. p.1135-1142.

Gunter, W.D., E.H. Perkins, T.J. McCann. 1993. Aquifer disposal of $co_2$-rich gases: reaction design for added capacity. Energy Conservation and Management V.34 no.9-11 p.941-948.

Gunzler, H. and A. Williams (eds). 2001. Handbook of analytical techniques volume II. Wiley-Vch, Germany. 1182pp.

Harrington J.F., and S.T. Horseman, 1999. Gas transport properties of clays and mudrocks. In: Aplin, A.C., A.J. Fleet, and J.H.S. Macquaker (eds). Muds and mudstones: physical and fluid-flow properties, Geological Society, London, Special Publications V.158, p.107-124.

Harrison, W.J., R.F. Wendlandt, and E.D. Sloan. 1995. Geochemical interactions resulting from carbon dioxide disposal on the sea floor. Applied Geochemistry V 10, No.3 p.461-475.

Head, K.H. 1982. Manual of soil laboratory testing volume 2:permeability, shear strength and compressibility tests. John Wiley and Sons, USA. 747pp.

Hedberg, H.D., 1974. Relation of methane generation to undercompacted shales, shale diapirs and mud volcanoes. Bulletin, American Association of Petroleum Geologists, V 58 p.661-673.

Hildenbrand, A., S. Schlömer, and B.M. Krooss. 2002. Gas breakthrough experiments on fine-grained sedimentary rocks. Geofluids V.2 p.1-21.

Hoek, E. and J.A. Franklin. 1968. A simple triaxial cell for field and laboratory testing of rock. Transactions of the Institution of mining and metallurgy V. 77 p.A22-26.

Holloway, S. 1997. Safety of underground disposal of carbon dioxide. Energy Conservation and Management V.38 Suppl. p.S241-S245.

Holloway, S., J.P. Heederik, L.G.H. van der Meer, I. Czernichowski-Lauriol, R. Harrison, E. Lindeberg, I.R. Summerfield, C. Rochelle, T. Schwarzkopf, O. Kaarstad, B. Berger 1996. The underground disposal of carbon dioxide summary report, Joule II. British Geological Survey, Keyworth, Nottingham, UK. 24pp.

Holloway, S. and D. Savage. 1993. The potential for aquifer disposal of carbon dioxide in the UK. Energy and Conversion Management V.34 no.9-11 p.925-932.

Horseman, S.T., J.J.W. Higgo, J. Alexander and J.F. Harrington, 1996. Water, gas and solute movement through argillaceous media. Report CC-96/1 Nuclear Energy Agency. 306pp.

Houghton, J. 1997. Global warming the complete briefing. 2nd Ed. Lion Publishing Inc., Oxford, England. 251pp.

Humé, H.B. 1993. Procedures and apparatus for measuring diffusion and distribution coefficients in compacted clays. AECL Research Report 10981 Whiteshell Laboratories, Pinawa Manitoba. 40pp.

Hsieh, P.A., J.V. Tracy, C.E. Neuzil, J.D. Bredehoeft, S.E. Silliman. 1981. A transient laboratory method for determining the hydraulic properties of tight rocks – I theory. International Journal of Rock Mechanics and Mining Sciences & Geomechanics Abstracts V.18 p.245-252.

Ingram, G.M., J.L. Urai, and M.A. Naylor, 1997. Sealing processes and top seal assessment, *In*: Moller-Pedersen, P., and A.G. Koestler (eds). Hydrocarbon Seals: Singapore, Norwegian Petroleum Society, Special Publications, Elseveir, p.165-174.

Issac, B.A., Dusseault, M.B., Lobb, G.D., Root, J.D. 1982. Characterization of the lower cretaceous overburden for oil sands surface mining within Syncrude Canada Ltd. Leases northeast, Alberta, Canada, *In:* Balkema, A.A (ed) Proceedings of the International Association of Engineering Geology, V.2 p.371-384.

Jenkins, R.C.L., P.M. Nelson, and L. Spirer. 1970. Calculation of the transient diffusion of a gas through a solid membrane into a finite outflow volume. Faraday Society Transactions V.66 pt.2 p.1391-1401.

Johnson, J.W., J.J. Nitao, C.I. Steefel, and K.G. Knauss. 2001. Reactive transport modeling of geologic $CO_2$ sequestration in saline aquifers: the influence of intra-aquifer shales and the relative effectiveness of structural, solubility, and mineral trapping during prograde and retrograde sequestration. Pre-print from: First National Conference on Carbon Sequestration 60pp. U.S. DOE, Washington, D.C.

Katsube, T.J., B.S. Mudford, and M.E. Best. 1991. Petrophysical characteristics of shales from the scotian shelf. Geophysics, V.56 no.10 p.1681-1689.

Katsube, T.J, and J.B. Walsh. 1987. Effective aperture for fluid-flow in microcracks. International Journal of Rock Mechanics and Mining Sciences & Geomechanics Abstracts V.24 no.3 p.175-183.

Ko, H-W, and H-K Juang. 1983. Absorption of $CO_2$ by alkaline electrolyte and its effect on electrical discharge. Journal of applied electrochemistry V.13 p.725-730.

Krom, T.D., F. Lyngsie Jacobsen, and K. Hvid Ipsen. 1993. Aquifer based carbon dioxide disposal in denmark: capacities, feasibility, implications, and state of readiness. Energy Conservation and Management V.34 no.9-11 p.933-940.

Krooss, B.M., S. Schloemer, R. Ehrlich, 1998. Experimental investigation of molecular tranposrt and fluid flow in unfaulted and faulted pelitic rocks. *In:* Jones, G., Q.J. Fisher, R.J. Knipe, (eds). Faulting, fault sealing and fluid flow in hydrocarbon reservoirs, Geological Society, London Special Publications V.147 p.135-146.

Krooss, B.M., and D. Leythaeuser. 1997. Diffusion of methane and ethane through the reservoir cap rock: implications for the timing and duration of catagenesis: discussion. The American Association of Petroleum Geologists Bulletin V.81 no.1 p.155-161.

Krooss, B.M., D. Leythaeuser, R.G. Schaefer. 1992a. The quantification of diffusive hydrocarbon losses through cap rocks of natural gas reservoirs – A re-evaluation. The American Association of Petroleum Geologists Bulletin V.76 no.3 p.403-406.

Krooss, B.M., D. Leythaeuser, R.G. Schaefer. 1992b. The quantification of diffusive hydrocarbon losses through cap rocks of natural gas reservoirs – A re-evaluation: Reply. The American Association of Petroleum Geologists Bulletin V.76 no.11 p.1842-1846.

Krooss, B.M. and D. Leythaeuser. 1988. Experimental measurements of the diffusion parameters of light hydrocarbons in water saturated sedimentary rocks – II results and geochemical significance. Organic Geochemistry V 12, p.91-108.

Krooss, B.M., and R.G. Schaefer. 1987. Experimental measurements of the diffusion parameters of light hydrocarbons in water saturated sedimentary rocks – I A new experimental procedure. Organic Geochemistry V 11, no.3 p.193-199.

Kyle, B.G. 1992. Chemical and process thermodynamics, 2nd Edition. Prentice-Hall, USA. 567pp.

Law, D.H.-S. and S. Bachu. 1996. Hydrogeological and numerical analysis of $CO_2$ disposal in deep aquifers in the Alberta Sedimentary Basin. Energy Conservation and Management V.37 no.6-8 p.1167-1174.

Lemmon, E.W., M.O. McLinden and D.G. Friend. 2001. Thermophysical Properties of Fluid Systems *In*: NIST Chemistry WebBook, NIST Standard Reference Database Number 69 Linstrom, P.J. and W.G. Mallard (Eds). National Institute of Standards and Technology, Gaithersburg MD, 20899 (http://webbook.nist.gov).

Lewis, G.N. and M. Randall. 1961. Thermodynamics 2nd Ed. McGraw-Hill Inc. 723pp.

Leythaeuser, D., R.G. Schaefer, and A. Yukler. 1982. Role of diffusion in primary migration of hydrocarbons, AAPG Bulletin V.66, p.408-429.

Liu, X. and P. Ortoleva. 1996. A coupled reaction and transport model for assessing the injection, migration and fate of waste fluids. SPE 36640. Annual Technical Conference and Exhibition held in Denver, Colorado, USA October 6-9 p.661-673.

Lu, X., F. Li, and A.T. Watson. 1995. Adsorption measurements in devonian shales. Fuel V.74 p.599-603.

Mackay, P.L., E.K. Yanful, R.K. Rowe, and B. Kazem. 1998. A new apparatus for measuring oxygen diffusion and water retention in soils. Geotechnical Testing Journal, GTJODJ, V 21 no. 4 p.289-296.

Malinin, S.D. and N.I. Savelyeva, 1972. The Solubility of $CO_2$ in NaCl and $CaCl_2$ solutions at 25, 50, and 75° under elevated $CO_2$ pressures. Geochemistry International p.410-417.

Markham, A.E. and K.A. Kobe, 1941. The solubility of carbon dioxide and nitrous oxide in aqueous salt solutions, Journal of the American Chemical Society V.64 p.449-454.

McPherson, B.J.O.L., and B.S. Cole. 2000. Multiphase $CO_2$ flow, transport, and sequestration in the Powder River Basin, Wyoming, USA. Journal of Geochemical Exploration, V. 69-70, p.65-69.

Mitchell, J.K. 1993. Fundamentals of soil behaviour, 2nd Ed. John Wiley & Sons. 437pp.

Morgenstern, N.R. and B.I. Balasubramonian. 1980. Effects of pore fluid on the swelling of clay-shale, In: (ed) Snethen, D. Proceedings of the 4th International conference on Expansive soils held in Denver, Colorado, USA June 16-18 p.190-205. American Society of Civil Engineers.

Mossop, G.D., and I. Shetsen. 1994. Introduction to the geological atlas of the western canada sedimentary basin, chapter 1. In Geological atlas of the Western Canada Sedimentary Basin. G.D. Mossop and I. Shetsen (eds.). p.1-11. Alberta Research Council and Canadian Society of Petroleum Geologists.

Nelson, J.S., and E.C. Simmons. 1992. The quantification of diffusion hydrocarbon losses through cap rocks of natural gas reservoirs – A re-evaluation: Discussion. The American Association of Petroleum Geologists Bulletin V.76 no.11 p.1839-1841.

Nelson, J.S., and E.C. Simmons, 1995. Diffusion of methane and ethane through the reservoir cap rock: implications for the timing and duration of catagenesis. The American Association of Petroleum Geologists Bulletin V.79 no.7 p.1064-1073.

Nelson, J.S., and E.C. Simmons, 1997. Diffusion of methane and ethane through the reservoir cap rock: implications for the timing and duration of catagenesis: Reply. The American Association of Petroleum Geologists Bulletin V.81 no.1 p.162-167.

Neuzil, C.E. 2000. Osmotic generation of 'anomalous' fluid pressures in geological environments. Nature V.403 p.182-184.

Neuzil, C.E. 1994a. How permeable are clays and shales? Water Resource Research V.30 no.2 p.145-150.

Neuzil, C.E. 1994b. Characterization of flow properties, driving forces, and pore-water chemistry in the ultra-low-permeability Pierre shale, North America. Hydraulic and hydrochemical characterization of argillaceous rocks proceedings of an international workshop, June 7-9. p.65-74. Nottingham, UK.

Neuzil, C.E., C. Cooley, S.E. Silliman, J.D. Bredehoeft, P.A. Hsieh. 1981. A transient laboratory method for determining the hydraulic properties of tight rocks – II application. International Journal of Rock Mechanics and Mining Sciences & Geomechanics Abstracts V.18 p.253-258.

Parkhomenko, E.I. 1967. Electrical properties of rocks. Plenum Press, New York, USA. 314pp.

Pastorek, R.L. and R.A. Rapp. 1969. Solubility and diffusion of $O_2$ in solid copper from electrochemical measurements. Transactions of the Metallurgical society AIME V 245 no.8 p.1711-1720.

Pearce, J.M., S. Holloway, H. Wacker, M.K. Nelis, C. Rochelle, and K. Bateman. 1996. Natural occurrences as analogues for the geological disposal of carbon dioxide. Energy and Conversion Management V.37 no.6-8 p.1123-1128.

Pearson, F.J., 1999. What is the porosity of a mudrock? *In:* Aplin, A.C., A.J. Fleet, and J.H.S. Macquaker (eds). Muds and mudstones: physical and fluid-flow properties, Geological Society, London, Special Publications no. 158 p9-21.

Perkins E.H. and W.D. Gunter. 1996. Mineral traps for carbon dioxide, *In:* Hitchon, B (ed) Aquifer disposal of carbon dioxide hydrodynamic and mineral trapping-proof of concept. p.93-112.

Petroleum Research Corporation. 1958. Principles of osmosis applicable to oil hydrology. Research report B-2, Denver, Colorado, USA. 66pp.

Rebour, V., J. Billiotte, M. Deveughele, A. Jambon, C. le Guen, 1997. Molecular diffusion in water-saturated rocks: A new experimental method. Journal of contaminant hydrology V.28 p.71-93.

Reddy, T.V.K. and N. J. Raju. 1990. A statistical approach between total dissolved solids and electrical conductivity – A study. Journal of the institution of engineers (India) Civil Engineering Division. p. 151-152.

Reeder, S. and D.C. Entwisle. 1994. Pore fluid extraction by mechanical squeezing. Hydraulic and hydrochemical characterization of argillaceous rocks proceedings of an international workshop, June 7-9. p.247-256. Nottingham, UK.

Renner, T.A. 1986. Measurement and correlation of diffusion coefficients for $CO_2$ and rich gas applications. SPE 15391. Presented at the 61st Annual Technical Conference and Exhibition of the Society of Petroleum Engineers in New Orleans, October 5-8 p.1-12.

Rodwell, W.R., A.W. Harris, S.T. Horseman, P. Lalieux, W.Müller, L. Ortiz Amaya, and K. Preuss. 1999. Gas Migration and To-Phase Flow through Engineered and Geological Barriers for a Deep Repository for Radioactive Waste. EC/NEA Status Report.

Rostron, B.J. 1993. Numerical simulations of how cap-rock properties can control differential entrapment of oil. Presented at the 68th Annual Technical Conference in Houston, Texas October 3-6 p.263-275.

Schatz, J.F., A.J. Olszewski and R.A. Schraufnagel. 1993. Scale dependence of mechanical properties: Application to the oil and gas industry. SPE Rocky Mountain Regional/Low permeability reservoir symposium. Denver, CO, USA April 12-14 1993 p.615-624.

Schettler, P.D., and C.R. Parmely. 1991. Physicochemical Properties of Methane Storage and Transport in Devonian Shale. Gas Research Institute. 65pp.

Schlomer, S. and B.M. Krooss. 1997. Experimental characterization of the hydrocarbon sealing efficiency of cap rocks. Marine and Petroleum Geology, V. 14 no. 5 p.565-580.

Sen, P.N., P.A. Goode, and A. Sibbit. 1988. Electrical conduction in clay bearing sandstones at low and high salinities. Journal of Applied Physics V.63 no.10 p.4832-4840.

Shelby, J.E. 1996. Handbook of gas diffusion in solids and melts. ASM International, USA. 240pp.

Sobkowicz, J.C. 1982. The mechanics of gassy sediments. PhD Thesis University of Alberta. 531pp.

Span, R., and W. Wagner. 1996, A new equation of state for carbon dioxide covering the fluid region from the triple-point temperature to 1100 K at pressures up to 800 MPa, J. Phys. Chem. Ref. Data, V. 25 p.1509-1596.

Sterne, K.B. 1981. Hollow cylinder testing of oil sands. MSc. Thesis. University of Alberta. 228pp.

Stesky, R.M. 1986. Electrical conductivity of brine-saturated fractured rock. Geophysics, V.51 no.8 p.1585-1593.

Stevens, S.H., J.M. Pearce, A.J. Rigg, 2001. Natural analogs for geologic storage of $CO_2$: an integrated global research program. Pre-print from: First National Conference on Carbon Sequestration 12pp. U.S. DOE, Washington, D.C.

Stevens, S.H., C.E. Fox, L.S. Melzer. 2000. McElmo Dome and St. Johns natural $CO_2$ deposits: analogs for geologic sequestraion. Fifth International Conference on Greenhouse Gas Control Technologies, p.317-321 Cairns, Queensland, Australia, August 13-16.

Stevens, S.H., V.A. Kuuskraa, and J.J. Taber. 1999. Sequestration of $CO_2$ in depleted oil and gas fields: barriers to overcome in implementation of $CO_2$ capture and storage (disused oil and gas fields) IEA/CON/98/31 Final Report. 116pp.

Takenouchi, S. and G.C. Kennedy. 1965. The solubility of carbon dioxide in NaCl solutions at high temperatures and pressures. American Journal of Science, V.263 p.445-454.

Tanaka, S., H. Koide, and A. Sasagawa. 1995. Possibility of underground $CO_2$ sequestration in Japan. Energy Conservation and Management V.36 no.6-9 p.527-530.

Tavenas, F., P. Jean, P. Leblond, and S. Leroueil. 1983. The permeability of natural soft clays. part I: Methods of laboratory measurement. Canadian Geotechnical Journal V.20 p.629-644.

Telford, W.M., Geldart, L.P., Sheriff, R.E. 1990. Applied geophysics 2nd Ed. Cambridge Univ. Press. 770pp.

Terzaghi, K., R.B. Peck, and G. Mesri. 1996. Soil mechanics in engineering practise, 3rd Ed. John Wiley & Sons. 549pp.

Thimm, H. 1999. Repressurization of depleted gas caps surmont area, rebuttal by Gulf Canada Resources Limited Application number 960953 attachment R8. 17pp.

Thomas J., and B.F. Bohor. 1968. Surface area of montmorillonite from the dynamic sorption of nitrogen and carbon dioxide. Clays and Clay Minerals V.16 p.83-91.

Thomas J., and B.F. Bohor. 1969. Surface area of vermiculite with nitrogen and carbon dioxide as adsorbates. Clays and Clay Minerals V.17 p.205-209.

Thomas, J.Jr., R.R. Frost. 1980. Adsorption/desorption studies of gases through shales. *In* Bergstrom, R.E., Shimp, N.F., and Cluff, R.M. (eds) Geologic and Geochemical Studies of the New Albany Shale Group, University of Illinois/Illinois State Geological Survey.

Tissot, B., and R. Pelet. 1971. Nouvelles donnees sur les mecanismes de genese et de migration du petrole simulation mathematique et application a la prospection: 8th World Petroleum Congress, Moscow, Proceedings V.2 p.35-46.

van der Meer, L.G.H. 1992. Investigations regarding the storage of carbon dioxide in aquifers in the Netherlands. Energy Conservation and Management V.33 no.5-8 p.611-618.

van Olphen. 1977. An introduction to clay colloid chemistry: for clay technologists, geologists, and soil scientists 2nd Ed. Wiley Publishing. 318pp.

Vazquez, U.G., R.F. Chenlo, G.G Pereira, and L.J. Peaguda. 1994. Solubility of $CO_2$ in aqueous solutions of saccharose, glucose, fructose, and glycerin. Journal of Chemical and Engineering Data V.39 no. 4 Oct 1994, p.639-642.

Volzone, C., J.G. Thompson, A. Melnitchenko, J. Ortiga, and S.R. Palethorpe. 1999. Selective gas adsorption by amorphous clay-mineral derivatives. Clays and Clay Minerals V.47 no.5 p.647-657.

Wang, L.-S, Z.-X Lang, T.-M. Guo. 1996. Measurement and correlation of the diffusion coefficients of carbon dioxide in liquid hydrocarbons under elevated pressures. Fluid Phase Equilibria V. 117 p.364-372.

Watts, N.L. 1987. Theoretical aspects of cap-rock and fault seals for single and two-phase hydrocarbon columns. Marine and Petroleum Geology V.4 p.274-307.

Wedlake, G.D. and D.B. Robinson. 1979. Solubility of carbon dioxide in silicone oil. Journal of Chemical and Engineering Data. V. 24. no.4 p.305-306.

Weemees, I.A. 1990. Development of an electrical resistivity cone for groundwater contamination studies. MSc. Thesis. University of British Columbia. 77pp.

White, S.P., G.J. Weir, and W.M. Kissling. 2001. Numerical simulation of $CO_2$ sequestration in natural $CO_2$ reservoirs on the Colorado Plateau. Pre-print from: First National Conference on Carbon Sequestration 12pp. U.S. DOE, Washington, D.C.

Wiebe, R and V.L. Gaddy, 1941. Vapour phase composition of carbon dioxide-water mixtures at various temperatures and at pressures up to 700 atmospheres. Journal of the American Chemical Society, V 63 p.475.

**Appendix A – Triaxial Cell Schematics**
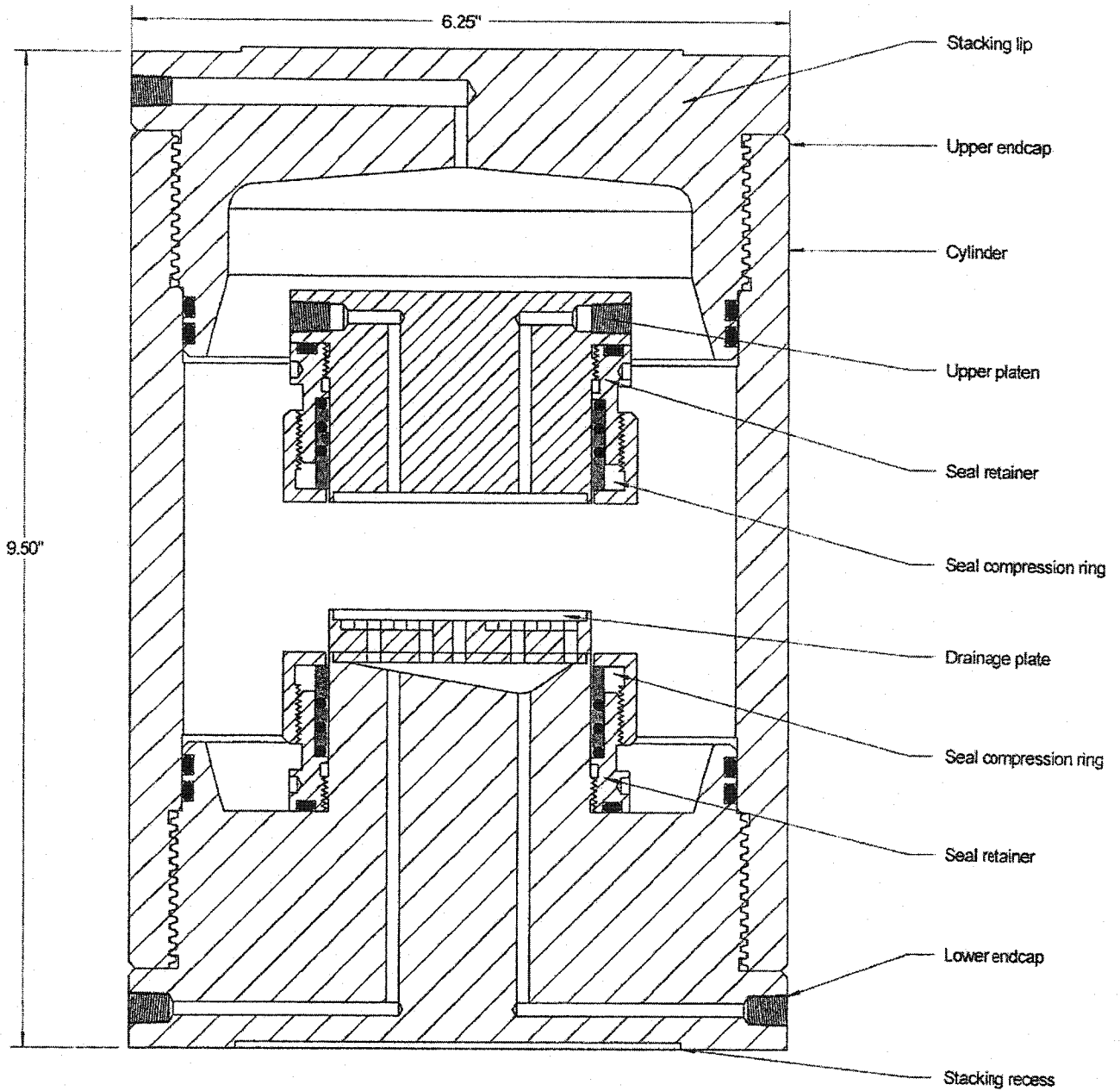
**Figure A- 1: 20MPa Triaxial Test Cell**
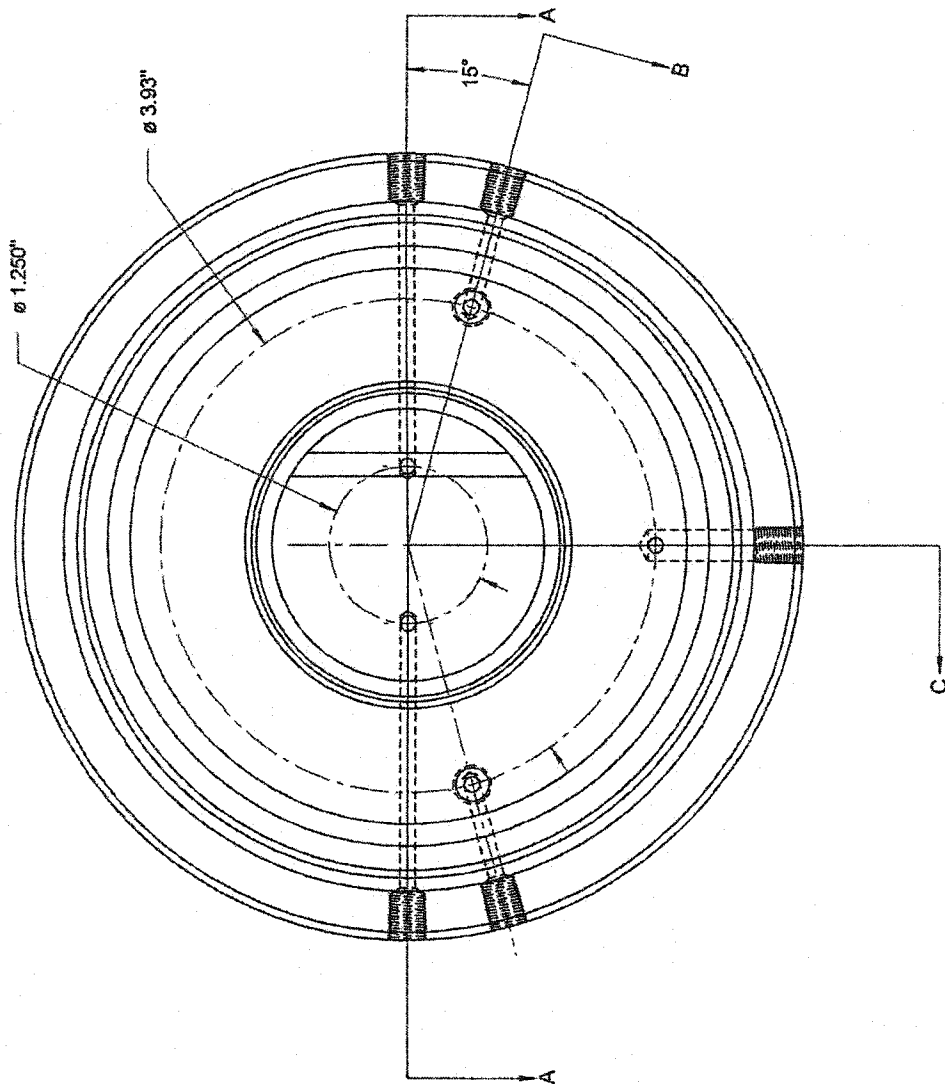
**Figure A- 2: Plan View of Bottom**
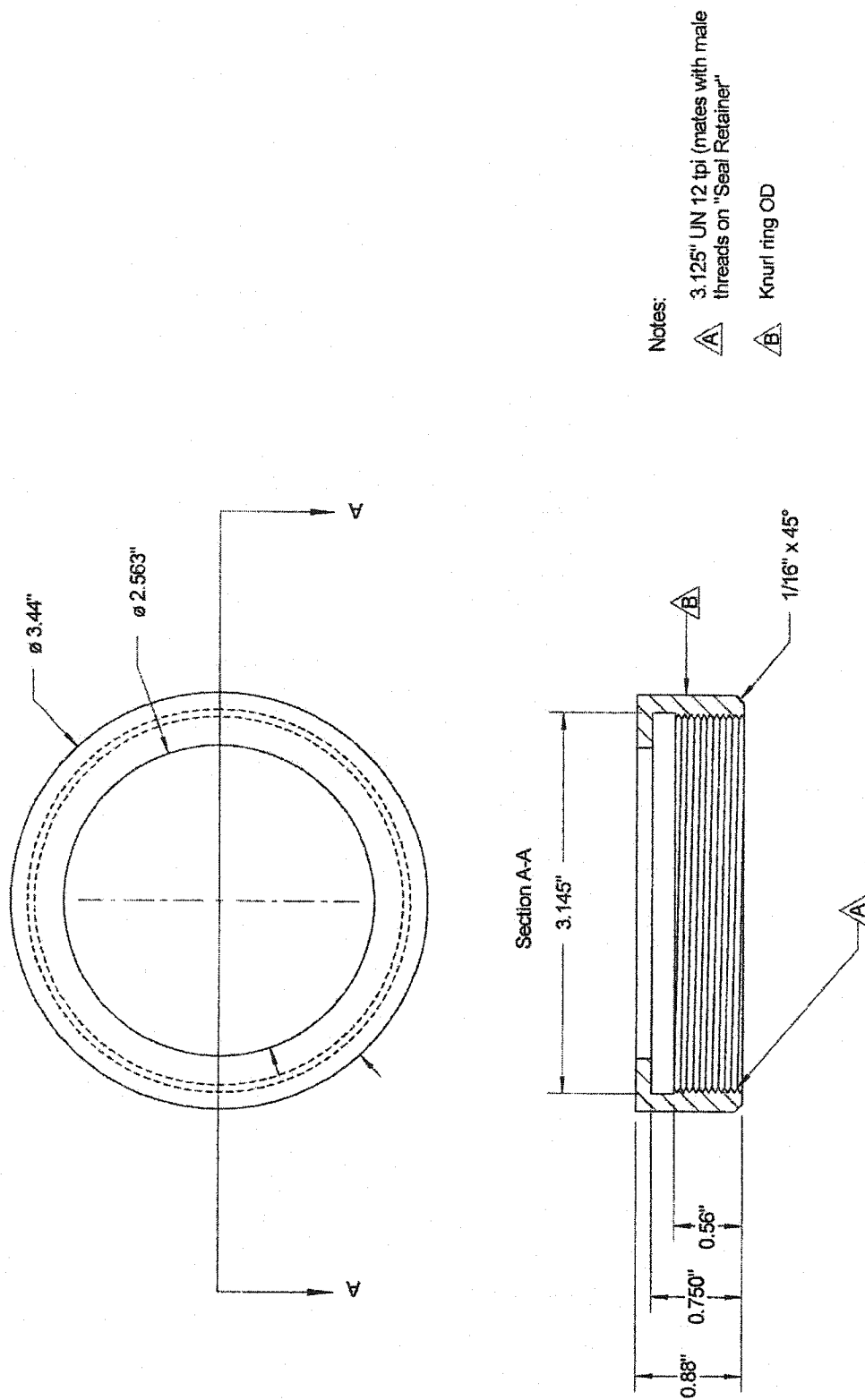
**Figure A- 3: Seal Compression Ring**

**Figure A-4: Cylinder**

Notes:

Mill Test Report (Certificate) required

Both ends of cylinder identical

⚠ A  5.500" ACME 8tpi class 2G (mates with upper and lower endcaps)

⚠ C  Knurled surface, in middle of cylinder

Detail B

ø5.341"

30°

3"

5.25"

5.281" +0.002" / -0.000"

6.25"

1.38"

1.50"

2.224"

16-32

8.00"

1/16" x 45° typ.

99
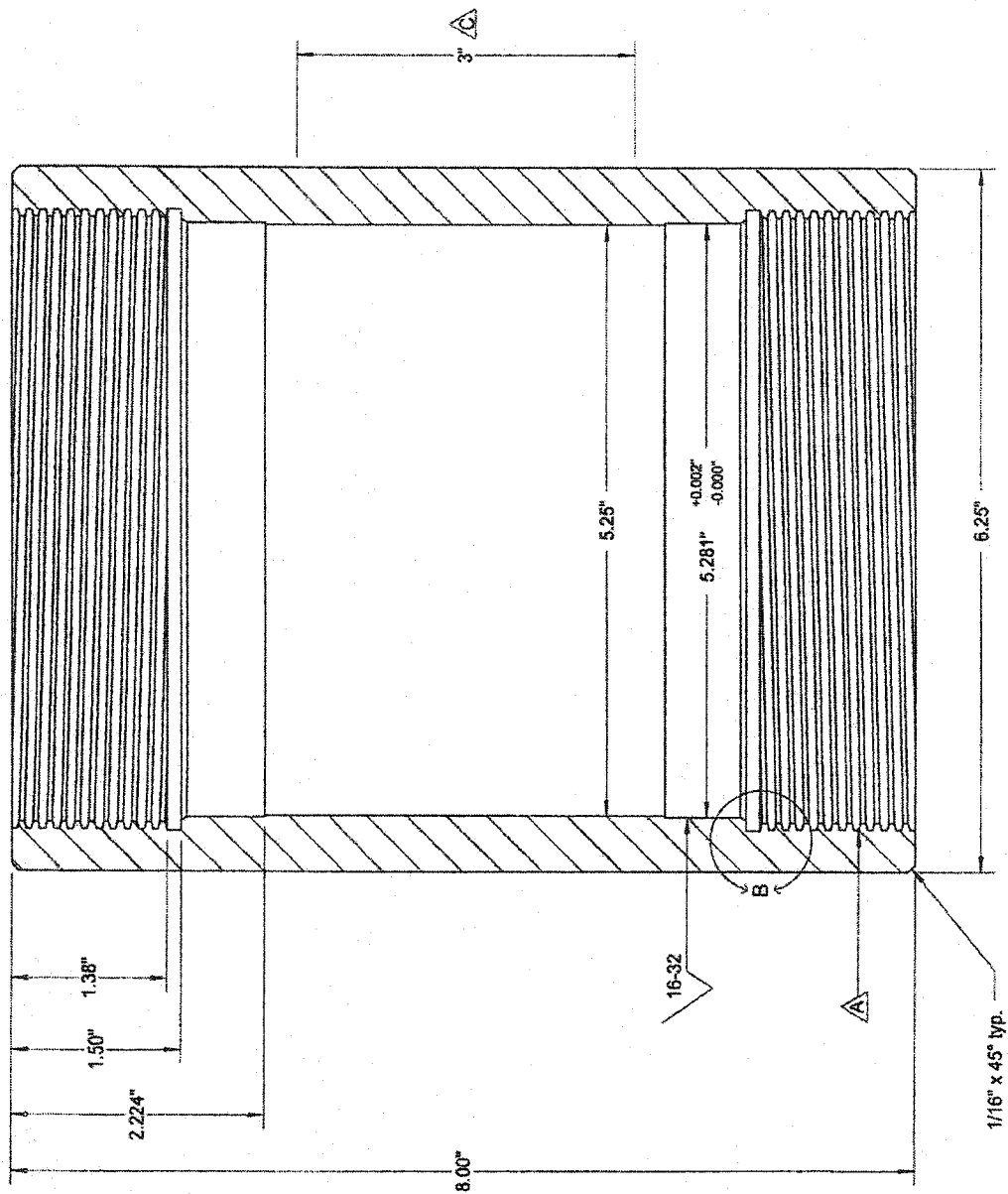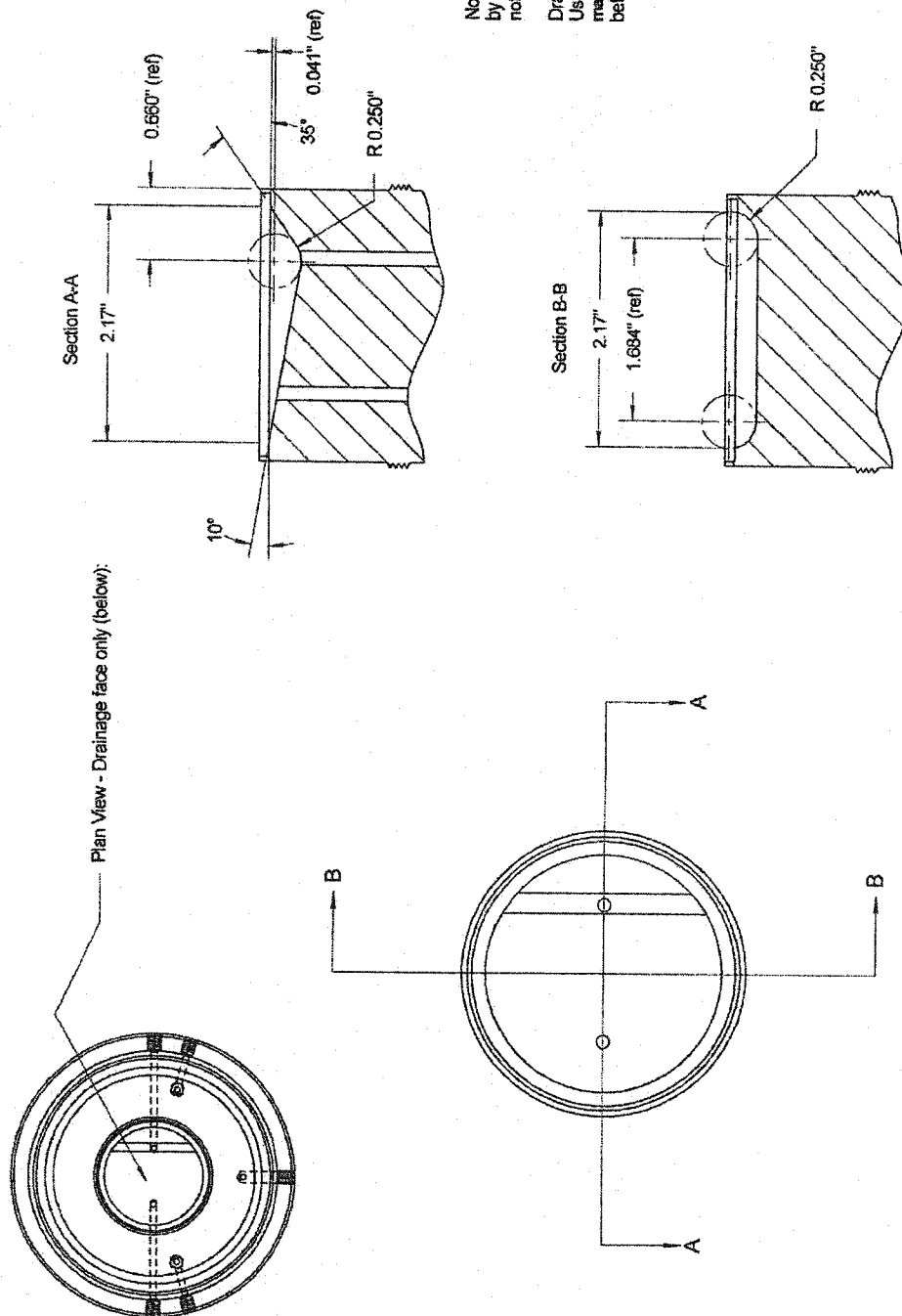
Note, drainage profile is constructed by intersecting two flat planes. It is not an eccentric conical surface.

Drainage profile surface roughness: Using an R0.25" ball end mill, maximum horizontal step distance between passes is 0.125".

Section A-A

0.660" (ref)

0.041" (ref)

35°

R 0.250"

2.17"

10°

Section B-B

R 0.250"

2.17"

1.684" (ref)

Plan View - Drainage face only (below):

A

B

B

A

**Figure A- 5: Lower End Cap Drainage Profile**

100

All holes ∅1/8"
All slots 1/8" wide

∅ 2-1/8"
∅ 1-5/8"
∅ 1-1/8"
∅ 5/8"

A

A

Section A-A

2.500"
+0.000"
-0.005"

2.420"

2.410"

0.094"

0.50"

0.094"

0.09"
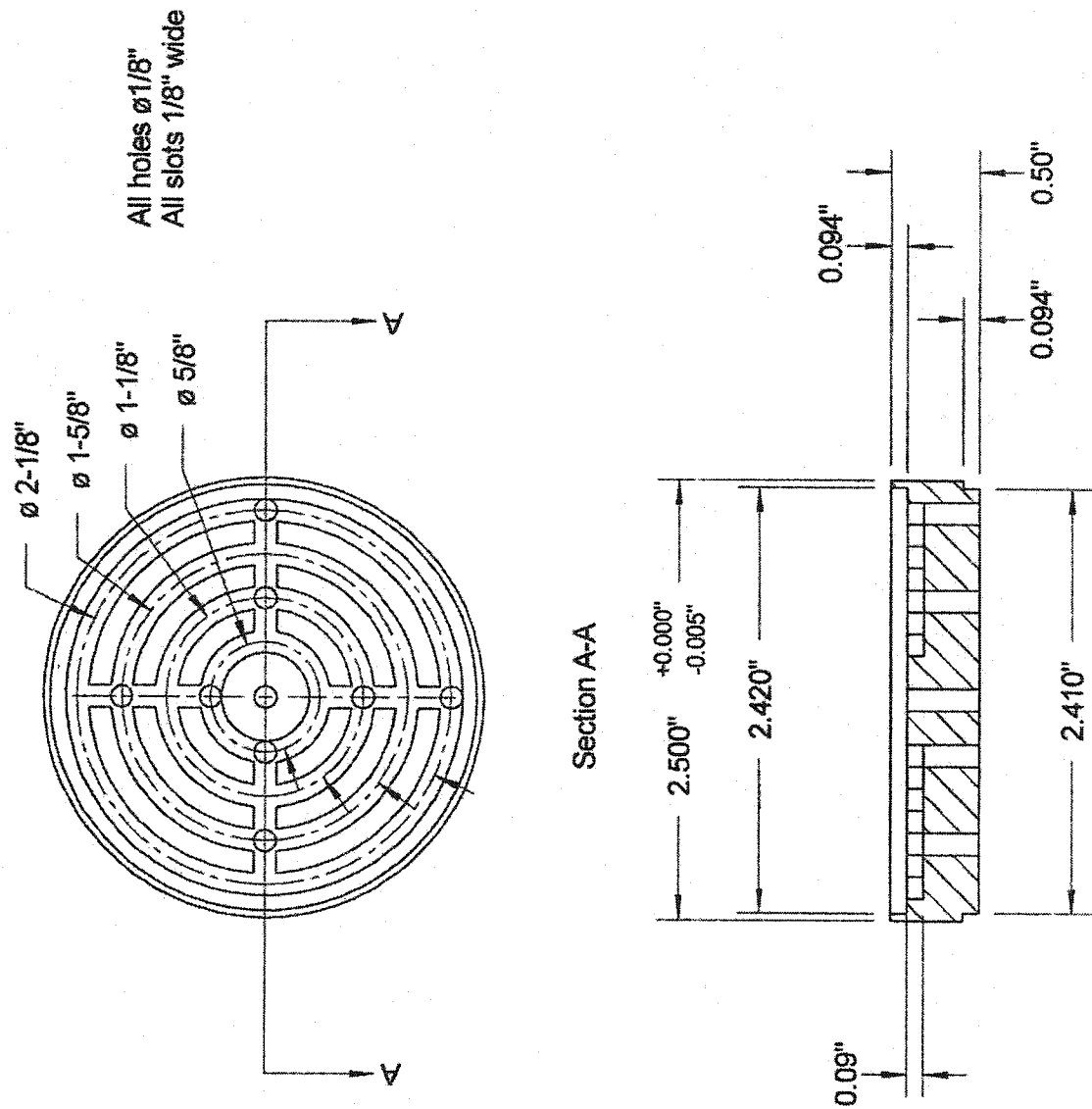
**Figure A- 6: Drainage Plate**

**Figure A- 7: Brass Spacers**

**Notes:**

A — 2.625" UN 12 tpi (mates with male threads on "Upper Platen" and "Lower Endcap")

B — 3.125" UN 12 tpi (mates with "Seal Compression Ring")

C — Four ø5/32" holes drilled 1/8" dp. spaced 90° apart

**Figure A- 8: Seal Retainer**

103

**Figure A- 9: Top Cap**

One 1/16" NPT
Tap drill to cross-
link with ø1/8"

0.05"

3/8"

ø5.335" (relief)

R 0.25"

1.41"

15°

5°

ø1/8"

6.25"

4.22"

3.26" drill dp. (ref)

4.422"

4.841"

+0.003"
−0.003"

0.190" typ.

5.059"  +0.000"
        −0.002"

5.277"  +0.000"
        −0.002"

1/8" x 45°

0.125"

0.378"

1/8" x 45°

0.66"

2.04"

2.16"

2.96"

Notes:

Mill Test Report (Certificate) required

5.500" ACME 8 tpi Class 2G (mates with Cylinder)

Knurled OD
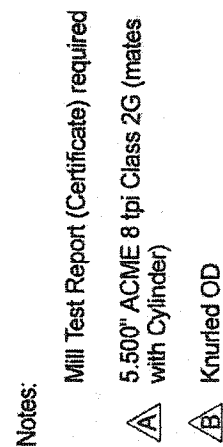
104

**Figure A- 10: Upper Platen**

105

Section A-A

Notes:

△A 2.625" UN 12 tpi (mates with "Seal Retainer")

△B Drainage profile details on sheet #5

△C 5.500"ACME 8 tpi Class 2G (mates with "Cylinder")

△D Knurl OD
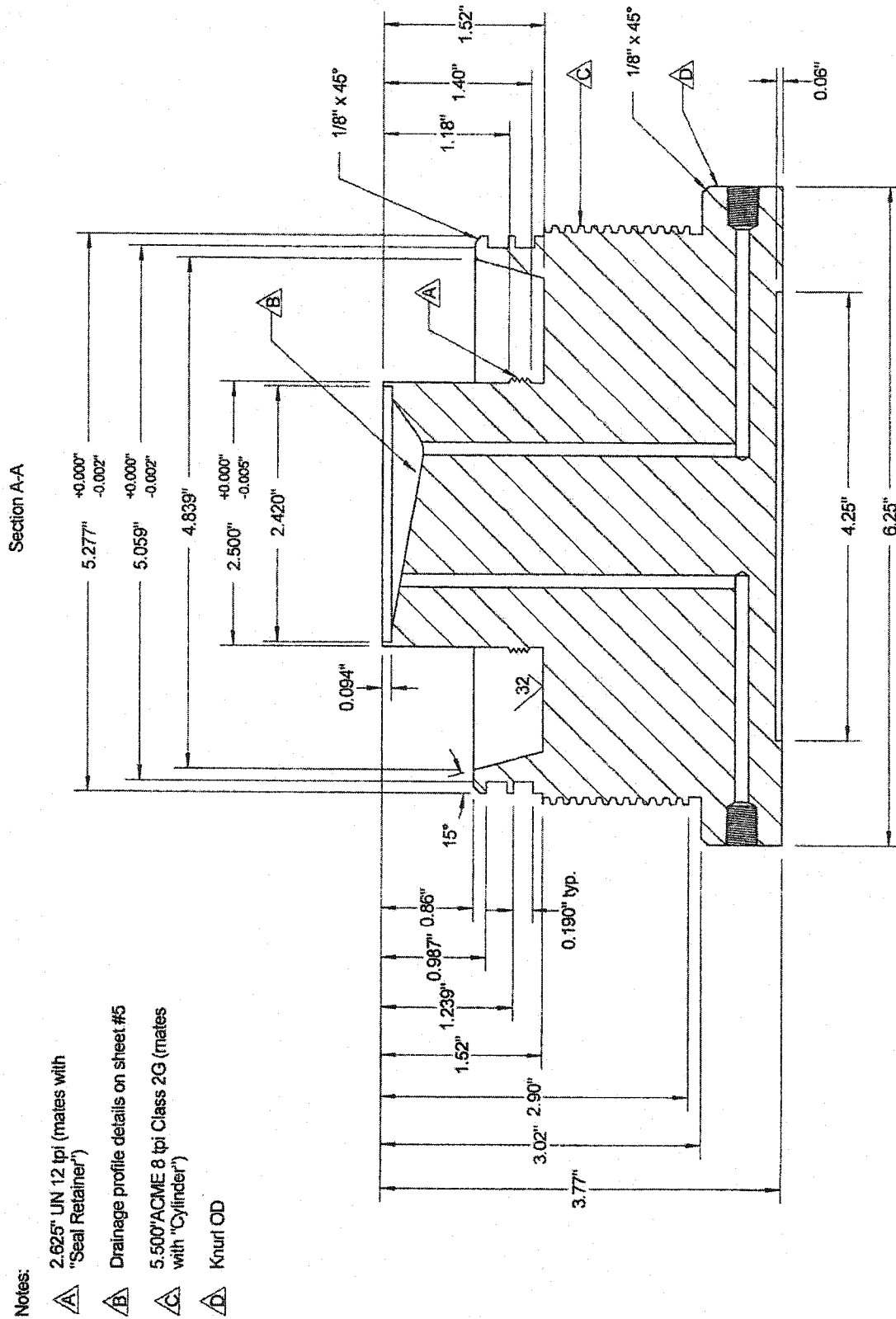
**Figure A- 11: Lower End Cap Section A-A**

106

All tapped holes are 1/16" NPT. Tap drill as shallow as possible on 1/16" NPT holes that lead into ø1/8" holes. Cross-linked ø1/8" holes need not intersect exactly on hole center-lines (reduced flow area at intersection is not critical).

Section A-B

1.88" ref.

3/8" typ.

1/8"

1/8"

1.26" ref.

2.60" ref.

1/8"

3.22" ref.

1/8"
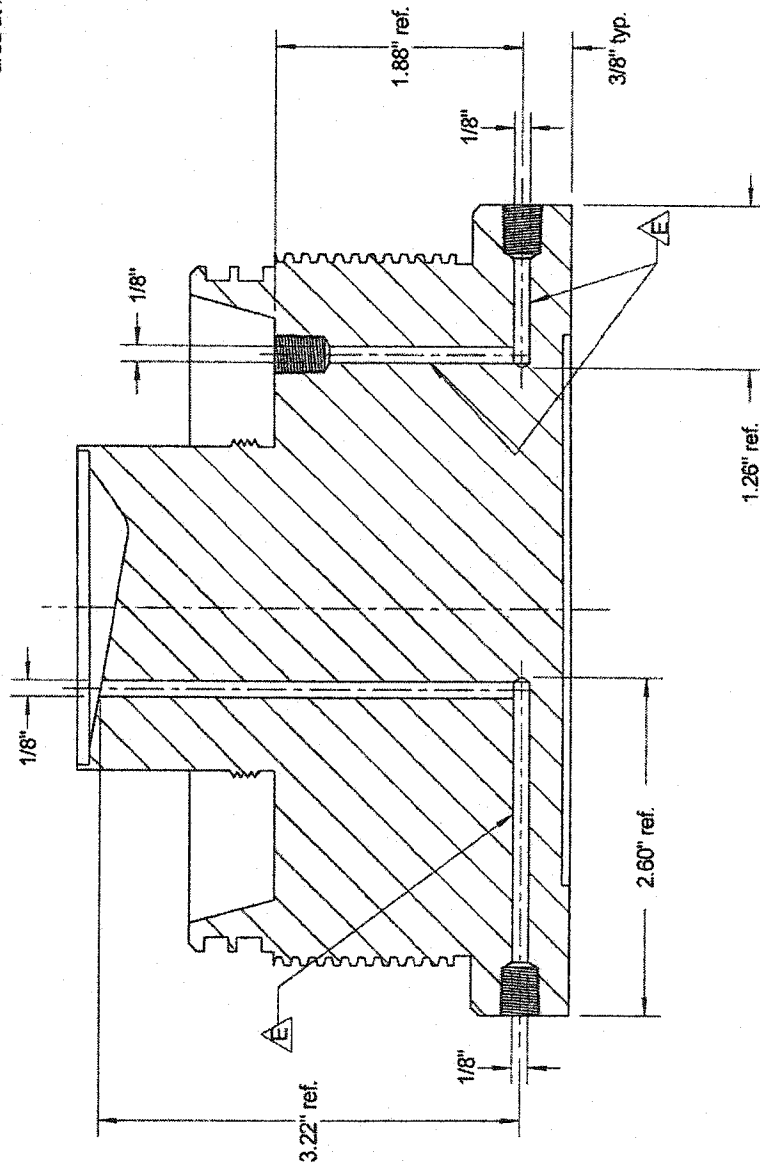
**Figure A- 12: Lower End Cap Section A-B**
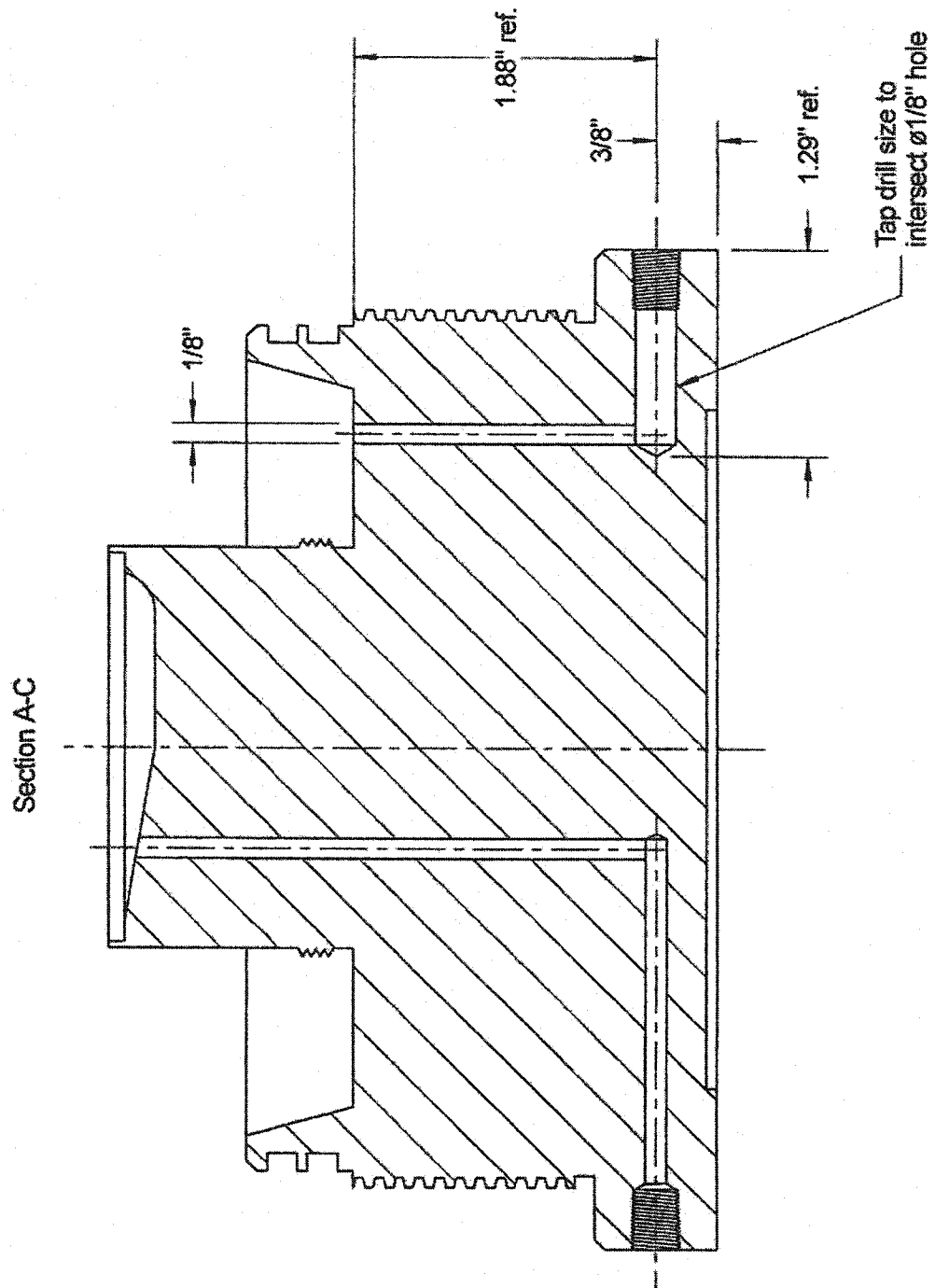
**Figure A- 13: Lower End Cap Section A-C**
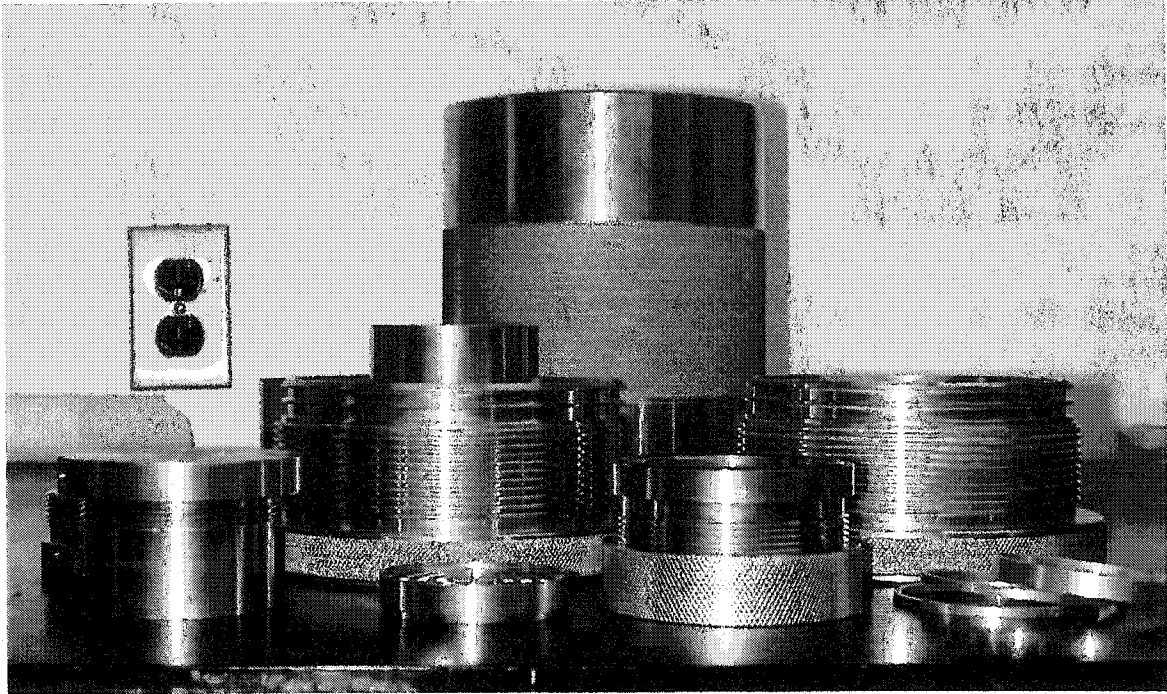
**Figure A- 14: Photo of Triaxial Assembly**

**Figure A- 15: Photo of Triaxial Assembly Plan View**
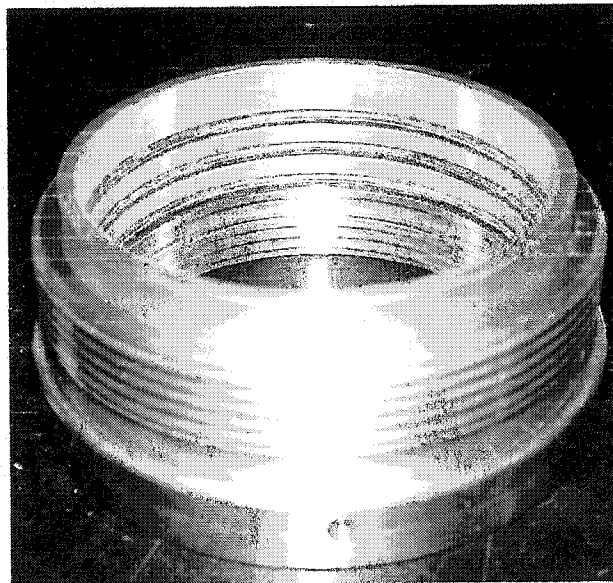

**Figure A- 16: Photo of Sealing Assembly**
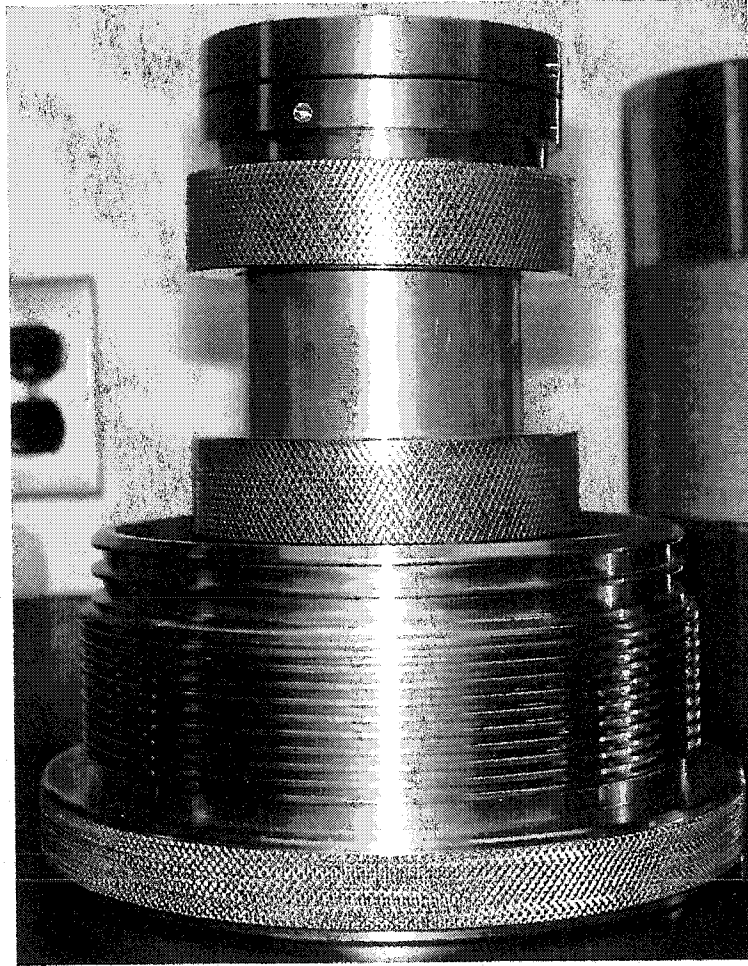
**Figure A- 17: Photo of Sealing Mechanism Set-Up**
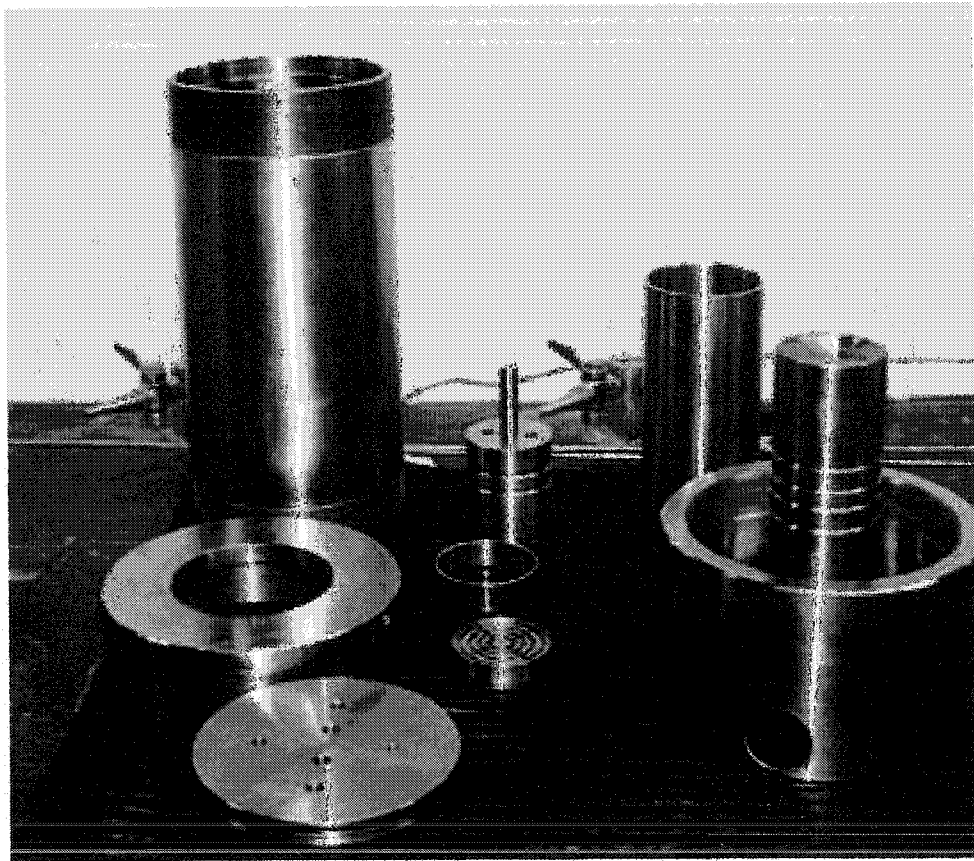
**Figure A- 18: First Triaxial Design**
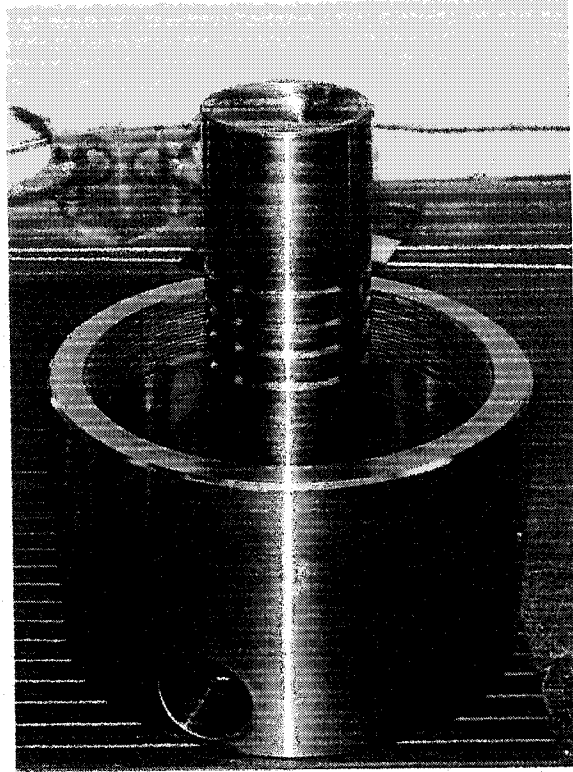
**Figure A- 19: Bottom Pedestal**

**Figure A- 20: Initial Triaxial Cell Schematic**

114
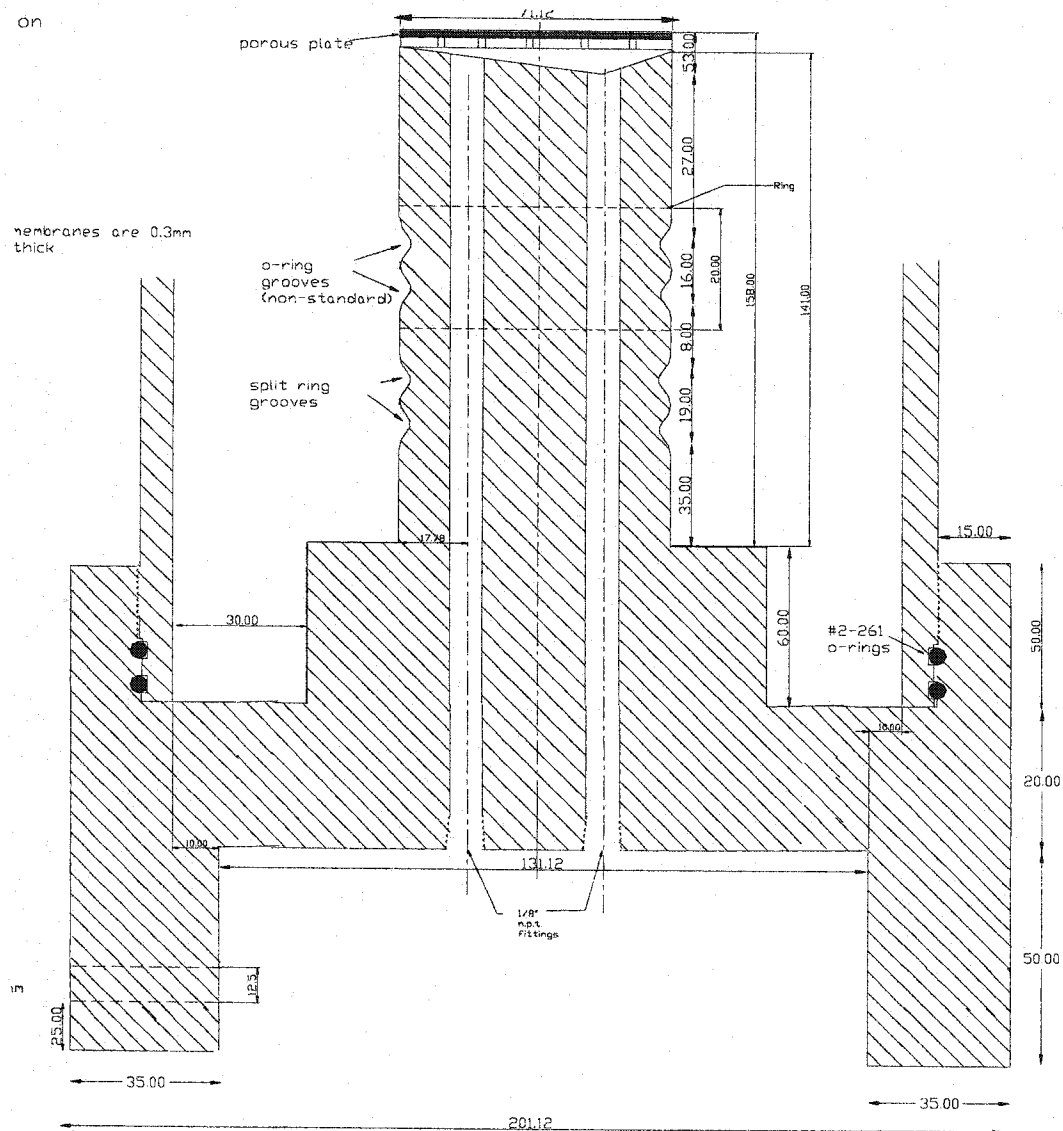
**Figure A- 21: Schematic of initial Triaxial Design, Bottom Platen**

**Figure A- 22: Drainage Setup in Initial Design**

**Figure A- 23: Schematic of Initial Design of Top Platen**

116

Triaxial Cell - Bottom
View
Drawing Not to Scale
Dimensions in mm

d=3.175mm or 1/8"

1/8" n.p.t with
1/8" (3.175mm)
hole

slot
dimensions:
12.5
wide
by
10
high

R17.28
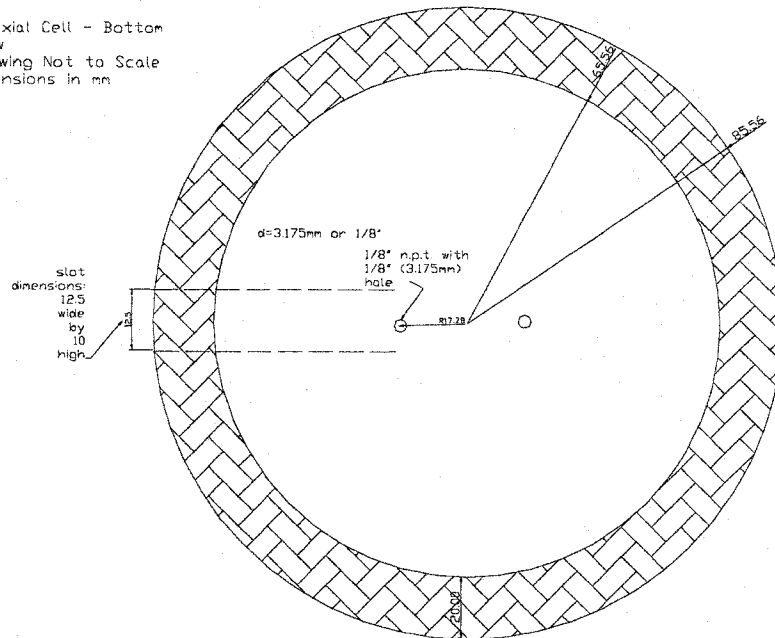
Triaxial Cell - Top
View
Drawing not to
scale
Dimensions in mm

1/8"
n.p.t.
with
1/8"
hole
through
(4)

100.56

55.56

Top Cap

vent

vent

R12.78

vent: 1/4" n.p.t
with 1/8" hole
through
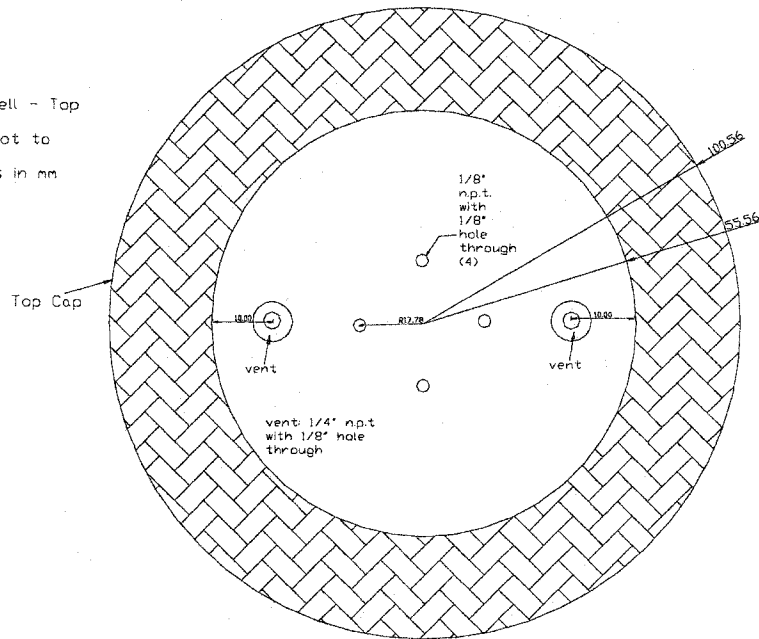
**Figure A- 24: Schematic of Plan view of Initial Cell**

117
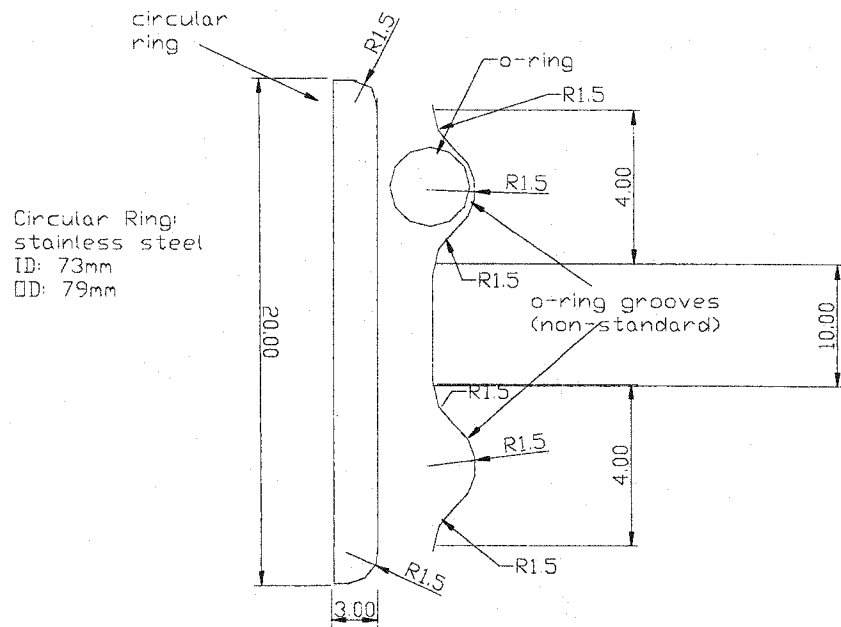
**Figure A- 25: Schematic of Initial O-ring Design**

## Appendix B – Water Bath Temperature Control
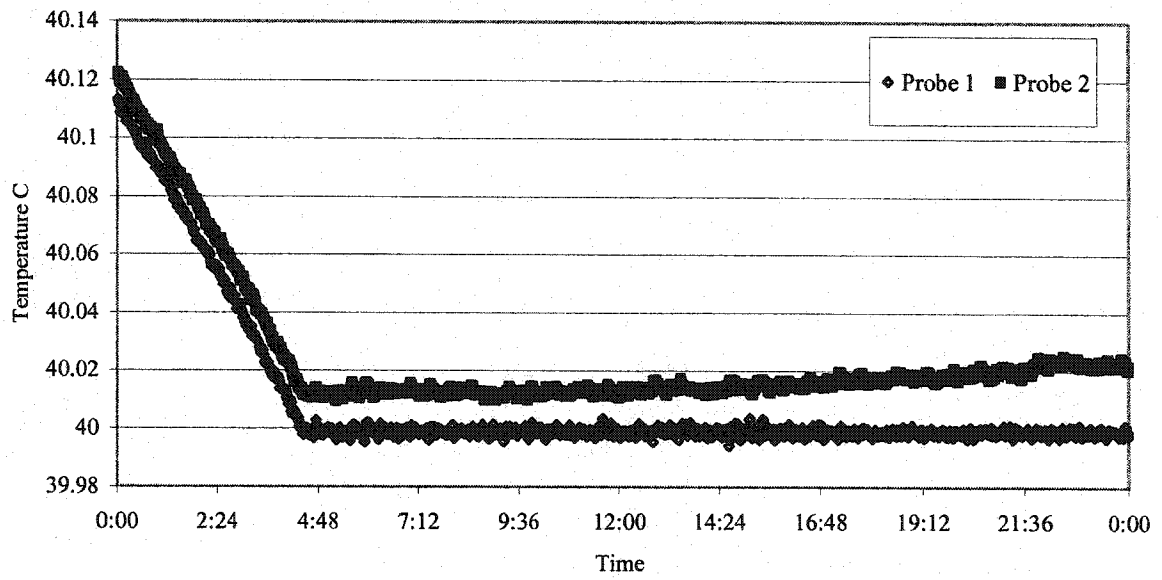
**Figure B- 1: Temperature Control August 6**
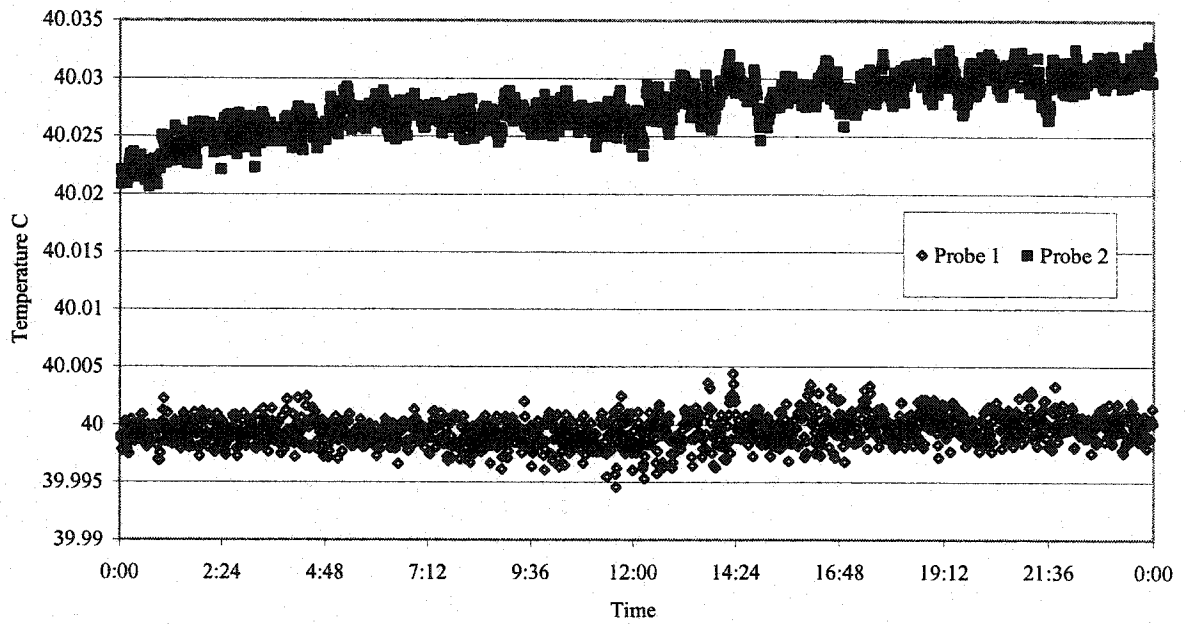


**Figure B- 2: Temperature Control Steady State, August 7**
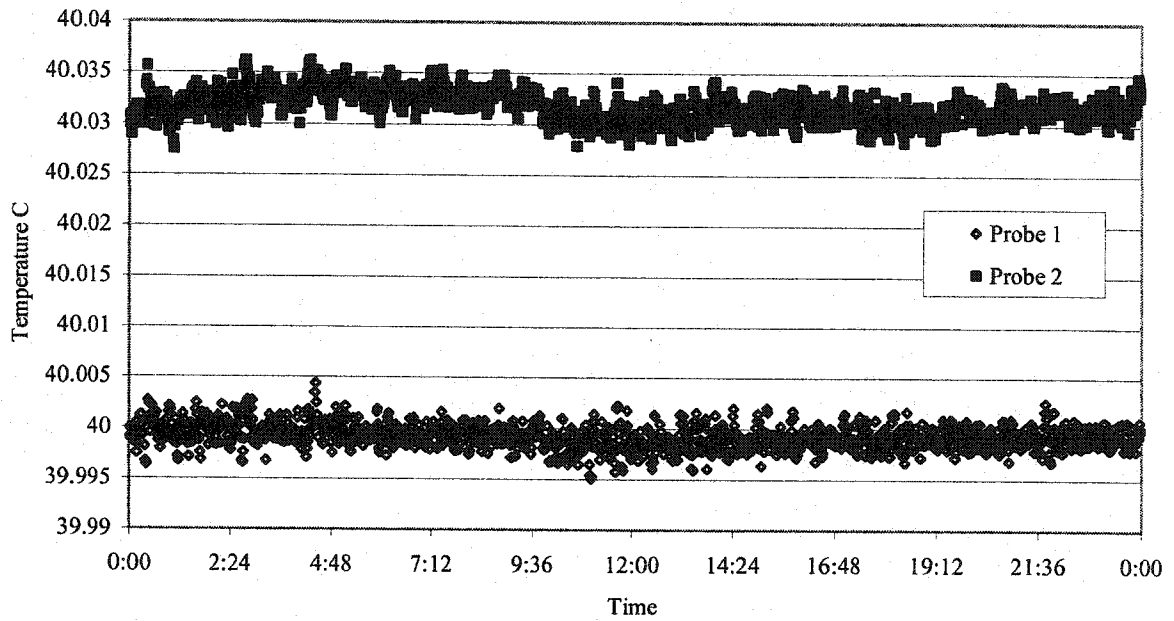
**Figure B- 3: Temperature Control Steady State, August 8**
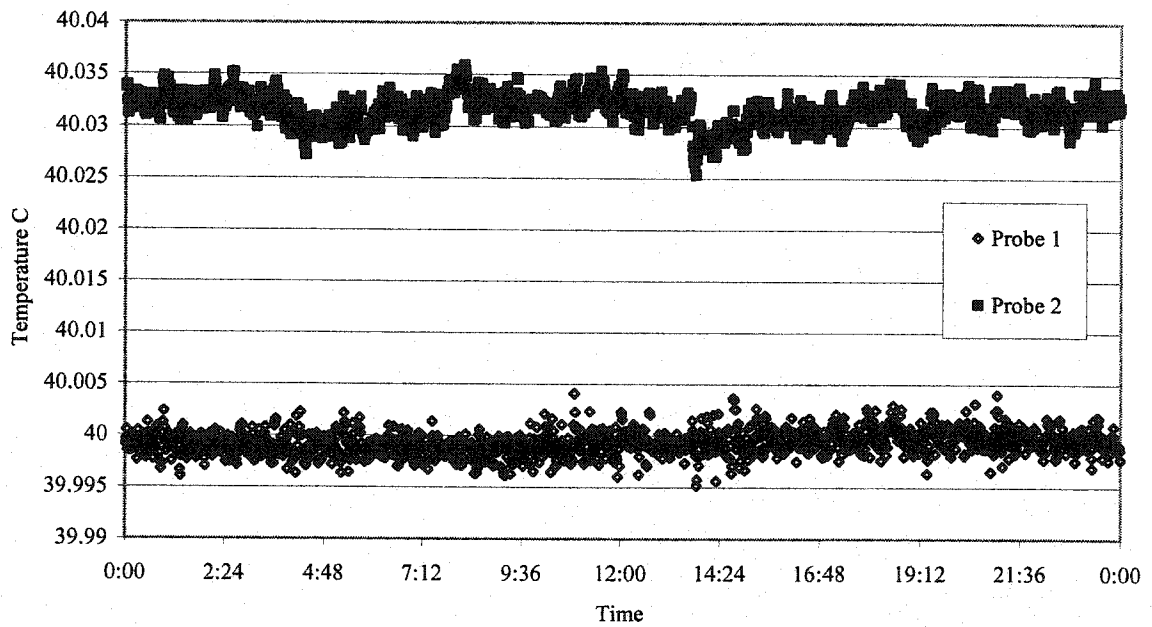


**Figure B- 4: Temperature Control Steady State, August 9**
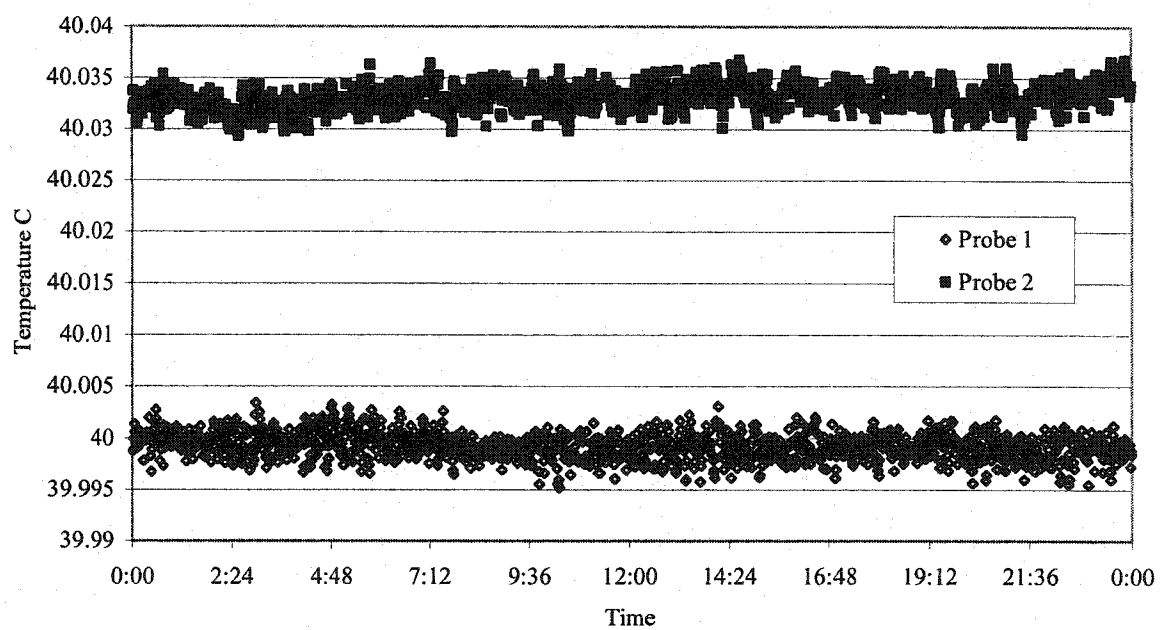
**Figure B- 5: Temperature Control Steady State, August 10**

# Appendix C – Electrical Resistivity Measurements
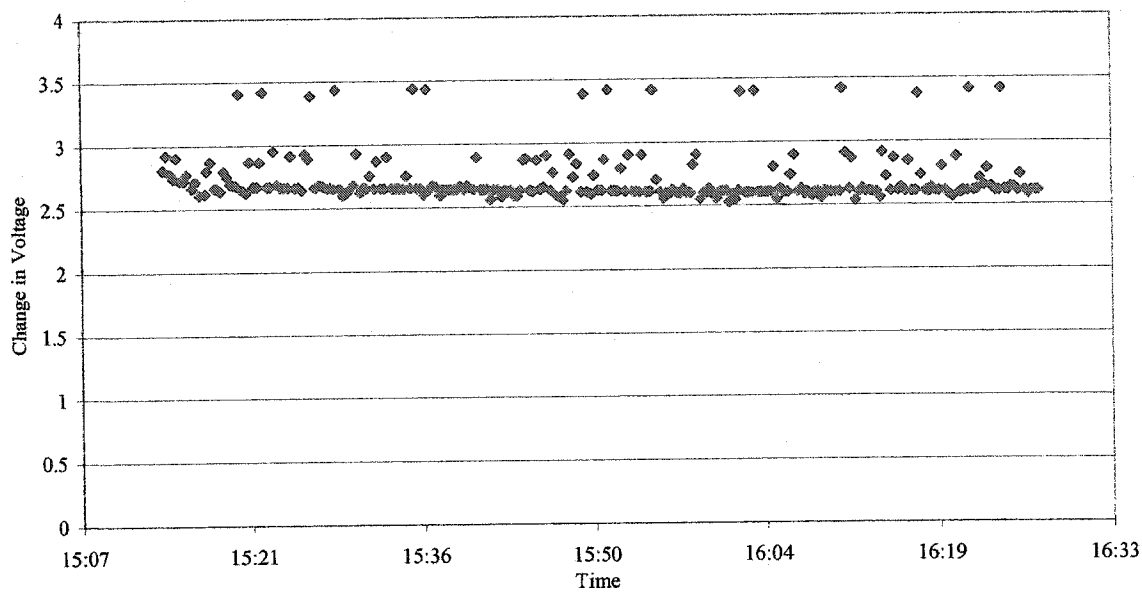
**Figure C- 1: Electrical Resistivity of Water in a Sample Cylinder**
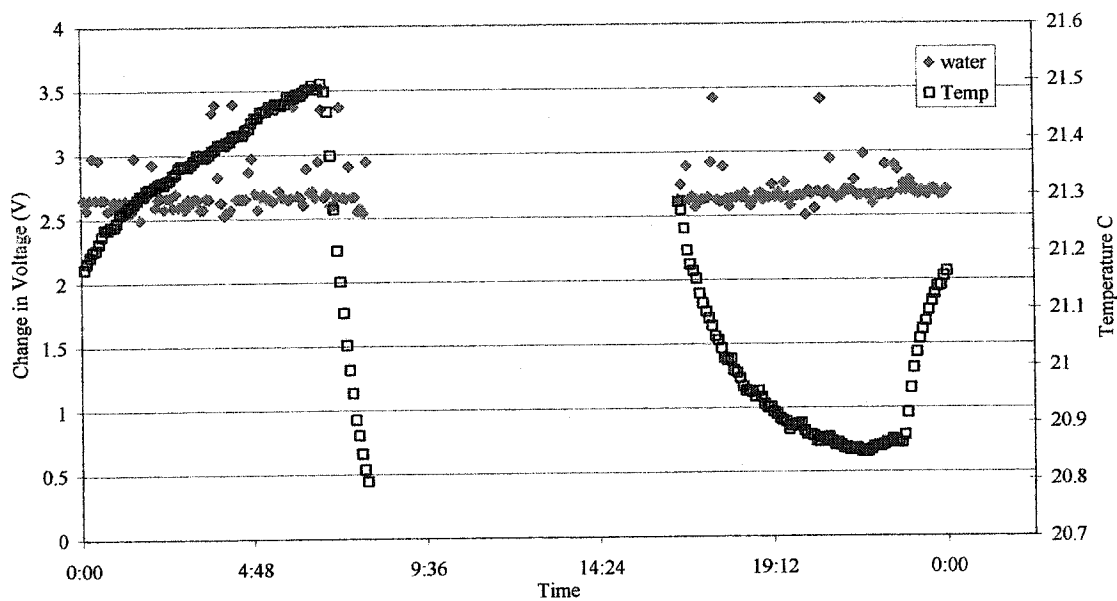


**Figure C- 2: Changes in Electrical Resistivity with Temperature**
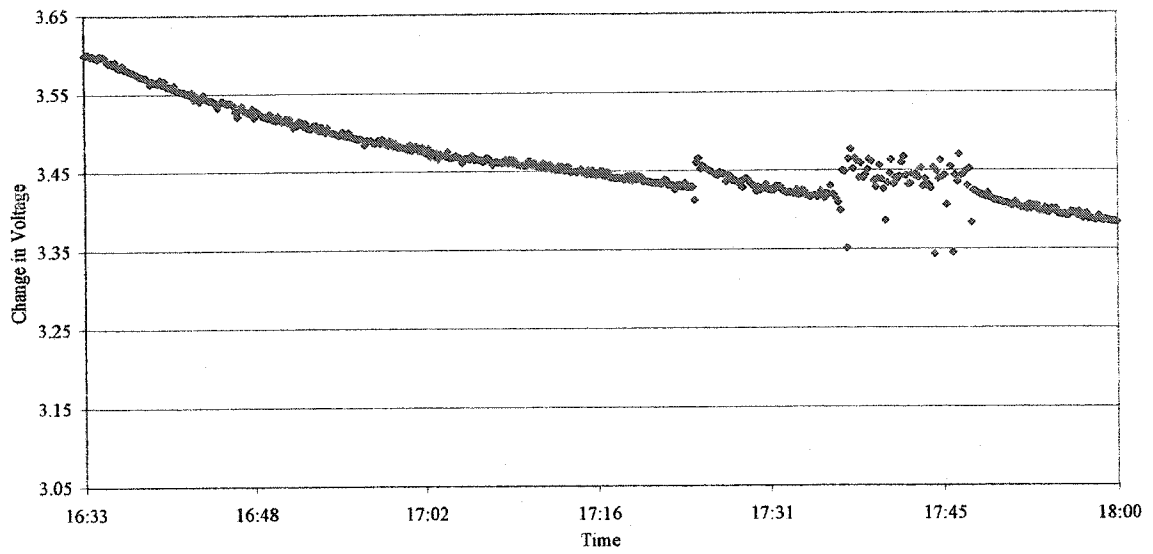
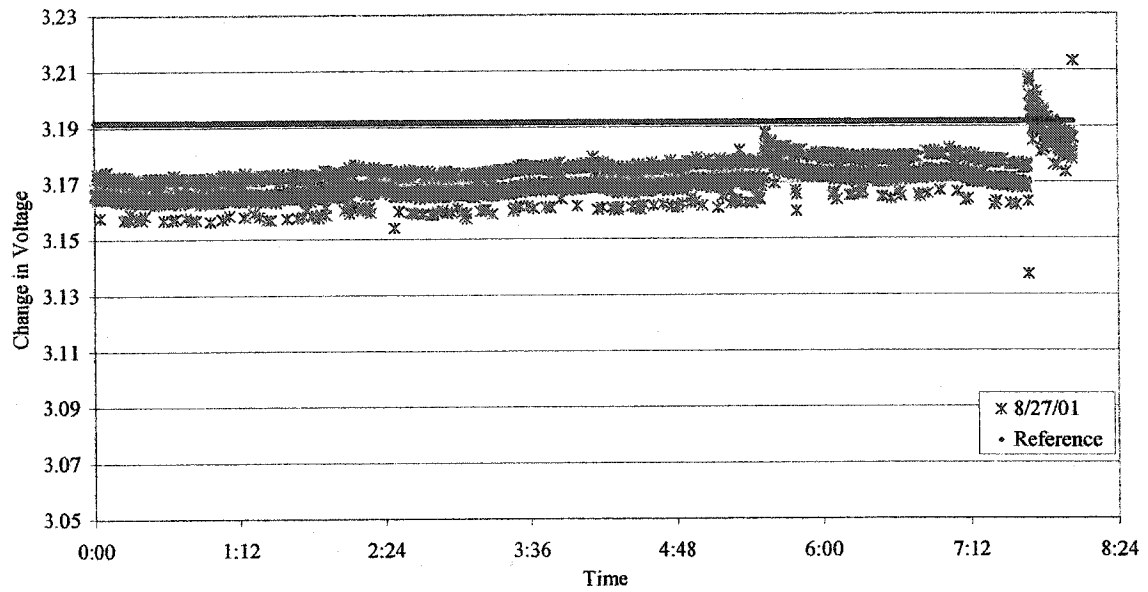**Figure C- 3: Changes in the Electrical Resistivity of a KOH solution**
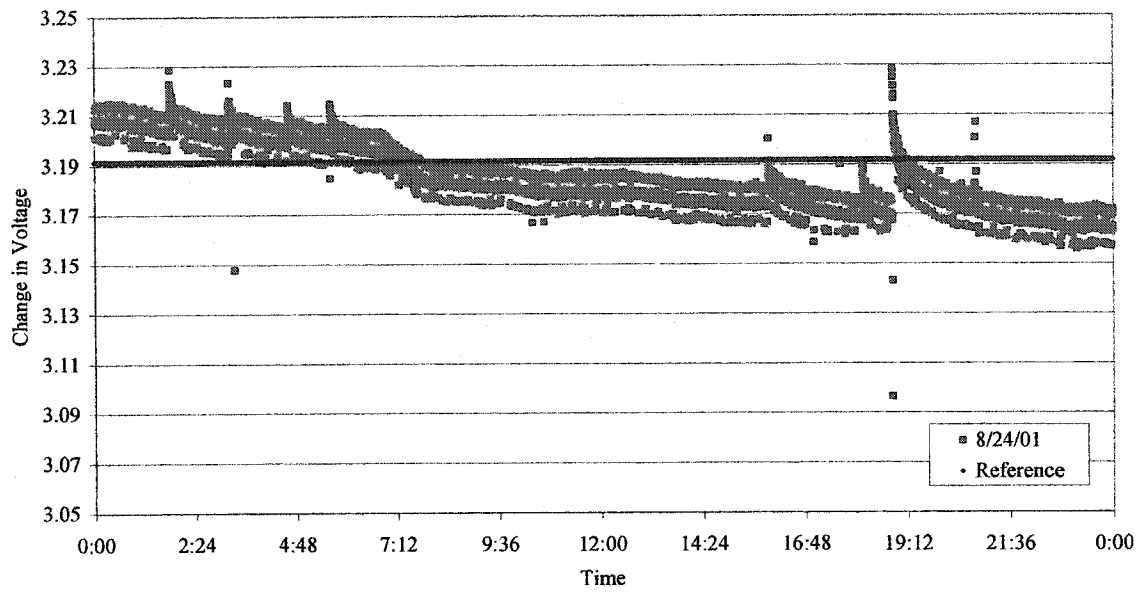


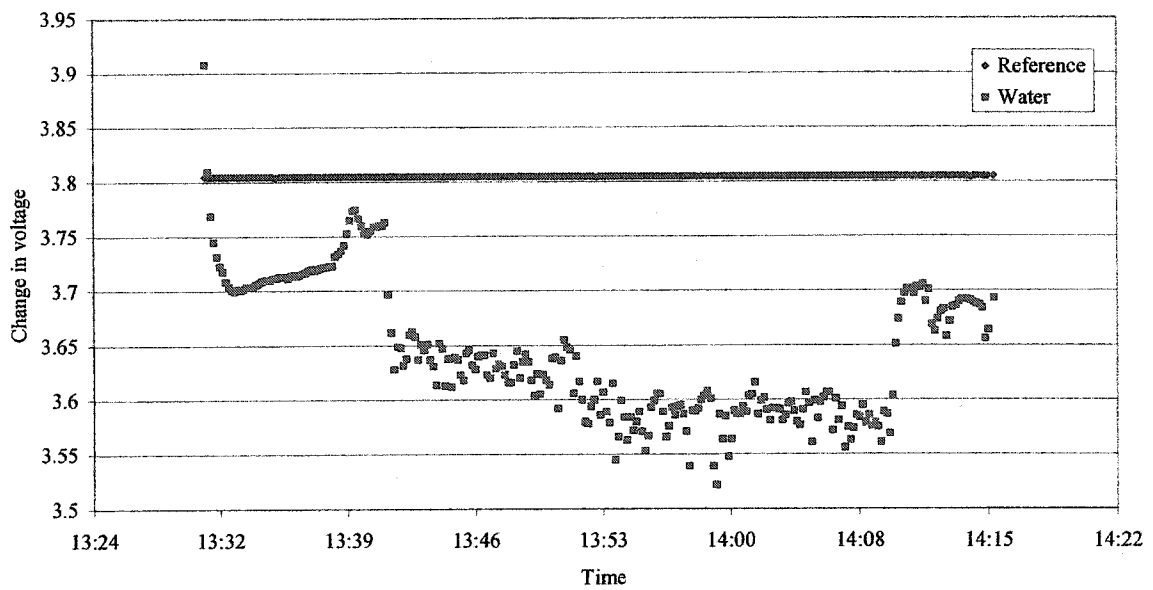**Figure C- 4: Changes in the Electrical Resistivity of a KOH solution (Day 2)**
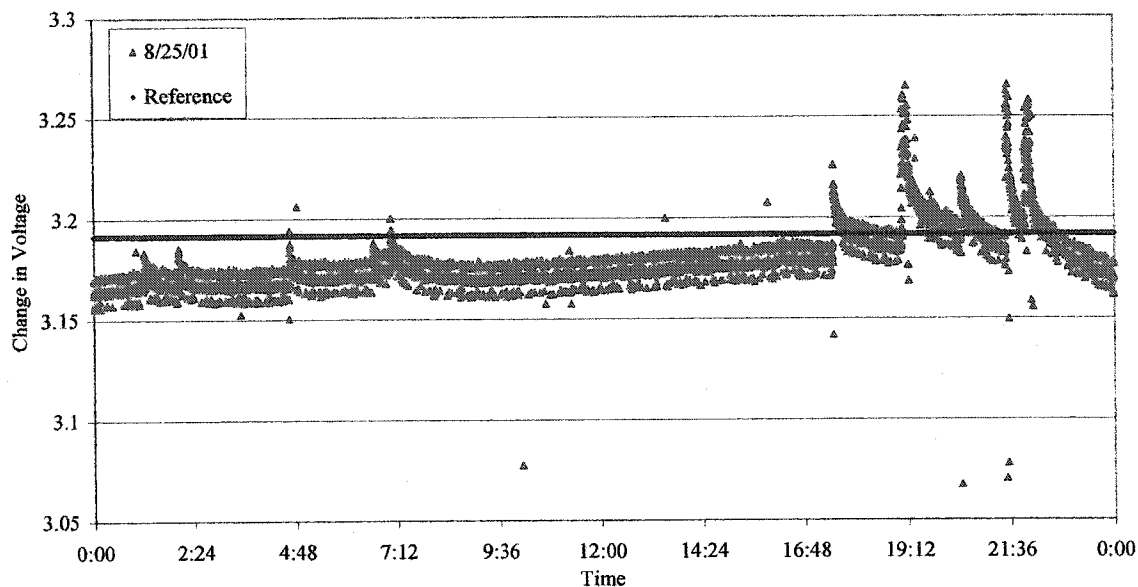
**Figure C- 5: Changes in the Electrical Resistivity of a KOH solution (Day 3)**
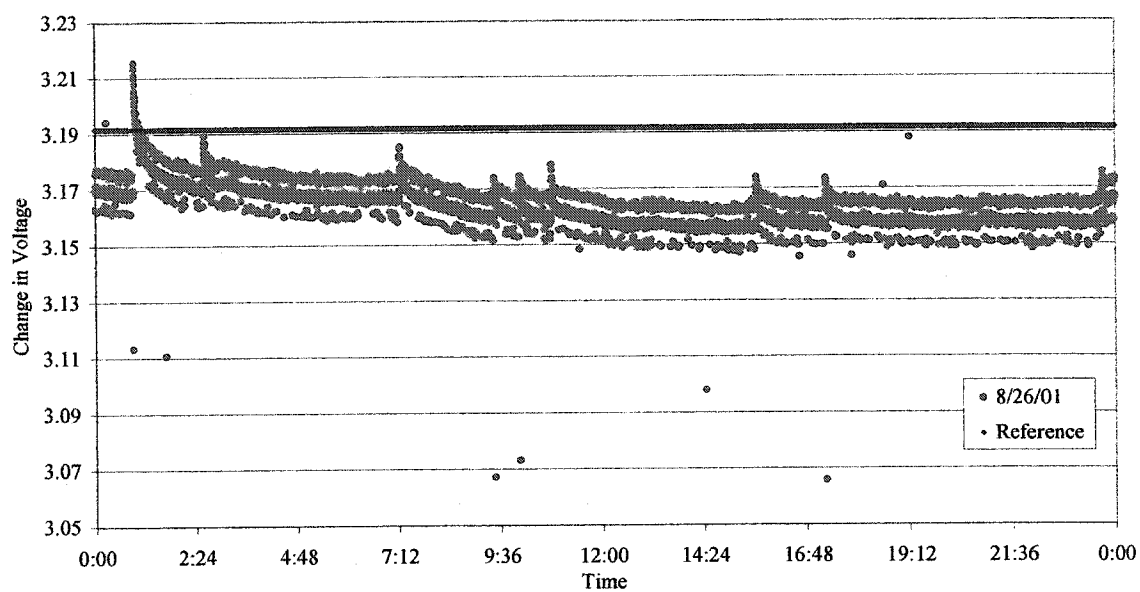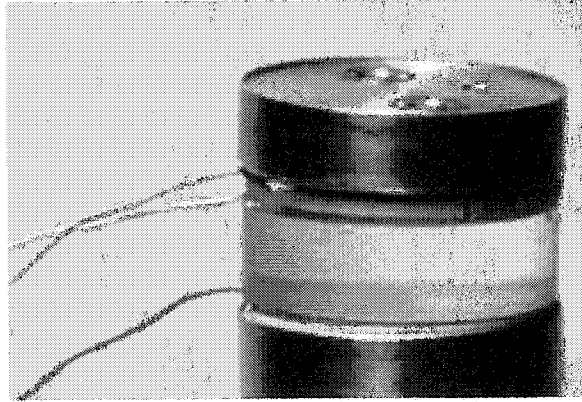


**Figure C- 6: Changes in the Electrical Resistivity of a KOH solution (Day 4)**
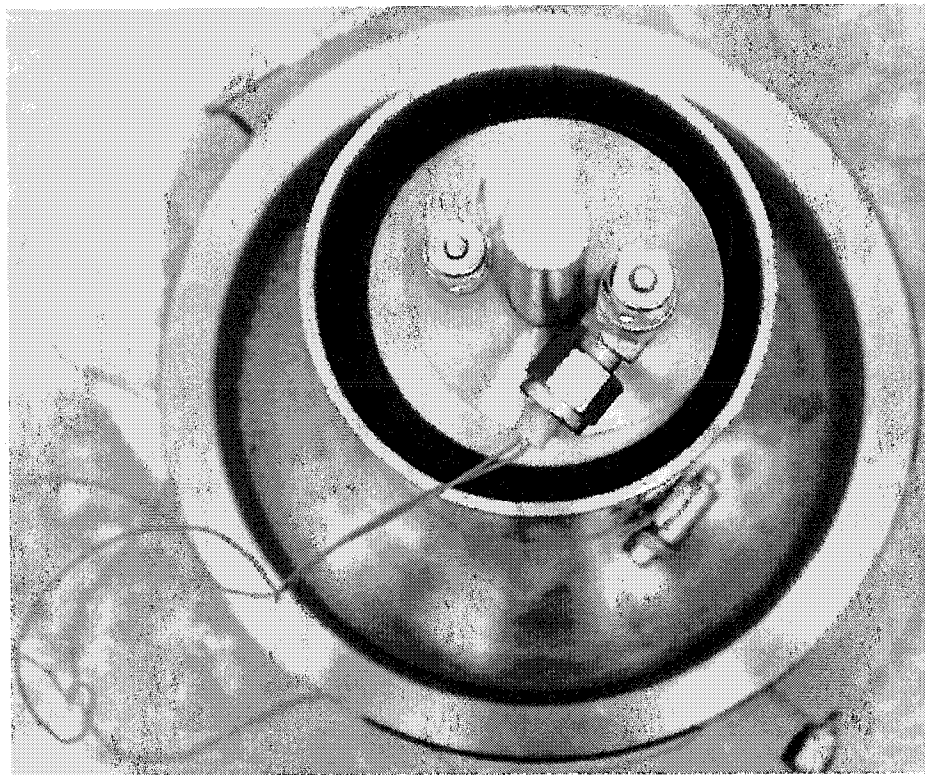
126

**Figure C- 7: Changes in the Electrical Resistivity of a KOH solution (Day 5)**



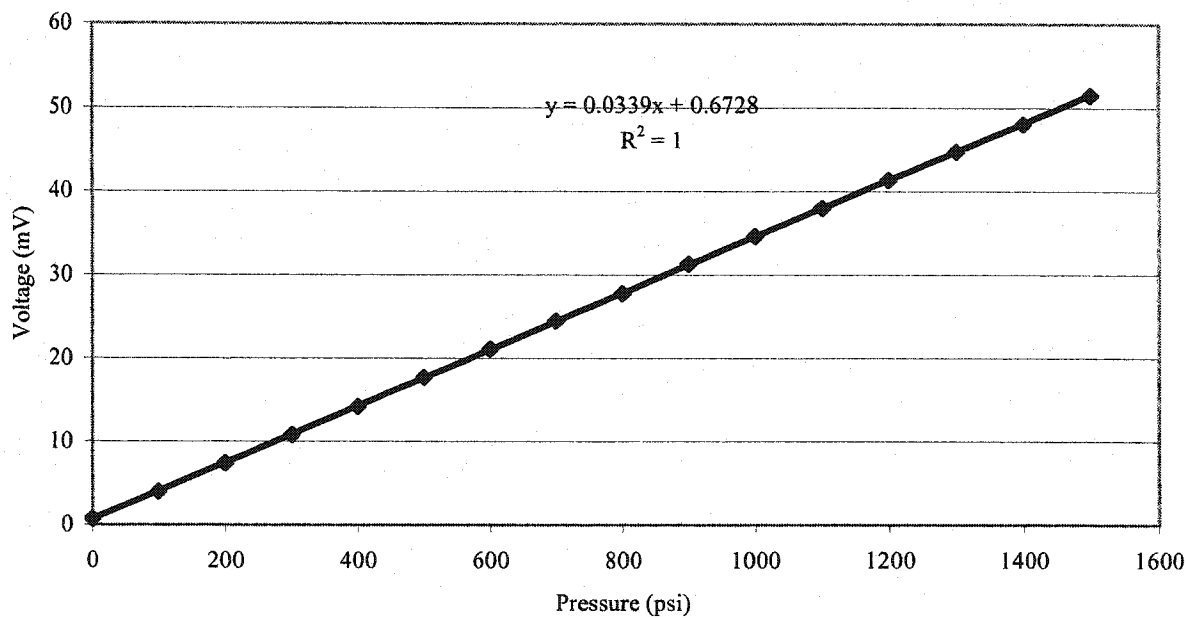**Figure C- 8: Changes in Electrical Resistivity across a Specimen**

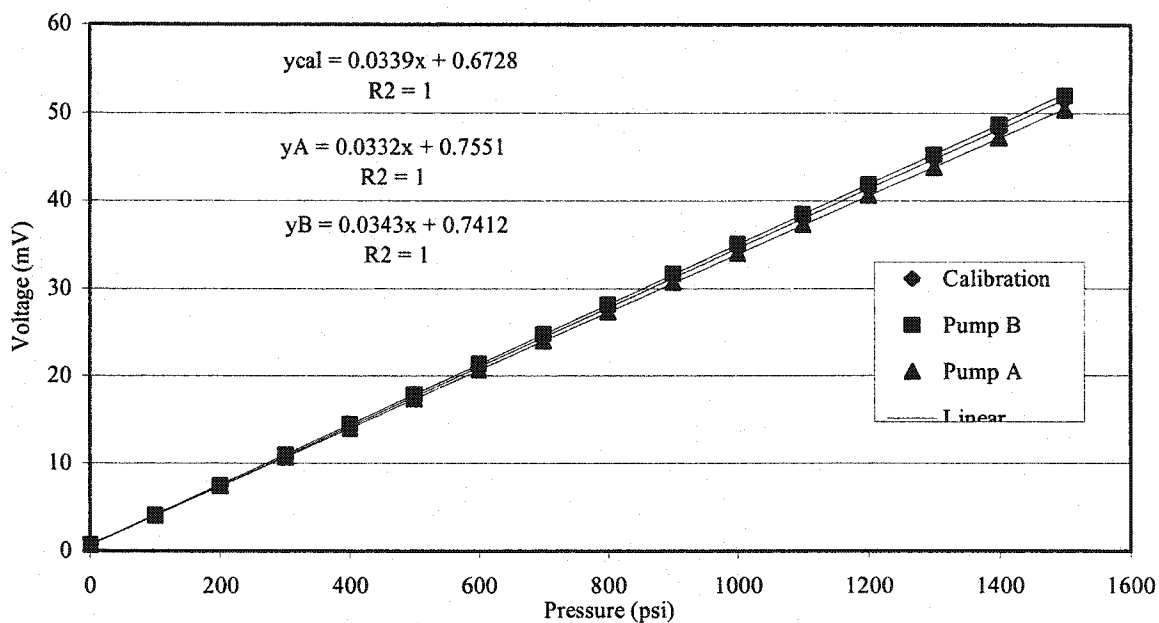**Figure C- 9: Electrical Resistivity Setup across the Specimen**



**Figure C- 10: Photo of Electrical Resistivity in Triaxial**

**Appendix D – Calibrations**

**Figure D- 1: Calibration of Pressure Transducer**



**Figure D- 2: Calibration of ISCO 500 D Pumps**

yA = 8.1166x - 0.2008
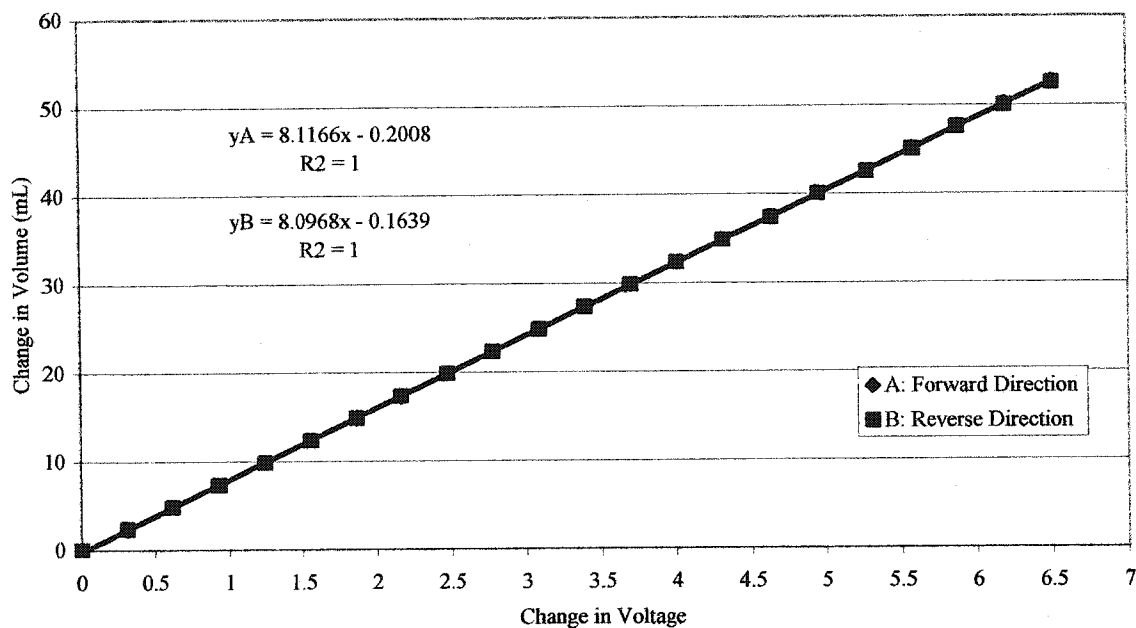R2 = 1

yB = 8.0968x - 0.1639
R2 = 1

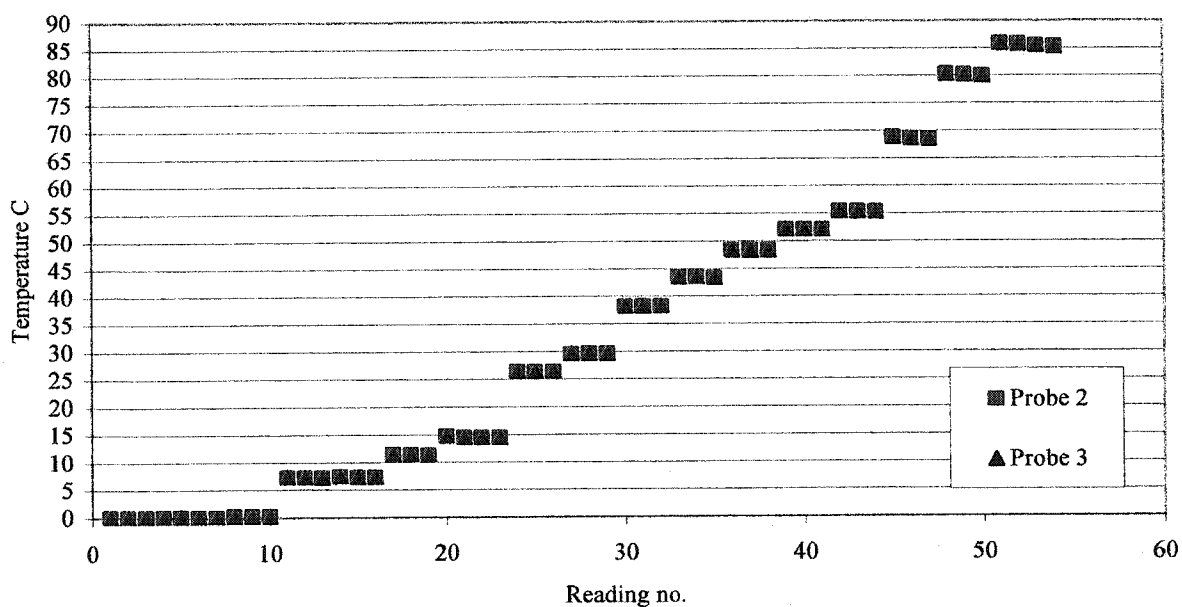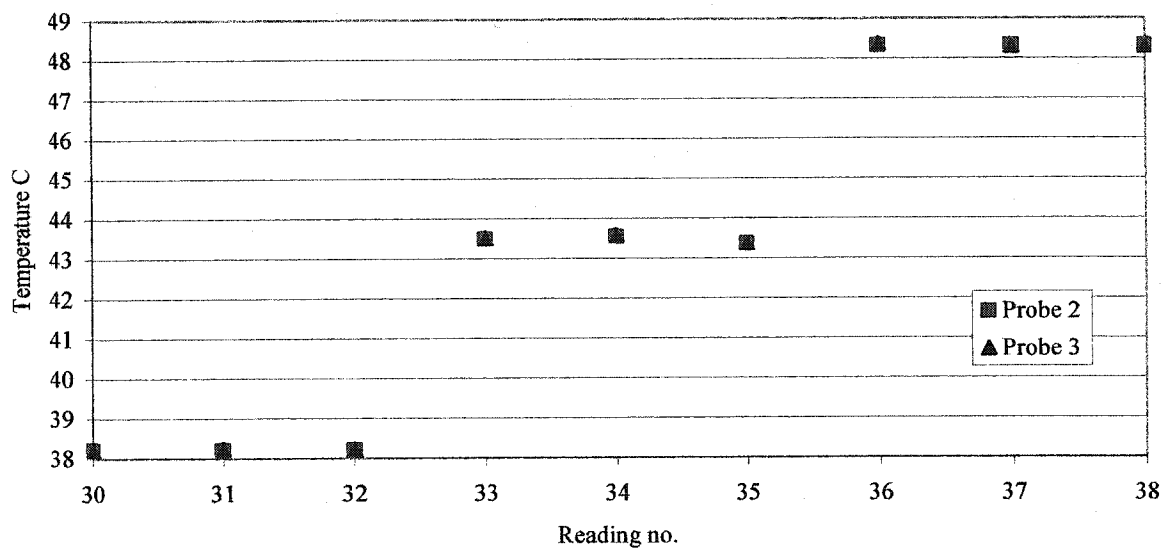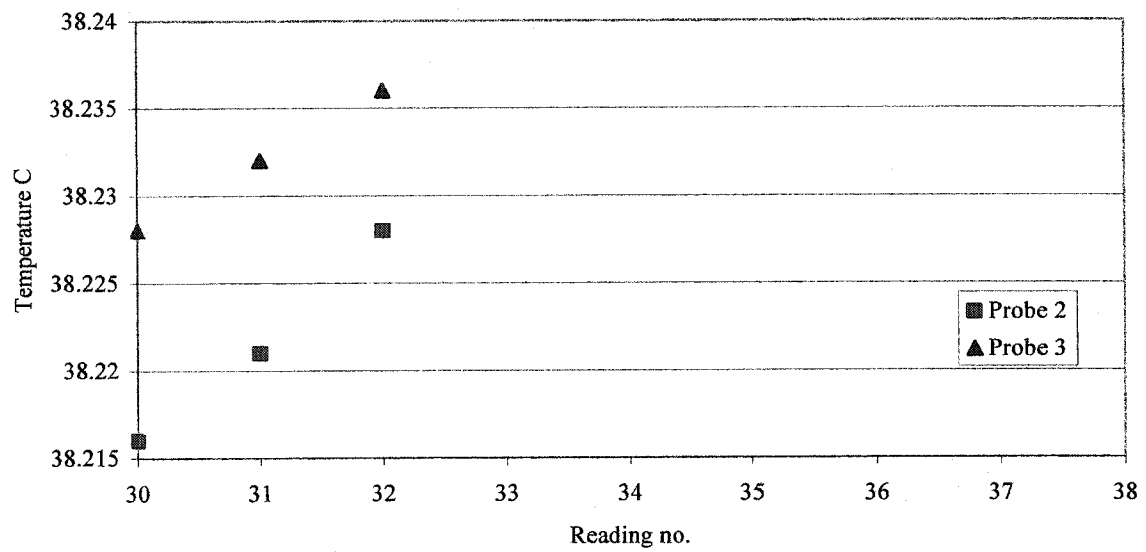**Figure D- 3: Calibration of High Pressure Volume Change Device**



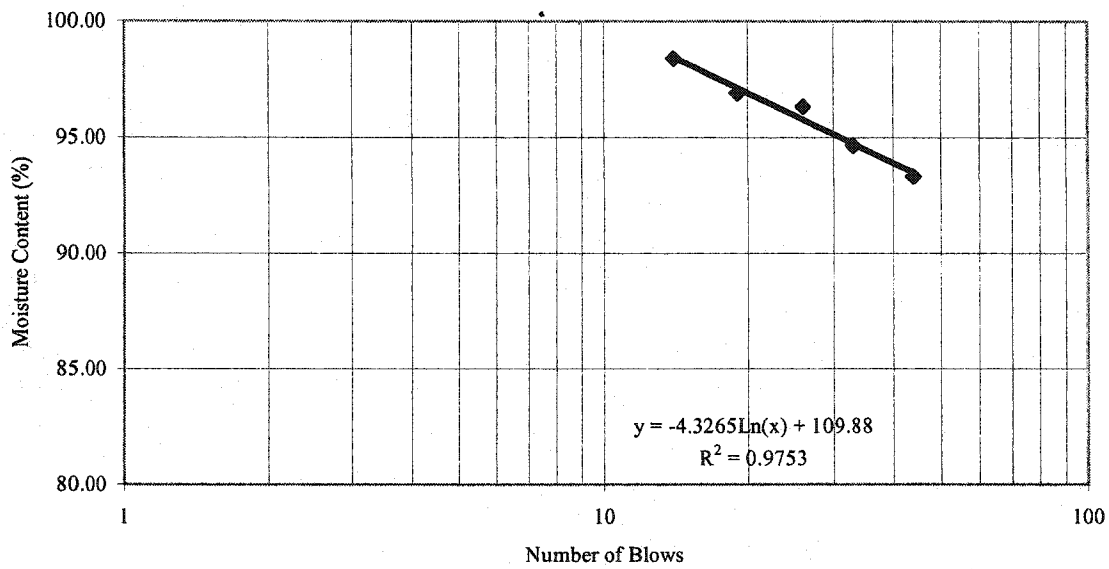**Figure D- 4: Calibration of Azonix Temperature Probes**

**Figure D- 5: Temperature Probe Calibration**



**Figure D- 6: Temperature Probe Calibration @ ~38°C**

**Appendix E –Clay Shale Data from the Clearwater Formation**

**Figure D- 1: Liquid Limit of Clearwater Clay Shale Run 17**

**Table D- 1: Liquid Limit Data Run 17**

| Well: 13-22-83-6W4 | | | | | |
|---|---|---|---|---|---|
| **Run:** | 17 | Core: | 2 of 2 | **Depth:** | 252.1 |
| No. | Wt. Of Tin | Wt of Tin + Wet Soil | Wt of Tin + Dry Soil | Moisture Content (%) | Number of Blows (N) |
| 1 | 1.00 | 14.61 | 7.86 | 98.40 | 14 |
| 2 | 0.98 | 12.58 | 6.98 | 93.33 | 44 |
| 3 | 1.00 | 12.74 | 6.98 | 96.32 | 26 |
| 4 | 1.09 | 17.15 | 9.34 | 94.67 | 33 |
| 5 | 1.04 | 23.35 | 12.37 | 96.91 | 19 |
| 6 | | | | | |

**Liquid Limit (%):**　　95.95

**Table D- 2: Plastic Limit Data Run 17**

| No. | Wt. Of Tin | Wt of Tin + Wet Soil | Wt of Tin + Dry Soil | Moisture Content (%) |
|---|---|---|---|---|
| 1 | 1.11 | 4.41 | 3.63 | 30.95 |
| 2 | 1.09 | 4.40 | 3.54 | 35.10 |
| 3 | 1.04 | 4.92 | 3.96 | 32.88 |

**Plastic Limit (%):**　　32.98

| Well No: | 13-22-83-6W4 |
|---|---|
| Run No: | 17 (2 of 2) |
| Cut (m): | 3 |
| Recovered (m): | 3 |
| Depth (m): | 250.5-253.5 |

Date: 11-Aug-00

*DS - Discontinutiy Spacing
*DP - Discontinuity Persistence

| Depth (cm) | DS (mm) | DP (m) | Roughness | Description | Observations | | |
|---|---|---|---|---|---|---|---|
| Sec 1 0-16cm | | | | Sec1- fissured | XXX-small sections of | | 0 |
| | | | | Sec2-fissured | sand grains. | A.L. | 4 |
| | | | | relativly intact. | (section split when | | 8 |
| | | | | Sec3- highly | opened). | | 12 |
| Sec 2 16-24cm | | | | fissured. | | | 16 |
| | | | | Sec4- highly | | | 20 |
| | | | | fissured. | | | 24 |
| Sec 3 24-32cm (waxed) | | | | Sec5-more intact. | | m.c. 1 | 28 |
| | | | | Sec6-more intact | | | 32 |
| | | | | with hidden larger | | | 36 |
| Sec 4 32-67cm (waxed) | | | | fractures. | | | 40 |
| | | | | Sec8-in chunks | | | 44 |
| | | | | (large few cm). | | | 48 |
| Sec 5 67-80cm | | | | Sec9-small pieces | | | 52 |
| | | | | (crumbled) more | | | 56 |
| | | | | sandy. | | | 60 |
| Sec 6 80-104cm (waxed) | | | | | | | 64 |
| | | | | | | | 68 |
| | | | | | | | 72 |
| Sec 7 104-117cm | | | | | | | 76 |
| | | | | | | | 80 |
| | | | | | | XXX | 84 |
| Sec 8 117-133cm | | | | | | m.c. 2 | 88 |
| | | | | | | | 92 |
| | | | | | | | 96 |
| Sec 9 133-143cm | | | | | | | 100 |
| | | | | | | | 104 |
| | | | | | | | 108 |
| | | | | | | | 112 |
| | | | | | | | 116 |
| | | | | | | | 120 |
| | | | | | | | 124 |
| | | | | | | | 128 |
| | | | | | | | 132 |
| | | | | | | | 136 |
| | | | | | Crumbled Pieces | | 140 |
| | | | | | | | 144 |
| | | | | | | | 148 |
| | | | | | | | 152 |
| | | | | | | | 156 |
| | | | | | | | 160 |
| | | | | | | | 164 |
| | | | | | | | 168 |

**Figure D- 2: Logging Data Run 17 (2of2)**